PHOSPHORYLATION OF HISTONE PROTEINS DURING CELL CYCLE & GENOMIC ANALYSES OF THE MAIZE SHOOT APICAL MERISTEM

by

XIAOLAN ZHANG

(Under the Direction of Michael J. Scanlon and R. Kelly Dawe)

ABSTRACT

This dissertation contains two distinct sections. The first section characterizes the phosphorylation of the maize centromeric histone H3 variant (CENH3) at Ser50. Phosphorylation of histone H3 occurs at Ser10/28 and Thr3/11, and marks chromosome arms or pericentromeres during cell division. Using molecular and cytological methods, we find that maize CENH3 is efficiently phosphorylated at Ser50 in a prophase-telophase pattern that mirrors known H3 phosphorylation events. These data extend the proposed "histone code" to centromeres. We propose that the primary role of histone H3 phosphorylation is to demarcate distinct chromosomal domains (i.e. centromere, pericentromere, chromosome arm) so that chromosomes can align and segregate properly. CENH3 phosphorylation may function as a component of the anaphase checkpoint, and/or mediate kinetochore maturation.

The second section describes the meristem-specific transcript profiling analyses of two maize leaf developmental mutants, narrow sheath1 (ns1) and ragged seedling2 (rgd2). ns mutant plants harbor mutations in the duplicate genes *ns1* and *ns2*, and display narrow leaves due to the loss of a mediolateral domain. The ns genes encode duplicate WUSCHEL1-like homeobOX

(WOX) transcription factors that function redundantly and non-cell autonomously to direct recruitment of leaf founder cell-initials in a lateral domain of the shoot apex. Our analyses indicated that genes predicted to be involved in hormonal transport and signaling, signal transduction, and growth are especially implicated during NS-mediated leaf founder cell recruitment and mediolateral axis specification. Moreover, potentially conserved WOX gene functions during the regulation of two component response pathways and of jasmonate-induced gene expression are identified.

RGD2 is required to coordinate leaf lateral expansion and dorsiventral patterning. rgd2-R mutant plants display narrow to radial leaves that fail to expand laterally, with no reduction of adaxial or abaxial identity. This peculiar phenotype enables the use of the rgd2-R mutant as a genetic tool to re-examine a widely accepted model for dorsiventral and mediolateral patterning in plants. Transcriptome analyses revealed that genes predicted to be involved in transcription regulation, chromatin remodeling, signal transduction, and proteolysis/protein fate are especially misexpressed in the rgd2-R mutant apex. Our data suggest that RGD2 may function through either the ARP (ASYMMETRIC LEAVES 1/ROUGH SHEATH2/PHANTASTICA) pathway or via a previously undescribed proteolytic pathway to coordinate dorsiventral patterning and mediolateral growth during maize leaf development.

INDEX WORDS: maize, histone H3, CENH3, phosphorylation, centromere, leaf development, *narrow sheath*, founder cells, *ragged seedling2*, adaxial, abaxial, laser microdissection, microarray

PHOSPHORYLATION OF HISTONE PROTEINS DURING CELL CYCLE & GENOMIC ANALYSES OF THE MAIZE SHOOT APICAL MERISTEM

by

XIAOLAN ZHANG

B.S., China Agricultural University, P. R. China, 1999

M.S., China Agricultural University, P. R. China, 2002

A Dissertation Submitted to the Graduate Faculty of The University of Georgia in Partial Fulfillment of the Requirements for the Degree

DOCTER OF PHILOSOPHY

ATHENS, GEORGIA

2007

PHOSPHORYLATION OF HISTONE PROTEINS DURING CELL CYCLE

& GENOMIC ANALYSES OF THE MAIZE SHOOT APICAL MERISTEM

by

XIAOLAN ZHANG

Major Professors:	Michael J. Scanlon R. Kelly Dawe
Committee:	Zheng-hua Ye Jeffrey Dean Gregory Schmidt

Electronic Version Approved:

Maureen Grasso
Dean of the Graduate School
The University of Georgia
August, 2007

DEDICATION

To my husband, my daughter, my parents, my sisters and my brothers for their love and support.

ACKNOWLEDGEMENTS

First of all, I would like to thank my major advisors Michael J. Scanlon and R. Kelly Dawe from the bottom of my heart for their help, guidance and support during the past five years. Michael and Kelly are great mentors who teach students not only how to do experiments, but also how to think and design experiments to address scientific questions, as well as how to manage a lab and balance your life. I am also very grateful to my wonderful committee members: Lee Pratt, Jeffrey Dean and Zhenghua Ye for their help, great comments and suggestions about my project. Lee and Jeffrey are especially helpful for the cDNA library construction and microarray data analyses, respectively. I would like to thank Gregory Schmidt who agreed to serve on my committee during my defense when Lee Pratt was out of the US. I would like to thank Sue Wessler for her terrific advice about my projects and my future career development. I would like to thank all current and past members in the Scanlon lab and Dawe lab, especially Suneng Fu, Dave Henderson, Jiabing Ji, Lee Brooks, Chris Topp, Yaqing Du, Yun Li, Brunie Burgos and Thomas Stahl for their help and friendship. I would like to thank Russell Malmberg, John Burk and Jim Leebens-Mack for their nice help after my home lab left for Cornell University. I would like to thank all departmental staff for their wonderful work, especially Susan Watkins and Elaine Dunbar for their great help to me. I am also very grateful to the greenhouse staff Andy Tull, Mike Boyd and Melanie Smith for their help and expertise caring for my plants. Also, I would like to thank many of my friends, especially Meizhu Du,

Xiaoming Wang, Tianle Chen, Zhijue Liu, Liang Shen, Renyi Liu and Guojun Yang for helping me have a happy and wonderful life in Athens.

Special thanks to my husband Xuexian Li and my daughter Anna Li for their love, support and understanding, as well as for giving me a loving and happy family. I would also like to thank all my big family members: my parents, sisters, brothers for their moral support.

TABLE OF CONTENTS

Page

LIST OF TABLES

Page

LIST OF FIGURES

Page

CHAPTER 1

INTRODUCTION AND LITERATURE REVIEW

PART A CELL BIOLOGY

Mitosis and Meiosis

In higher eukaryotes, cell division falls into two basic classes: mitosis and meiosis. Mitosis is for vegetative/somatic reproduction, which involves one round of DNA replication and subsequent chromosome division, and produces two daughter cells with identical genetic information. Mitosis is therefore called equational division. Meiosis, in contrast, is for sexual reproduction, which undergoes two rounds of chromosome division (meiosis I and meiosis II) following only one round of DNA replication, and generates four genetically different daughter cells. Each daughter cell contains half the chromosome number of the mother cell (haploid). Thus, meiosis is called reductional division. Two haploid gametes (male and female) then fuse to regenerate a diploid embryonic cell and complete the sexual cycle.

The cell cycle can be divided into several distinct substages, including interphase, prophase, metaphase, anaphase, telophase, and cytokinesis. The following unique features make meiosis the heart of genetic diversity and stability. First, homologous chromosomes experience a high frequency of recombination during prophase I. This cytogenetic event is achieved by a series of chromosome modifications, including pairing of homologous chromosomes (Schwacha and Kleckner, 1994, 1997), introduction of double strand breaks (Keeney, 2001), formation of the synaptonemal complex, and initiation of interhomolog recombination (Roeder, 1997; Keeney, 2001). Second, homologous chromosomes, rather than sister chromatids, segregate to the opposite poles during anaphase I. Coincidently, meiotic cohesion is destroyed in a stepwise

manner. Only chromosome arm cohesion is released during anaphase I, whereas centromeric cohesion remains until anaphase II (Kitajima et al., 2003; Kitajima et al., 2004; Watanabe, 2005).

The centromere/ kinetochore complex

To maintain genome stability, genetic information needs to be equally distributed into daughter cells by the end of the cell cycle. Chromosome missegregation may lead to aneuploidy (an abnormal number of chromosomes), a common feature of many human cancer and clinical syndromes (Draviam et al., 2004). The centromere/kinetochore complex is crucial for faithful chromosome segregation. It is required for microtubule-chromosome attachment, metaphase/anaphase checkpoint monitoring, sister chromatids cohesion and separation, and heterochromatin establishment (Pluta et al., 1995; Craig et al., 1999; Cleveland et al., 2003; Maiato et al., 2004; Vos et al., 2006). Errors in any of above processes will result in defective chromosome segregation. For example, anaphase is delayed by unattached or loose kinetochores (Rieder et al., 1995; Chan and Yen, 2003). Release of centromeric cohesion prior to meiosis II leads to random chromosome segregation and aneuploidy (Watanabe, 2004).

The 'classic' centromere refers to the primary chromosome constriction with highly repetitive DNA sequences (Rieder, 1982; Dawe and Henikoff, 2006). The size of centromeres varies from 125 base pairs in the budding yeast *S. cerevisiae,* to several megabases in higher eukaryotes, such as *Z. mays* (Cheeseman et al., 2002; Jin et al., 2004). Despite the tremendous variation in size, centromeres share two common features in higher eukaryotes. First, the centromere usually consists of large arrays of 150-180 bp satellite repeats (Heslop-Harrison et al., 2003), such as the 171 bp α-satellite in humans, 155 bp CentO in rice, and 156 bp CentC in maize (Spence et al., 2002; Zhong et al., 2002; Lee et al., 2006). However, the centromeric DNA sequences evolve so fast that there is no universally conserved centromeric DNA sequences

among different species (Henikoff et al., 2001). Moreover, centromeric DNA is neither required nor sufficient to assemble a functional centromere (Choo, 2001), indicating that centromeres are assembled and maintained at least partially, if not completely, by epigenetic mechanisms (Dawe and Henikoff, 2006). Second, the centromere is comprised of two distinct domains: the core centromeric domain and the surrounding pericentromeric domain (Pidoux and Allshire, 2004; Dawe and Henikoff, 2006). The core centromeric domain is the kinetochore binding region containing young and almost identical satellite repeats, while the pericentromeric domain is heterochromatic and consists of old divergent satellite repeats (Bernard et al., 2001; Schueler et al., 2001; Nonaka et al., 2002).

The kinetochore is the large proteinaceous structure that assembles on the core centromeric domain. The kinetochore appears as a multi-domain structure on the surface of pericentromeric heterochromatin under the traditional electron microscope (Brinkley and Stubblefield, 1966). The kinetochore plays essential roles in mediating microtubule attachment, chromosome biorientation, and anaphase onset. Even for the tiny 125 bp centromere in *S. cerecisiae*, 65 identified proteins are recruited to build a functional kinetochore (McAinsh et al., 2003). At least 34 kinetochore protein homologs have been characterized in humans (Vos et al., 2006), and 6 kinetochore subunits have been identified in maize (CENP-C, CENH3, MAD2, 3F3/2, MIS12, NDC80) (Yu et al., 2000; Zhong et al., 2002) (personal communication with Xuexian Li and Yaqing Du). These kinetochore proteins are broadly classified into two categories: constitutive proteins that associate with the centromere throughout the cell cycle, and transitory proteins that are recruited only in specific stages during the cell cycle. Constitutive kinetochore proteins are mainly structural components. They form the foundation platform to recruit transitory proteins. Depletion of constitutive kinetochore proteins, such as CENP-A,

CENP-C, CENP-H, CENP-I, MIS12, or CENP-U, leads to mitotic halt, chromosome misalignment, or slower growth rates (Fukagawa et al., 1999; Howman et al., 2000; Fukagawa et al., 2001; Nishihashi et al., 2002; Fukagawa, 2004; Minoshima et al., 2005). In humans, eight constitutive kinetochore proteins have been characterized, CENP-A, CENP-C, CENP-H, CENP-I, MIS12, CENP-G, CENP-B and CENP-U(50) (Amor et al., 2004; Vos et al., 2006). They all localize to the inner kinetochore and associate with the core centromeric DNA. Transitory kinetochore proteins, on the other hand, include three classes: spindle checkpoint proteins, such as Mad2, Bub1, ZW10, Ndc80, Nuf2, Spc24 and Spc25 (Sullivan, 2001; Vos et al., 2006); passenger proteins, such as INCENP, Aurora kinases, Survivin and Borealin (Vagnarelli and Earnshaw, 2004); and motor proteins, such as CENP-E, dynein and kinesin (Fukagawa, 2004). Transitory kinetochore proteins play roles in interacting with the spindle and ensuring accurate chromosome segregation during cell division. Loss-of-function of transitory proteins results in defects in spindle checkpoint, mitotic delay or even mitotic arrest (Chen et al., 1996; Wojcik et al., 2001; Putkey et al., 2002).

Phosphorylation of histone H3

The nucleosome is the fundamental unit of all eukaryotic chromatin, and is composed of an octamer of core histones (two copies of each of histones H2A, H2B, H3 and H4) wrapped up with 147 base pair of DNA into two left-handed superhelical turns (Luger et al., 1997). Each core histone contains a histone-fold domain which mediates histone-histone interaction within the nucleosome octamer, and a flexible N-terminal tail that extends from the surface of nucleosome core particle. Notably, the N-terminal tails of core histones are subjected to extensive post-translational modifications, including phosphorylation of serine (K) and threonine (T), acetylation of lysines (K), methylation of lysine (K) and arginine (R), ubiquitination and

sumoylation of lysine (K), glycosylation, ADP-ribosylation of glutamic acid (E), carbonylation of lysine (K) and arginine (R), deimination of arginine (R), and isomerization of proline (P) (Wondrak et al., 2000; Fuchs et al., 2006). These covalent modifications may affect the contacts between nucleosomes via charge change to switch chromatin "on" or "off". Alternatively, covalent modifications regulate the interactions between histones and chromatin remodeling factors or transcription factors to induce downstream effects (Strahl and Allis, 2000; Nowak and Corces, 2004). Collectively, these post-translational modifications are called a "histone code" that is implicated in various biological processes, such as alteration of chromatin structure and regulation of gene expression (Strahl and Allis, 2000). Furthermore, some histone modifications, such as phosphorylation, acetylation and methylation, are reversible and highly dynamic (Kouzarides, 2007). Given the huge number of nucleosomes in each cell, the versatile modifications on each histone, and large variety of sequential combinations of certain modifications, the genome coding capacity is greatly expanded by these epigenetic modifications (Jenuwein and Allis, 2001; Fischle et al., 2003).

On the N-terminal tail of histone H3, sixteen residues were shown to be epigenetically modified, including through phosphorylation, methylation, acetylation and isomerization (Figure 1.1). Four out of sixteen modified residues are known to be phosphorylated (Hendzel et al., 1997; Gernand et al., 2003; Preuss et al., 2003; Polioudaki et al., 2004; Houben et al., 2005). All these phosphorylation events display similar kinetics in all species studied: undetectable or low levels at interphase, increasing at prophase, peaking at metaphase, and decreasing during anaphase and telophase (Hendzel et al., 1997; Gernand et al., 2003; Preuss et al., 2003; Polioudaki et al., 2004; Houben et al., 2005). However, the precise modification pattern varies, and the underlying

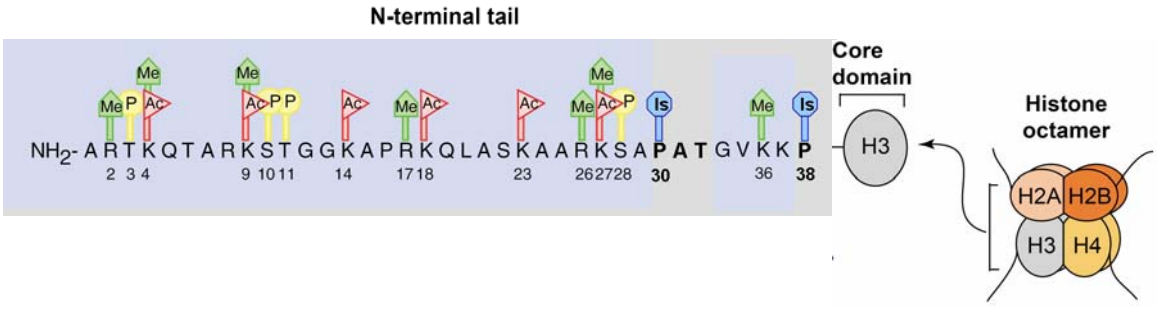

Figure 1.1 Post-translational modifications of histone H3 on the N-terminal tail. The residue modifications are indicated as follows: methylation as a green pentagon, phosphorylation as a yellow circle, acetylation as a red triangle and isomerization as a blue octagon [Redrawn and modified from Nowak and Corces, 2000; Peterson and Laniel, 2004].

biological functions remain controversial. In mammalian cells, the phosphorylation of H3-Ser10 and H3-Ser28 initiates in pericentric heterochromatin and spreads to chromosome arms during mitotic and meiotic metaphase, which temporally and spatially correlates with chromosome condensation (Hendzel et al., 1997; Goto et al., 1999). Further studies using competitive peptides or replacement of Ser10 suggest that H3-Ser10 phosphorylation may have a role in chromosome condensation (Van Hooser et al., 1998; Wei et al., 1998; de la Barre et al., 2000). However, other evidence indicates that H3-Ser10 phosphorylation and chromosome condensation are uncoupled events during cell cycle. Budding yeasts with mutated Ser10 show no cell cycle defects (Hsu et al., 2000), and loss of H3-Ser10 phosphorylation in Xenopus egg cells by Aurora B depletion did not comprise chromosome condensation (MacCallum et al., 2002).

In plants, H3-Ser10 and H3-Ser28 phosphorylation begins in late prophase after the initiation of chromosome condensation in both mitosis and meiosis (Kaszas and Cande, 2000; Gernand et al., 2003). Unlike in animals, H3-Ser28 phosphorylation never extends beyond pericentric regions in both mitosis and meiosis. H3-Ser10 phosphorylation is restricted to the pericentromeric region during mitosis and meiosis II, and only during meiosis I is the entire chromosome modified (Houben et al., 1999; Kaszas and Cande, 2000; Manzanero et al., 2000; Gernand et al., 2003). These studies suggest that plant H3-Ser10 phosphorylation is involved in sister chromatid cohesion instead of chromosome condensation (Kaszas and Cande, 2000; Gernand et al., 2003).

In contrast to the phosphorylation of H3 serines 10 and 28, phosphorylation of H3 threonines 3 and 11 in mammalian cells is enriched mainly in the centromeric/pericentromeric regions, whereas it occurs along chromosome arms in plant cells (Preuss et al., 2003; Polioudaki et al., 2004; Dai et al., 2005; Houben et al., 2005). Therefore, animal H3 threonine

phosphorylations may serve as an epigenetic mark for centromere assembly, while plant H3 theonine phosphorylations are correlated with chromosome condensation (Preuss et al., 2003; Polioudaki et al., 2004; Dai and Higgins, 2005; Dai et al., 2005; Houben et al., 2005).

Several lines of evidence show that histone H3 serine/threonine phosphorylations may also play roles in transcriptional activation of specific genes in both animals and plants. In fibroblast cells, activation of immediate-early response genes, such as *c-fos* and *c-jun* is correlated with the rapid phosphorylation of histone H3 at Ser10 (Mahadevan et al., 1991; Barratt et al., 1994; Strelkov and Davie, 2002). Phosphorylation of H3 Ser10 and acetylation of H3 Lysine 14 activate together the expression of cellular differentiation genes in ovarian granulose cells (DeManno et al., 1999; Salvador et al., 2001). Convincingly, the phosphorylation level of H3 Ser10 increases at heat shock loci in *Drosophila*, despite the global drop of phosphorylation levels in response to heat shock (Nowak and Corces, 2000). Similar correlation of histone H3 phosphorylation and gene activation has been reported in plants. The enhancement of H3 phosphorylation is observed during the mitogen-activated protein kinase cascade (Clayton and Mahadevan, 2003). Sucrose and salt stresses lead to the phosphorylation of H3 at Ser10 and Threonine 3, and the activation of stress response in tobacco cells (Houben et al., 2007).

Taken together, the function of histone phosphorylation is largely dependent on the specific species, residue and context. The phosphorylation of histone H3 may be involved in gene activation under certain conditions, but it primarily appears to identify different chromosomal domains and mark their progress during the cell cycle progression (Prigent and Dimitrov, 2003).

Histone H3 kinases

Several kinases have been implicated in histone H3 phosphorylation. Aurora B kinase has been well characterized as responsible for phosphorylation of H3 at Ser 10 and Ser 28 during the cell cycle in many organisms, including *S. cerevisiae* (Hsu et al., 2000), *S. pombe* (Petersen et al., 2001), *C. elegans* (Hsu et al., 2000), *D. melanogaster* (Giet and Glover, 2001), and mammals (Crosio et al., 2002; Goto et al., 2002). Aurora B kinase is a passenger protein that localizes to the centromere region from G2 to metaphase, and moves to the central spindle microtubules during anaphase (Vagnarelli and Earnshaw, 2004). Aurora B can phosphorylate H3 Ser 10 and Ser28 *in vitro*, and mutation or knock-down of aurora B decreases H3 phosphorylation at both Ser10 and Ser28 *in vivo* (Hsu et al., 2000; Giet and Glover, 2001; Goto et al., 2002).

The plant aurora kinase family has been recently shown to contain three members, *Arabidopsis thaliana* Aurora kinases 1-3 (AtAUR1-3). AtAUR1 and AtAUR2 localize in the perinuclear membrane during interphase, move to microtubule spindles and then concentrate at the cell plate in anaphase. AtAUR3 appears as discrete dots on chromosomes during prophase and then localizes to the metaphase plate (Demidov et al., 2005; Kawabe et al., 2005; Kurihara et al., 2006). AtAUR1 preferentially phosphorylates histone H3 at Ser10, but not at Ser28, as detected by immunostaining and an *in vitro* kinase assay (Demidov et al., 2005; Kawabe et al., 2005). AtAUR3, however, has been shown to mediate the phosphorylation of both H3 Ser10 and Ser28 *in vitro* and *in vivo* (Kurihara et al., 2006).

In contrast, the kinases involved in H3 threonine phosphorylation are poorly characterized. Haspin kinase phosphorylates H3 at threonine 3 in mammalian cells both *in vitro* and *in vivo* (Dai et al., 2005). Haspin belongs to a novel group of kinases present in most eukaryotes (Higgins, 2001). Depletion of haspin by RNAi and overexpression of haspin result in

chromosome misalignment and retarded cell progression, respectively (Dai et al., 2005). Nevertheless, the role of haspin on H3 Thr3 phosphorylation is not universal. Haspin-like genes Alk1 and Alk2 fail to phosphorylate histone H3 in *S. cerevisiae* (Nespoli et al., 2006). As to the kinase implicated in H3 Thr11 phosphorylation, the only report came from mammalian cells, wherein death-associated protein (DAP)-like kinase (DLK) phosphorylated H3 at Thr11 in vitro and correlated with H3 Thr11 phosphorylation in a strict temporal and subcellular (centromere) manner (Preuss et al., 2003).

Phosphorylation of CENH3

Centromeric Histone H3 (CENH3) is a histone H3 variant required for centromere identity and kinetochore assembly (Choo, 2001; Amor et al., 2004; Heit et al., 2006). CENH3 shares the histone-fold domain with conventional H3, but is characterized by a very divergent N-terminal tail (Henikoff et al., 2000). CENH3 is incorporated exclusively into the centromere during interphase, and serves as a centromere epigenetic marker and kinetochore "foundation" protein (Choo, 2001; Amor et al., 2004; Heit et al., 2006). Little is known about covalent modifications on the N-terminal tail of CENH3 compared to those on canonical H3. Zeitlin and colleagues (2001) showed that human CENPA (CENH3 ortholog) was phosphorylated on Ser7 during mitosis. This phosphorylation event initiates in prophase, reaches its peak in prometaphase and decreases in anaphase. Interestingly, double labeling of phosphorylation of CENH3 Ser7 and H3 Ser10 indicated that pericentric H3 phosphorylation occurred first, followed by chromosome arm H3 phosphorylation and then CENH3 phosphorylation in the centromere. Furthermore, phosphorylation of CENPA on Ser7 is required for proper chromosome alignment (Zeitlin et al., 2001b; Zeitlin et al., 2001a; Kunitoku et al., 2003). Aurora A initiates the phosphorylation of CENH3 Ser7 in prophase, and aurora B maintains the

phosphorylation to ensure proper chromosome segregation (Kunitoku et al., 2003). This raises the potential that the "histone code" may apply to the centromere and play similar or distinct biological functions during cell division. To test this hypothesis, further studies on CENH3 covalent modifications, especially phosphorylation of other CENH3s, are imperative.

PART B LEAF DEVELOPMENT

Leaves are plant lateral organs specialized for light harvesting and gas exchange. Despite these conserved functions, plants have evolved extreme and exquisite variation in leaf shape, size, and complexity. For example, the maize leaf is strap-like and simple; the *Arabidopsis* simple leaf forms a distal lamina at the end of a stem-like petiole; whereas tomato has a unipinnately dissected leaf comprised of multiple leaflets arranged about the central rachis. Leaves originate from founder cells that are recruited from the periphery of the shoot apical meristem (SAM). Subsequently, leaf patterning occurs along the proximodistal (base-tip), mediolateral (middle-margin) and dorsiventral (top-bottom) axes to establish a leaf primordium. Continued growth and differentiation give rise to the mature leave form. Therefore, understanding the molecular mechanisms of leaf founder cell recruitment and patterning in the leaf primordium will help to unravel the mystery as to how leaves attain such complex and diverse developmental morphology.

SAMs Produce Lateral Organs

All above-ground organs come from the shoot apical meristem (SAM), a specialized pluripotent pool of stem cells located at the apex of the shoot. The SAM is formed during embryogenesis and functions as an organogenic center to produce phytomers in a regular and reiterative manner. Phytomers are the repeating plant segment; each phytomer is composed of a

leaf, a node, an internode and an axillary bud (McSteen and Leyser, 2005). The SAM can be divided into the clonally distinct tunica and corpus layers. The tunica is the outer sheath comprised of either a single-cell layer (L1 in maize and most monocots) or two cell layers (L1 and L2 in *Arabidopsis* and most dicots and eudicots). Anticlinal (i.e. cell division plane perpendicular to the plane of the cell layer) cell divisions predominate in the tunica (Fleming, 2006). The corpus is the interior layer (L2 in maize and most monocots, L3 in most dicots) wherein both anticlinal and periclinal (i.e. cell division plane parallel to the plane of the cell layer) cell divisions take place. The SAM is also organized into different histological zones. The mitotically-active peripheral zone (PZ) is the site of leaf organogenesis and is located on the flank of the meristem. The central zone (CZ) comprises the self-renewing stem cells situated at the apex of the meristem and is characterized by a slower rate of cell division. The CZ functions to replenish cells that have been lost to the PZ during organ formation. Beneath the CZ is the rib zone, which gives rise to the central pith of the stem.

Regulation of SAM function

The primary functions of the SAM are to produce lateral organs reiteratively from the PZ and to maintain the stem cell population in the CZ. Performance of these two essential functions requires a delicate balance between cell proliferation and cell differentiation in the SAM. Multiple regulators have been identified to be involved in the precise control of the SAM function. SHOOT MERISTEMLESS (STM), a member of the class I KNOTTED1-like homeobox (KNOX) gene family, is required for the maintenance of the meristematic identity in the SAM (Barton and Poethig, 1993; Clark et al., 1996; Long et al., 1996; Gallois et al., 2002). Null mutations at STM results in the loss of meristem identity and premature termination of shoot development (Barton and Poethig, 1993; Long et al., 1996). STM is expressed throughout

the indeterminate cells of the SAM, but is down-regulated in the leaf founder cells and in leaf primordia (Long et al., 1996). Moreover, the closely related class 1 KNOX gene family members KNAT1, KNAT2 and KNAT6, play partially redundant roles with STM to maintain meristematic identity. The expression of KNAT1, KNAT2 and KNAT6 is limited to specific regions in the SAM and is excluded from young leaf primordia (Chuck et al., 1996; Byrne et al., 2000; Byrne et al., 2002; Xu et al., 2003). The STM-related KNOX genes function in three genetic pathways to maintain indeterminate cell fate in the SAM. First, KNOX genes function to repress the expression of ASYMMETRIC LEAVES1 (AS1) and its interactor ASYMMETRIC LEAVES2 (AS2) in the SAM proper, so that AS1 and AS2 are expressed in the incipient leaf primordium (Byrne et al., 2000; Byrne et al., 2002). Secondly, KNOXes negatively regulate gibberellin (GA) biosynthesis in the SAM to prevent cells from entering a determinate cell fate (Tanaka-Ueguchi et al., 1998; Hay et al., 2002; Jasinski et al., 2005). Lastly, KNOXes induce cytokinin (CK) biosynthesis in the SAM, which positively regulates cell division and meristem size (Shani et al., 2006). Overexpression of STM leads to rapid accumulation of CK and the induction of the CK-synthesis gene ISOPENTENYL TRANSFERASE7 (IPT7) (Jasinski et al., 2005; Yanai et al., 2005) (Figure 1.2).

WUSCHEL (WUS) is another key player that functions to specify and maintain the stem cell niche in the SAM, a role that is complimentary to KNOX. Loss of WUS function causes a failure to maintain stem cell fate in the SAM, whereas ectopic expression of WUS results in ectopic stem cell identity (Laux et al., 1996; Schoof et al., 2000). WUS encodes another class of homeodomain transcription factors and is expressed in the organizing center (OC) of the SAM (shown in orange in Figure 1.2), comprised of a few corpus cells below the CZ. WUS functions non-cell autonomously in the OC to specify overlying stem cell identity in the CZ by activating

the expression of the small peptide ligand CLAVATA3 (CLV3) (Laux et al., 1996). The CLV3 ligand moves through the apolastic space in the CZ of the SAM and binds to the heterodimeric, leucine-rich receptor like protein kinases CLAVATA1 and CLAVATA2. Binding of the CLV3 ligand subsequently activates the CLV signaling pathway and results in repression of WUS expression (Figure 1.2). Therefore, the WUS and the CLV genes function in a negative feedback loop to maintain stem cell homeostasis in the SAM (Figure 1.2) (Clark et al., 1997; Mayer et al., 1998; Jeong et al., 1999; Trotochaud et al., 2000; Rojo et al., 2002; Lenhard and Laux, 2003). Null mutations in CLV1, CLV2, and CLV3 result in an expanded WUS-expressing domain in the SAM and an enlarged meristem, whereas overexpression of CLV3 mimics the wus mutant phenotype, illustrating that the CLV genes negatively regulate WUS activity in the SAM (Brand et al., 2000).

WUS promotes stem cell fate by directly repressing transcription of several two-component ARABIDOPSIS RESPONSE REGULATOR genes (ARR5, ARR6, ARR7 and ARR15) (Leibfried et al., 2005). ARRs are negative regulators of the CK signaling pathway and meristem size; constitutive activation of ARR7 causes a reduction in SAM size, whereas null mutations in the maize ARR7 orthologue ABPHYLL1 result in an enlarged SAM (Giulini et al., 2004; Leibfried et al., 2005) (Figure 1.2).

However, KNOXes and WUS are not the sole regulators of SAM function. Recently, several chromatin remodeling factors have been shown to function during SAM maintenance, mainly by regulating WUS expression. FASCIATA1 (FAS1) and FASCIATA2 (FAS2) negatively regulate WUS expression in the SAM, and encode two subunits of the CHROMATIN ASSEMBLY FACTOR (CAF-1) complex that is involved in chromatin

reconstitution and inheritance of heterochromatin states (Loyola and Almouzni, 2004). Loss-of-function mutations in FAS1 or FAS2 result in ectopic expression of WUS and aberrant shoot development (Kaya et al., 2001). BRUSHY1 (BRU1), a nuclear protein involved in chromatin stabilization following DNA replication, is shown to be a positive regulator of WUS expression (Takeda et al., 2004). Furthermore, SPLAYED (SYD), a SWI2/SNF2 class ATP-dependent chromatin remodeling factor, is as a direct positive regulator of WUS (Figure 1.2). SYD mutants display defective organ initiation and reduction of WUS and CLV3 expression in the SAM (Kwon et al., 2005). Similarly, RNAi knockdowns of another SWI2/SNF2 class ATPase, AtBRAHMA (AtBRM), leads to small plants with curled leaves (Farrona et al., 2004). Multiple transcription factors are also involved in the regulation of the WUS-expression domain in the SAM. HANABA TARARU (HAN), a GATA transcription factor, negatively regulates WUS-expressing cells during early embryogenesis, prior to the initiation of CLV1, CLV2, or CLV3 expression (Zhao et al., 2004). Null mutations in HAN result in the expansion of the WUS expression domain in the SAM (Zhao et al., 2004). However, the SAND domain transcription factor ULTRAPETALA1 (UTL1), represses WUS expression after the floral transition, but functions in a different pathway than the CLV proteins (Carles et al., 2004; Carles et al., 2005). Loss-of-function mutations in ULT1 cause an enlarged WUS-expression domain, over-sized inflorescence and floral meristems, supernumerary flowers and floral organs, and delayed termination of floral meristems (Carles et al., 2004; Carles et al., 2005). Furthermore, STIMPY/WOX9 (STIP), a WUSCHEL-related homeobOX (WOX) gene family member, functions as a positive regulator of WUS expression. Mutations in STIP result in a defective SAM devoid of WUS and CLV3 expression. Sucrose rescues the STIP mutant phenotype,

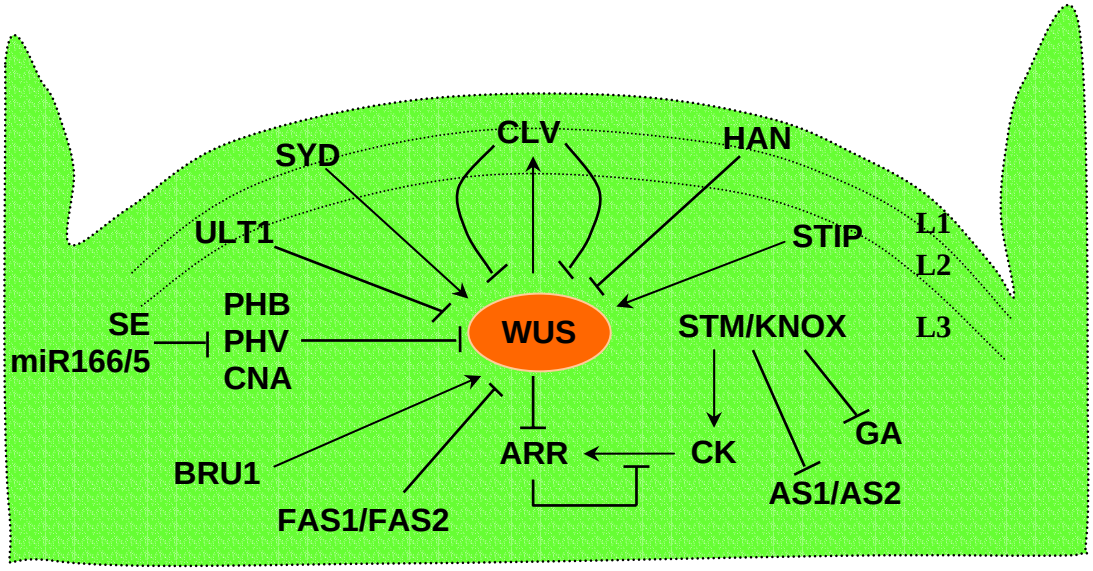

Figure 1.2 Molecular regulation of the shoot apical meristem (SAM). KNOX function maintains the meristematic identity by repressing AS1/AS2 and GA accumulation, and activating CK biosynthesis in the SAM. WUS and CLV form a negative feedback loop to control stem cell homeostasis and function complimentary to the KNOX pathways. WUS directly represses the expression of ARRs, which are negative regulators of the CK signaling pathway. Chromatin remodeling factors, including FAS1/FAS2, SYD and BRU1, modify SAM function through regulation of the WUS expression domain (shown in orange). Additional transcription factors, including HAN, ULT1, STIP and HD-ZIPIII proteins (PHB, PHV and CAN), are also involved in the regulation of WUS expression and thus contribute to SAM function [Redrawn and modified from Williams and Fletcher, 2005].

suggesting that sugar signaling or the metabolic induction of entry into the cell cycle can bypass the need for STIP to activate cell division and WUS expression (Wu et al., 2005; Francis and Halford, 2006). Recently, a role for the HD-ZIPIII- microRNA166/5 pathway in WUS regulation has been uncovered. HD-ZIPIII genes encode class III homeodomain-leucine zipper transcription factors and are well-characterized targets of microRNA166/5. Three members of the HD-ZIPIII family, CORONA (CNA), PHABULOSA (PHB) and PHAVOLUTA (PHV), function redundantly to repress WUS expression and thus limit the size of the SAM CZ. Correspondingly, microRNA166/5 and its regulator SERRATE (SE) activate WUS expression by targeting the destruction of HD-ZIPIII transcripts, and thereby indirectly induce SAM activity (Grigg et al., 2005; Williams et al., 2005; Yang et al., 2006) (Figure 1.2).

Leaf initiation from the SAM

Leaf development is initiated by recruitment of leaf founder cells from the PZ region of the SAM. Once recruited, cells change their identity from an indeterminate meristematic fate to a determinate leaf fate. The process of founder cell recruitment is marked by the downregulation of KNOX accumulation in the PZ, as demonstrated by the expression profile of the founding member of the KNOX gene family, *knotted1* (Smith et al., 1992; Jackson et al., 1994). The variations in leaf shape observed in the plant kingdom partly result from differing extents of leaf founder cell recruitment (Byrne et al., 2001). For example, each maize leaf arises from about 200 founder cells that are recruited from the entire circumstance of the SAM, so that the base of the leaf primordium encircles the SAM (Poethig, 1984; Poethig and Szymkowiak, 1995). In contrast, each *Arabidopsis* leaf originates from about 25 initials cells that are recruited from one flank of the SAM with minimal lateral spreading during founder cell recruitment. Thus, the base of the young primordium does not encircle the SAM in *Arabidopsis* and many eudicots (Irish and

Sussex, 1992; Long and Barton, 2000) (Figure 1.3). After leaf initiation, the maintenance of determinate cell fate in the leaf primordium requires the function of the ARP class of MYB transcription factors (AS1 in *Arabidopsis*, RS2 in maize and PHAN in *Antirrhinum*). ARP proteins function as general repressors of *knox* gene expression to keep meristematic identity extinguished in young leaf primordia. Mutations in ARP genes result in ectopic *knox* expression in leaf primordia, although KNOX down-regulation in the P0 is not changed (Schneeberger et al., 1998; Waites et al., 1998; Timmermans et al., 1999; Theodoris et al., 2003). For example, null mutations in the *rs2* gene result in a defective blade-sheath boundary and is correlated with ectopic expression of *kn1*, *rough sheath1 (rs1)* and *liguless3 (lg3)* in maize leaf primordia (Schneeberger et al., 1998). Similarly, loss of AS1 function in *Arabidopsis* leads to ectopic expression of KNAT1, KNAT2 and KNAT6, indicating that the conserved ARP function is to keep knox genes in an "off" state during leaf development (Byrne et al., 2000; Byrne et al., 2002; Xu et al., 2003).

Leaves are produced from the SAM in a regular and predictable manner. Although the precise mechanisms controlling the timing and location of leaf initiation from the SAM remain elusive, several regulators are implicated in these processes. Auxin is a crucial player during leaf initiation and founder cell recruitment. Blocking polar auxin transport (PAT) either by mutation in the PINFORMED (PIN) class of auxin transporters, or by chemical inhibitors such as NPA, abolishes leaf initiation. Lateral organ formation can be restored in PIN mutants and NPA-arrested shoots via application of exogenous auxin (Reinhardt et al., 2003; Scanlon, 2003; Reinhardt, 2005). Moreover, auxin distribution in the shoot apex exhibits a gradient dynamic, with maximum accumulation at the incipient leaf primordium (Benkova et al., 2003; Tanaka et al., 2006). ABPHYL1 (ABPH1), a putative two-component response regulator, indirectly

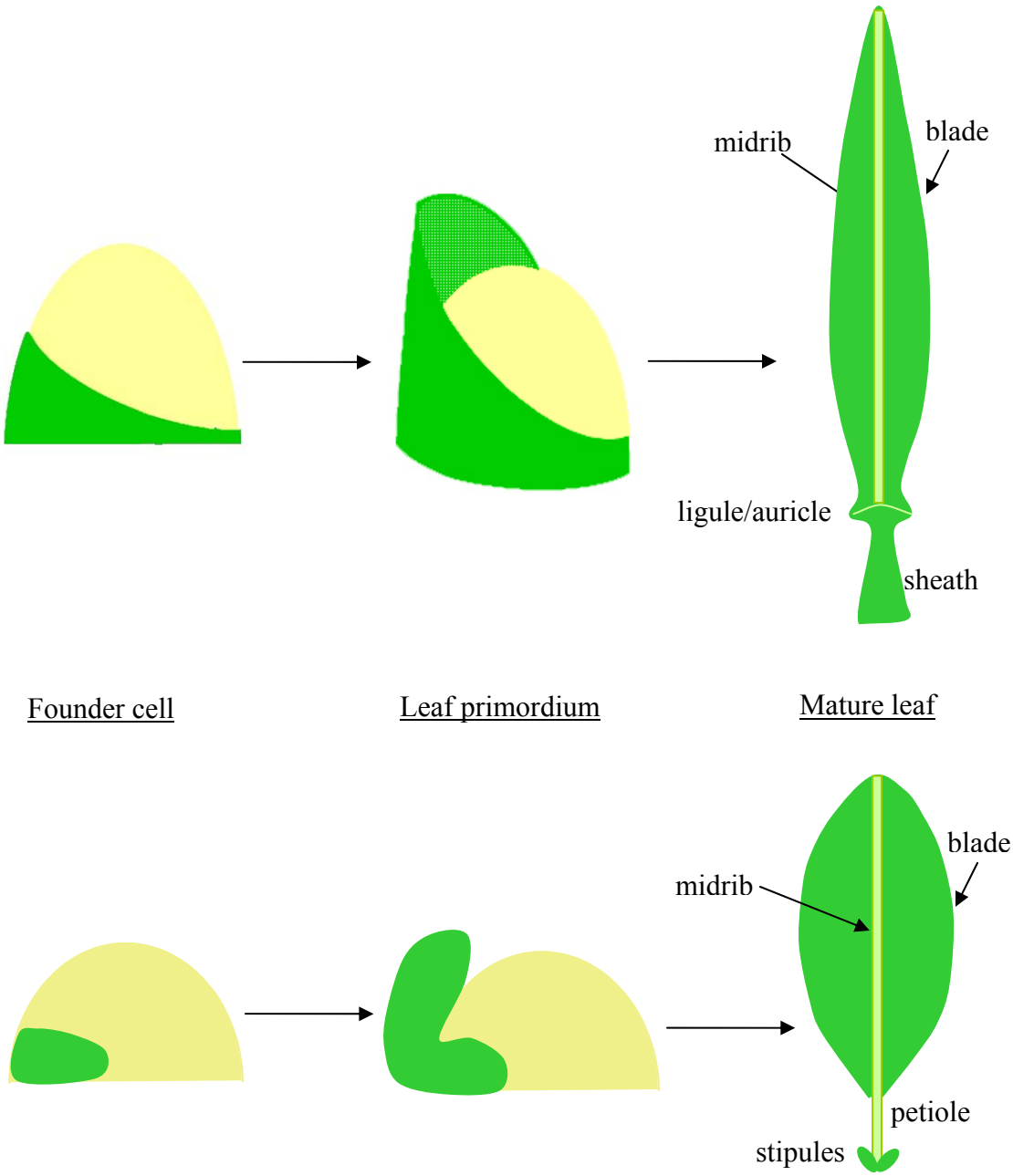

Figure 1.3 Cartoon of leaf development in a typical monocot (maize, top row) and eudicot (*Arabidopsis*, bottom row). Note that leaf founder cells (green) completely surround the shoot apical meristem (yellow) of maize, but not in *Arabidopsis*. A similar phenomenon is observed later in the disc of insertion of young leaf primordia and in the bases of mature leaves.

regulates leaf phyllotaxy by controlling SAM size in maize. Loss of ABPH1 function leads to an enlarged SAM and decussate phyllotaxy instead of distichous phyllotaxy. ABPH1 negatively regulates the CK-induced expansion of the SAM to limit the physical space for leaf initiation (Giulini et al., 2004). In addition, EXPANSINS, proteins that modulate cell wall extensibility, are also involved in the regulation of leaf formation. Local application of EXPANSINS induces leaf formation, and the *expansin* genes are upregulated at the site of new leaf initiation (Reinhardt et al., 1998; Pien et al., 2001). Further experiments are needed to clarify whether EXPANSINS are a cause or a consequence of leaf organogenesis from the SAM.

Leaf Patterning Occurs Along Three Axes to Produce Leaf Primordia

Concomitant with founder cell recruitment in maize, leaf patterning occurs along the proximodistal (length), mediolateral (width) and dorsiventral (height) axes to specify the three-dimensional polarized leaf primordium. Specification of the proximodistal axis requires the down-regulation of class I KNOX gene expression in developing leaves. *Knox* genes are expressed in the SAM, where they function to maintain meristematic identity by delaying the progression from cell proliferation to cell differentiation (Schneeberger et al., 1995; Schneeberger et al., 1998). Downregulation of *knox* genes in the leaf primordia ensures proper cell differentiation in the leaf tissue. Dominant gain of function in class I KNOX mutations, such as KNOTTED1 (KN1), ROUGH SHEATH1 (RS1), GNARLEY1 (GN1), LIGULELESS3 (LG3) and LIGULELESS4 (LG4), cause displacement of proximal sheath tissues into distal blade tissue and ectopic cell divisions (knots) in leaf tissues along the blade/sheath boundary (Smith et al., 1992; Sinha et al., 1993; Schneeberger et al., 1995; Muehlbauer et al., 1997; Foster et al., 1999; Muehlbauer et al., 1999; Bauer et al., 2004). RS2 functions to maintain KNOX gene expression in the "off" state within maize leaf primordia. Loss-of-function mutations in *rs2* display similar

proximodistal phenotype as observed in dominant, gain of function KNOX mutant plants (displacement of sheath into blade). RS2 is expressed uniformly within the developing leaf primordia and P0, but is excluded from the SAM proper (Timmermans et al., 1999; Tsiantis et al., 1999). Therefore, RS2 is a key regulator involved in maize leaf patterning along the proximodistal axis.

In addition, LIGULELESS1 (LG1) and LIGULELESS2 (LG2), which encode a SQUAMOSA PROMOTER-BINDING protein and a bZIP transcription factor, respectively, regulate differentiation along the proximodistal axis by specifying ligule and auricle formation in maize. The ligule and auricle together comprise a distinct boundary between the proximal sheath and the distal blade in the maize leaf (Emerson, 1912; Brink, 1933). Loss of LG1 or LG2 function leads to loss of the ligule and auricle, as well as a distal shift in the blade-sheath boundary (Emerson, 1912; Brink, 1933; Harper and Freeling, 1996; Moreno et al., 1997; Foster et al., 2004). Furthermore, a recently described dominant mutation, *Wavy auricle in blade (Wab1),* affects both proximodistal and mediolateral patterning in maize. Mutant plants exhibit displacement of auricle and sheath into the blade, as well as a narrower leaf blade. Double mutants of WAB and lg1 develop an extremely narrow leaf blade (Foster et al., 2004). Characterization of the *Wab1* gene product promises to shed more light on the regulation of leaf patterning along the mediolateral and proximodistal axes.

As for the specification of the mediolateral axis, the only well characterized regulators are the duplicate genes *narrow sheath1 (ns1)* and *narrow sheath2 (ns2)* in maize and their homologue PRESSED FLOWER (PRS) in *Arabidopsis* (Scanlon et al., 1996; Scanlon and Freeling, 1997; Scanlon, 2000; Matsumoto and Okada, 2001; Nardmann et al., 2004). Plants with recessive mutations at both *ns1* and *ns2* display narrow leaves due to a deletion of lateral and

marginal domains in the lower leaf. *ns1* and *ns2* encode duplicated WUSCHEL1-like homeobOX (WOX) transcription factors that are expressed at two lateral foci within the SAM . NS1 and NS2 function non-cell autonomously and redundantly to specify the recruitment of founder cells that give rise to this large lateral domain in mature maize leaves (Scanlon et al., 1996; Scanlon and Freeling, 1997; Scanlon, 2000; Nardmann et al., 2004). Our laser microdissection microarray analysis of gene expression in ns mutant and non-mutant SAMs (see chapter 3) implicates multiple hormonal (auxin and jasmonate) and other signaling pathways to function in NS-mediated founder cell recruitment mediolateral patterning. Moreover, our work suggests conserved WOX gene functions during the repression of two-component signaling pathways as well as the transcriptional activation of sugar-binding lectin genes.

Leaf patterning along the dorsiventral axis has been extensively characterized in a number of plant species. The dorsal (adaxial) side of the leaf refers to the top surface that is located closer to the SAM, whereas the ventral side of leaf is the bottom surface that is further away from the SAM. The anatomy of vascular bundles is also polarized, in that xylem is typically adaxial and phloem is abaxial. Mutant studies in maize, *Arabidopsis*, snapdragon and tomato have contributed to a model wherein juxtaposition of adaxial and abaxial developmental fields generates a positional signal that specifies patterning and expansion along the mediolateral and proximodistal axes of the leaf, thereby enabling lateral growth and margin development (Waites and Hudson, 1995; Eshed et al., 2001; Hudson, 2001; Bowman et al., 2002). Loss of either adaxial or abaxial identity causes a partial or completely filamentous leaf phenotype that is defective in lateral expansion (Waites et al., 1998; Siegfried et al., 1999; Timmermans et al., 1999; Tsiantis et al., 1999; Eshed et al., 2001; Kerstetter et al., 2001; McConnell et al., 2001). The determinants for adaxial identity are HD-ZIPIII family genes, which include PHABULOSA

(PHB), PHAVOLUTA (PHV) and REVOLUTA (REV) in *Arabidopsis*, and the REV orthologue ROLLED LEAF1(RLD1) in maize. HD-ZIPIII genes are expressed in the adaxial side of developing leaf primordia, within the xylem, and in the central zone of the meristem. HD-ZIPIII genes function to specify adaxial identity during leaf development. Gain-of-function mutation in HD-ZIPIII genes cause adaxialized leaves and enlarged meristems, whereas triple mutant constructs of recessive mutations in PHB, PHV, and REV result in abaxialized cotyledons and meristem arrest. These phenotypes support the proposed function of HD-ZIPIII genes during adaxial patterning and identity, and likewise reveal a requirement for adaxial identity in the maintenance of SAM cell fate (McConnell et al., 2001; Otsuga et al., 2001; Bowman et al., 2002; Emery et al., 2003; Prigge et al., 2005). HD-ZIPIII genes are mutually antagonistic to members of the KANADI (KAN) gene family, GARP transcription factors which promote abaxial identity (Figure 1.4). Comprised of four genes in *Arabidospis,* three members (KAN1, KAN2 and KAN3) are expressed in the abaxial side of leaf primordia and in the phloem of *Arabidopsis* vascular bundles. KAN genes also negatively regulate HD-ZIPIII expression, thereby promoting abaxial identity. Loss-of-function mutations in *kan1 kan2* double mutants lead to adaxialized leaves, whereas gain-of-function mutations in KAN genes cause abaxialized leaves and meristem arrest (Kerstetter et al., 2001; Emery et al., 2003; Eshed et al., 2004). HD-ZIPIII gene expression is also regulated by microRNA pathways; HD-ZIPIII transcripts are targeted for destruction by the miR166/5 class of plant microRNAs. Mature miR166/5 transcripts accumulate on the abaxial side of leaf primordia to restrict HD-ZIPIII expression domain to adaxial domains. Therefore, mutations in genes involved in the microRNA biosynthesis pathway, such as DICER-LIKE1 (DCL1), the pre-miRNA processor SERRATE (SE), and ARGONAUTE1 (AGO1), display

defects in leaf dorsiventrality via perturbation of the miR166/HD-ZIPIII pathway (Kidner and Martienssen, 2004; Baumberger and Baulcombe, 2005; Grigg et al., 2005; Williams et al., 2005).

Two genetic pathways are known to function redundantly to regulate the dorsiventral identity genes and thus leaf polarity. One is the plant-specific trans-acting small interfering RNA (ta-siRNA) pathway (purple in Figure 1.4), and the other is the ARP pathway (red in Figure 1.4). ta-siRNA promotes adaxial identity by targeting the destruction of mRNA transcripts of the abaxial determinants AUXIN RESPONSE FACTOR 3 (ARF3) and ARF4. ARF3 is expressed throughout the meristem and the leaf primordia, and ARF4 is expressed in the abaxial side of leaf primordia and in phloem. Loss of ARF3/ARF4 function in double mutants of *Arabidopsis* causes abaxialized leaf phenotypes (Pekker et al., 2005). Multiple components are involved in the ta3-siRNA biogenesis pathway, which is conserved in maize and *Arabidopsis*. ta3-siRNAs originate from the TAS3 precursor gene, whose transcripts are targeted for cleavage by miRNA390. The resultant TAS3 cleavage fragments are then converted into double strand RNAs via the activity of RNA-dependent RNA polymerase (RDR6) and the zinc-finger protein SUPPRESSOR OF GENE SILENCING3 (SGS3). These double stranded RNAs are subsequently recognized by dsRNA-BINDING PROTEIN4 (DRB4) and processed by DICER-LIKE4 (DCL4) into 21 base-pair (bp) ta-siRNAs. Finally, the ta-siRNAs mediates the cleavage of ARF3/ARF4 transcripts in an ARGONAUTE7 (AGO7)-dependent manner (Peragine et al., 2004; Allen et al., 2005; Gasciolli et al., 2005; Vaucheret, 2005; Yoshikawa et al., 2005; Adenot et al., 2006; Hunter et al., 2006; Nakazawa et al., 2007; Nogueira et al., 2007). Interestingly, mutant phenotypes vary among different components of the ta-siRNA pathway, and among or even the same component in different species. For example, null mutations of RDR6, SGS3, or

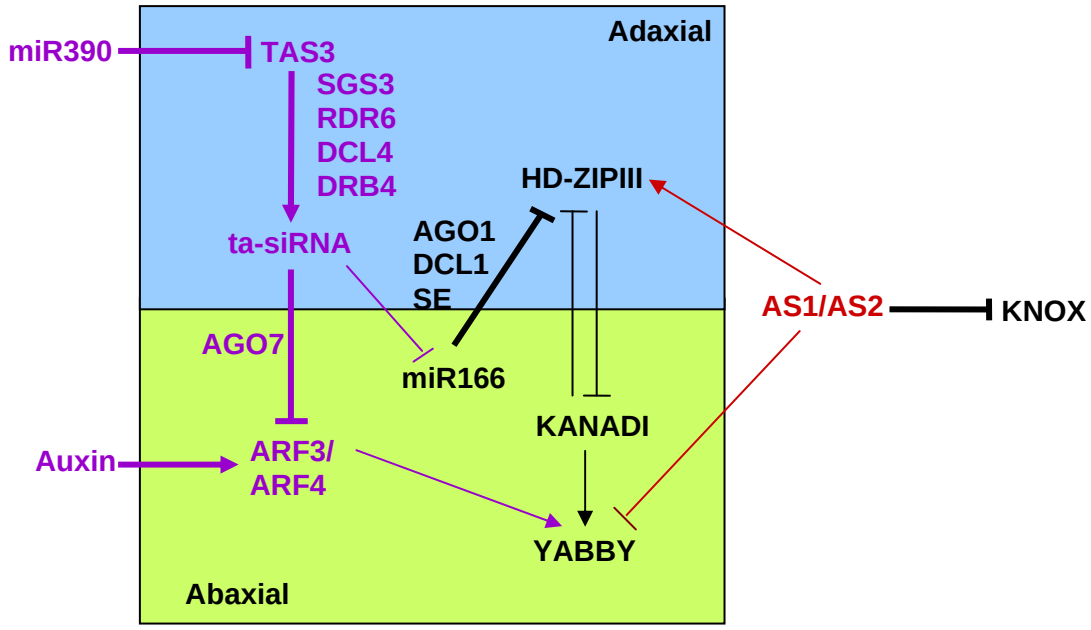

Figure 1.4 Genetic pathways regulating leaf dorsiventrality in *Arabidopsis.* HD-ZIPIII and KANADI genes are adaxial and abaxial identity determinants, respectively, that act via mutually antagonism to demarcate adaxial and abaxial cell fate. miR166 promotes adaxial identity by targeting HD-ZIPIII transcripts for destruction. AGO1, DCL1 and SE regulate the biogenesis or function of miR166 by an as-yet undetermined mechanism. The ta3-siRNA pathway (shown as purple) regulates dorsiventrality by targeting the abaxial-promoting genes ARF3/ARF4 for cleavage and thereby repressing further downstream expression of YABBY. SGS3, RDR6, DCL4 and DRB4 control the biogenesis of ta-siRNA, whereas AGO7 regulates the ta-siRNA-mediated cleavage of target transcripts. The ARP pathway (shown as red) activates HD-ZIPIII expression and represses transcription of YABBY, thereby affecting adaxial-abaxial polarity. The conserved ARP function is to repress KNOX expression in leaf primordia [Redrawn and modified from Kidner and Timmermans, 2007].

DCL4 result in no apparent leaf dorsiventrality defect in *Arabidopsis*, whereas mutation in AGO7 or DRB4 cause leaf morphology defects (Adenot et al., 2006; Fahlgren et al., 2006). Loss-of-function mutations in the maize SGS3 orthologue LEAF BLADELESS1 (LBL1) lead to thread-like abaxialized leaves, accompanied with the up-regulation of miR166 and downregulation of HD-ZIPIII transcripts (Nogueira et al., 2007). Orthologous mutations in the *Arabidopsis* gene have no apparent effect on leaf polarity, but result instead in defects in juvenile-to-adult phase change (Peragine et al., 2004). These phenotypic discrepancies observed between sgs3 mutants in maize and *Arabidopsis* may be partly due to various redundancies during the ta-siRNA biogenesis pathways, complimentary functions of the ta-siRNA pathway and the ARP pathway in promoting leaf polarity, and differential redundancies of these pathways in different species. In *Arabidopsis*, the ta-siRNA pathway and ARP pathway are antagonistic in the regulation of abaxial-promoting genes YABBY (Figure 1.4) (Chitwood et al., 2007; Kidner and Timmermans, 2007), whereas in maize the YABBY genes are expressed adaxially (Juarez et al., 2004).

ARP refers to the MYB transcription factor genes that negatively regulate KNOX gene expression (AS1 in *Arabidopsis*, RS2 in maize and PHAN in *Antirrhinum*). ARP genes are expressed uniformly within the developing leaf primordia and P0, but are excluded from the SAM proper (Waites and Hudson, 1995; Waites et al., 1998; Timmermans et al., 1999; Tsiantis et al., 1999; Byrne et al., 2000; Xu et al., 2003). First identified by mutant phenotypes in *Antirrhinum*, PHAN was also the first gene shown to affect leaf dorsiventrality. Null mutations in PHAN result in partially or completely abaxialized leaves in *Antirrhinum* , however loss- or gain-of-function of AS1 or RS2 cause no leaf dorsiventrality defects in *Arabidopsis* or maize, respectively (Waites and Hudson, 1995; Waites et al., 1998; Timmermans et al., 1999; Tsiantis et

al., 1999; Byrne et al., 2000; Iwakawa et al., 2002; Theodoris et al., 2003; Xu et al., 2003). However, overexpression of *as2*, which encodes a LOB transcription factor that acts a protein partner of AS1 in *Arabidopsis*, results in adaxialized leaves; this phenotype is dependent on AS1 function (Iwakawa et al., 2002; Lin et al., 2003). Solo mutations in either as1 or as2 in an *erecta (er)* background leads to increased accumulation of miR166/5 and partial loss of adaxial identity (Lin et al., 2003; Xu et al., 2003; Li et al., 2005). These data reveal that AS1 and AS2 also function to repress abaxial identity in *Arabidopsis*. The consistent and conserved ARP function that is shared in all species thus examined is the repression of *knox* gene expression in lateral organs, thereby delimiting *knox* transcripts to the SAM (Figure 1.4) (Waites et al., 1998; Timmermans et al., 1999; Tsiantis et al., 1999; Theodoris et al., 2003). The non-uniformity observed in ARP mutant phenotypes of maize, *Arabidopsis* and *Antirrhinum* may result from the various redundancies in dorsiventral patterning pathways inherent in particular species.

Members of the YABBY family, which include FILAMENTOUS FLOWER (FIL), YABBY2 and YABBY3 in *Arabidopsis*, are described to promote abaxial fate further downstream of the KANADI pathway (Figure 1.4) (Kidner and Timmermans, 2007). YABBYs are expressed in the abaxial side of *Arabidopsis* leaf primordia and in regions of laminar outgrowth. Recessive mutations in both fil and yab3 combine to condition adaxialized leaves and suppress outgrowth of ectopic lamina in kan1 kan2 mutant plants. Overexpression of YABBYs causes abaxialized leaves in *Arabidopsis* (Siegfried et al., 1999; Bowman, 2000; Kumaran et al., 2002; Eshed et al., 2004). GRAMINIFOLIA (GRAM) and PROLONGATA (PROL), YABBY orthologues in *Antirrhinum*, are abaxially expressed in leaf primordia and regulate leaf polarity by either promoting or repressing adaxial identity through distinct signaling pathways (Golz et al., 2004; Navarro et al., 2004). However, the role of YABBYs in abaxial fate specification is not

conserved. For example, ZmYABBY9 (ZYB9) and ZmYABBY14 (ZYB14), YABBY orthologues in maize, are expressed in the adaxial domain of leaf primordia where they probably function to direct lateral outgrowth instead of dorsiventrality (Juarez et al., 2004).

Tissue-Specific Expression Profiling via Laser Microdissection Microarray

Ever since 1995, microarrays have become one of the most effective and routine high-throughput transcript profiling technologies (Aharoni and Vorst, 2002; Imbeaud and Auffray, 2005). Microarray technology is a hybridization-based method which permits expression analyses of many thousands of genes in a single experiment (Schena et al., 1995; Richmond and Somerville, 2000; Aharoni and Vorst, 2002). The basis of the microarray assay is the specific hybridization of fluorescently-labeled cDNA probes and gene-specific DNA targets immobilized on the array. Microarray hybridizations enable the spatial separation of specific targets on the array so that precise quantification of hybridized fluorescent probe can be measured. Two distinct microarray platforms predominate. One format is on-slide-synthesis arrays and the second is the spotted array. The former includes short oligonucleotide (25-30 base) arrays that synthesize probes *in situ* by photolithographic methods, whereas the latter includes cDNA arrays and long oligonucleotide arrays, in which either cDNA fragments of variable length or 50-70 oligonucleotide base pairs, are presynthesized and spotted on the surface of a solid matrix (Heller, 2002; Rensink and Buell, 2005). Compared to cDNA arrays, oligonucleotide arrays have the advantage of reducing cross-hybridization between gene family members with significant sequence similarity, as well as a more uniform melting temperature (Duggan et al., 1999; Lipshutz et al., 1999; Aharoni and Vorst, 2002; Zhao and Bruce, 2003; Hardiman, 2004; Galbraith and Birnbaum, 2006).

The typical microarray experiment contains 39 key steps, and includes growth of multiple biological replicate samples under controlled conditions, array and sample preparation, hybridization and washing, data analyses and normalization, and data storage (Forster et al., 2003; Czechowski et al., 2004; Shippy et al., 2004; Imbeaud and Auffray, 2005; Draghici et al., 2006). Microarray sensitivity refers to the minimum number of copies of a specific mRNA that is required for accurate detection in a microarray measurement. For current microarray technology, the sensitivity is between one to ten copies of mRNA per cell (Draghici et al., 2006). Long cDNA arrays tend to perform with higher sensitivity, although their performance is somewhat compromised by lower gene-specificity. In terms of accuracy, microarrays can detect expression changes for 70-90% of the all genes expressed above the sensitivity threshold. Measurement of expression ratios in cDNA arrays is more accurate than measures of absolute expression in oligonucleotide arrays (Czechowski et al., 2004; Shippy et al., 2004). Reproducibility defines the degree to which repeated measurements give rise to the same or similar results. The reproducibility of technical replicates in published microarray experiments varies from 0.5 to 0.95 of the Pearson correlation coefficient (Jenssen et al., 2002; Handley et al., 2004; Bammler et al., 2005; Draghici et al., 2006). In addition, cross-hybridization and alternate splicing may greatly obscure the accuracy and reproducibility of microarrray measurement (Modrek et al., 2001; Zhang et al., 2005).

Microarray analyses require the input of 2-4 μg of RNA typically derived from whole organs and large tissue volumes, which effectively obscures the specific contributions of small tissues and single cell types (Lipshutz et al., 1999; Schnable et al., 2004). Laser microdissection (LM) is a new and powerful tool to harvest selected cells from complex tissues and organs (Kamme et al., 2004; Schnable et al., 2004; Nelson et al., 2006a, b)). There are two major ways

to isolate specific cells or regions from complex tissue sections. One procedure is termed "laser capture" and the other is "laser excision". Laser capture procedures harvest target cells in a “melt-stick-pull off” manner, in which a pulsed infrared laser melts a thermoplastic film overlaying the tissue. The melted film sticks to the cells of interest, which are then pulled off and extracted away from the original sample. Laser excision, on the other hand, harvests targeted cells in a cut-and-remove strategy. In this technique a UV laser cuts and destroys tissues surrounding the targeted cells, which are then isolated laser-mediated pressure catapulting (Kerk et al., 2003; Day et al., 2005; Klink et al., 2005; Cai and Lashbrook, 2006; Nelson et al., 2006a). Cells harvested by laser microdissection can be used for subsequent cell-specific analyses of DNA, RNA, protein or metabolites (Scutt et al., 1997; Kerk et al., 2003; Schad et al., 2005b; Schad et al., 2005a; Nelson et al., 2006a). For use in microarray profiling of specialized cell types, the combined use of laser microdissection with a linear, T7-based RNA amplification has been developed and widely-used in mammalian systems (Emmert-Buck et al., 1996; Kamme et al., 2004). Despite the peculiarities of plant cell structure (especially the rigid cell wall and large vacuoles), laser microdissection-microarray technology has been successfully applied to global expression analyses of maize vascular and epidermal tissues, maize roots, as well as *Arabidopsis* embryos, and floral organs (Nakazono et al., 2003; Casson et al., 2005; Woll et al., 2005; Cai and Lashbrook, 2006; Spencer et al., 2007). The combined use of laser microdissection and microarray technologies enables comparative analyses of discrete developmental fields while eliminating the transcriptional noise contributed by multiple tissues and downstream developmental events (Schnable et al., 2004).

Purpose of Study

In order to better understand the genetic mechanisms involved in leaf founder cell recruitment and leaf patterning along the mediolateral and dorsiventral axes, we performed SAM-specific transcript profiling analyses of two maize leaf developmental mutants, narrow sheath1 (ns1) and ragged seedling2 (rgd2), by laser microdissection microarray. The identified candidate genes were further characterized by quantitative real time RT-PCR, tissue-specific qRT-PCR and/or *in situ* hybridization. Subsequent reverse genetic analyses of selected differentially-expressed genes are in progress, in order to determine their role during SAM function and/or maize leaf development.

Chapter three of this dissertation, which has been published in PLoS Genetics, presents the data from our analyses of ns1. Our data illustrate the utility of laser microdissection microarray analyses to identify a relatively small number of genes that are differentially expressed within the SAM. Moreover, our analyses indicated that genes predicted to be involved in hormonal transport and signaling, signal transduction, and growth are especially implicated during NS-mediated leaf founder cell recruitment and mediolateral axis specification. Finally, potentially conserved WOX gene functions during the regulation of two component response pathways and of jasmonate-induced gene expression are identified.

Chapter Four of this dissertation presents the data from our rgd2 LMM experiment. RGD2 is an unknown gene product that is required for lateral expansion and dorsiventral patterning in maize leaf development. Our data identified putative transcription factors, chromatin remodeling genes, signal transduction components, genes involved in proteolysis and protein fate, as well as unknown predicted function as differentially expressed in the rgd2-R mutant SAMs. Moreover, our data suggest that RGD2 may function in the ARP pathway or via

an undescribed proteolytic pathway to coordinate dorsiventral patterning and mediolateral growth during maize leaf development.

Chapter Five summarizes and discusses the work from both part A (cell biology) and part B (leaf development).

REFERENCES

Adenot, X., Elmayan, T., Lauressergues, D., Boutet, S., Bouche, N., Gasciolli, V., and Vaucheret, H. (2006). DRB4-dependent TAS3 trans-acting siRNAs control leaf morphology through AGO7. Curr Biol **16,** 927-932.

Aharoni, A., and Vorst, O. (2002). DNA microarrays for functional plant genomics. Plant Mol Biol **48,** 99-118.

Allen, E., Xie, Z., Gustafson, A.M., and Carrington, J.C. (2005). microRNA-directed phasing during trans-acting siRNA biogenesis in plants. Cell **121,** 207-221.

Amor, D.J., Kalitsis, P., Sumer, H., and Choo, K.H. (2004). Building the centromere: from foundation proteins to 3D organization. Trends Cell Biol **14,** 359-368.

Bammler, T., Beyer, R.P., Bhattacharya, S., Boorman, G.A., Boyles, A., Bradford, B.U., Bumgarner, R.E., Bushel, P.R., Chaturvedi, K., Choi, D., Cunningham, M.L., Deng, S., Dressman, H.K., Fannin, R.D., Farin, F.M., Freedman, J.H., Fry, R.C., Harper, A., Humble, M.C., Hurban, P., Kavanagh, T.J., Kaufmann, W.K., Kerr, K.F., Jing, L., Lapidus, J.A., Lasarev, M.R., Li, J., Li, Y.J., Lobenhofer, E.K., Lu, X., Malek, R.L., Milton, S., Nagalla, S.R., O'Malley J, P., Palmer, V.S., Pattee, P., Paules, R.S., Perou, C.M., Phillips, K., Qin, L.X., Qiu, Y., Quigley, S.D., Rodland, M., Rusyn, I., Samson, L.D., Schwartz, D.A., Shi, Y., Shin, J.L., Sieber, S.O., Slifer, S., Speer, M.C., Spencer, P.S., Sproles, D.I., Swenberg, J.A., Suk, W.A., Sullivan, R.C., Tian, R., Tennant, R.W., Todd, S.A., Tucker, C.J., Van Houten, B., Weis, B.K., Xuan, S., and Zarbl, H. (2005). Standardizing global gene expression analysis between laboratories and across platforms. Nat Methods **2,** 351-356.

Barratt, M.J., Hazzalin, C.A., Cano, E., and Mahadevan, L.C. (1994). Mitogen-stimulated phosphorylation of histone H3 is targeted to a small hyperacetylation-sensitive fraction. Proc Natl Acad Sci U S A **91,** 4781-4785.

Barton, M.K., and Poethig, R.S. (1993). Formation of the shoot apical meristem in *Arabidopsis thaliana*: An analysis of development in the wild type and in the shoot meristemless mutant Development **119,** 823-831.

Bauer, P., Lubkowitz, M., Tyers, R., Nemoto, K., Meeley, R.B., Goff, S.A., and Freeling, M. (2004). Regulation and a conserved intron sequence of liguleless3/4 knox class-I homeobox genes in grasses. Planta **219,** 359-368.

Baumberger, N., and Baulcombe, D.C. (2005). *Arabidopsis* ARGONAUTE1 is an RNA Slicer that selectively recruits microRNAs and short interfering RNAs. Proc Natl Acad Sci U S A **102,** 11928-11933.

Benkova, E., Michniewicz, M., Sauer, M., Teichmann, T., Seifertova, D., Jurgens, G., and Friml, J. (2003). Local, efflux-dependent auxin gradients as a common module for plant organ formation. Cell **115,** 591-602.

Bernard, P., Maure, J.F., Partridge, J.F., Genier, S., Javerzat, J.P., and Allshire, R.C. (2001). Requirement of heterochromatin for cohesion at centromeres. Science **294,** 2539-2542.

Bowman, J.L. (2000). The YABBY gene family and abaxial cell fate. Curr Opin Plant Biol **3,** 17-22.

Bowman, J.L., Eshed, Y., and Baum, S.F. (2002). Establishment of polarity in angiosperm lateral organs. Trends Genet **18,** 134-141.

Brand, U., Fletcher, J.C., Hobe, M., Meyerowitz, E.M., and Simon, R. (2000). Dependence of stem cell fate in *Arabidopsis* on a feedback loop regulated by CLV3 activity. Science **289,** 617-619.

Brink, R.A. (1933). Heritable characters in maize XLVI – *liguleless2*. J. Hered **24,** 325 -326.

Brinkley, B.R., and Stubblefield, E. (1966). The fine structure of the kinetochore of a mammalian cell in vitro. Chromosoma **19,** 28-43.

Byrne, M., Timmermans, M., Kidner, C., and Martienssen, R. (2001). Development of leaf shape. Curr Opin Plant Biol **4,** 38-43.

Byrne, M.E., Simorowski, J., and Martienssen, R.A. (2002). ASYMMETRIC LEAVES1 reveals knox gene redundancy in *Arabidopsis*. Development **129,** 1957-1965.

Byrne, M.E., Barley, R., Curtis, M., Arroyo, J.M., Dunham, M., Hudson, A., and Martienssen, R.A. (2000). Asymmetric leaves1 mediates leaf patterning and stem cell function in *Arabidopsis*. Nature **408,** 967-971.

Cai, S., and Lashbrook, C.C. (2006). Laser capture microdissection of plant cells from tape-transferred paraffin sections promotes recovery of structurally intact RNA for global gene profiling. Plant J **48,** 628-637.

Carles, C.C., Lertpiriyapong, K., Reville, K., and Fletcher, J.C. (2004). The ULTRAPETALA1 gene functions early in *Arabidopsis* development to restrict shoot apical meristem activity and acts through WUSCHEL to regulate floral meristem determinacy. Genetics **167,** 1893-1903.

Carles, C.C., Choffnes-Inada, D., Reville, K., Lertpiriyapong, K., and Fletcher, J.C. (2005). ULTRAPETALA1 encodes a SAND domain putative transcriptional regulator that controls shoot and floral meristem activity in *Arabidopsis*. Development **132,** 897-911.

Casson, S., Spencer, M., Walker, K., and Lindsey, K. (2005). Laser capture microdissection for the analysis of gene expression during embryogenesis of *Arabidopsis*. Plant J **42,** 111-123.

Chan, G.K., and Yen, T.J. (2003). The mitotic checkpoint: a signaling pathway that allows a single unattached kinetochore to inhibit mitotic exit. Prog Cell Cycle Res **5,** 431-439.

Cheeseman, I.M., Drubin, D.G., and Barnes, G. (2002). Simple centromere, complex kinetochore: linking spindle microtubules and centromeric DNA in budding yeast. J Cell Biol **157,** 199-203.

Chen, R.H., Waters, J.C., Salmon, E.D., and Murray, A.W. (1996). Association of spindle assembly checkpoint component XMAD2 with unattached kinetochores. Science **274,** 242-246.

Chitwood, D.H., Guo, M., Nogueira, F.T., and Timmermans, M.C. (2007). Establishing leaf polarity: the role of small RNAs and positional signals in the shoot apex. Development **134,** 813-823.

Choo, K.H. (2001). Domain organization at the centromere and neocentromere. Dev Cell **1,** 165-177.

Chuck, G., Lincoln, C., and Hake, S. (1996). KNAT1 induces lobed leaves with ectopic meristems when overexpressed in *Arabidopsis*. Plant Cell **8,** 1277-1289.

Clark, S.E., Williams, R.W., and Meyerowitz, E.M. (1997). The CLAVATA1 gene encodes a putative receptor kinase that controls shoot and floral meristem size in *Arabidopsis*. Cell **89,** 575-585.

Clark, S.E., Jacobsen, S.E., Levin, J.Z., and Meyerowitz, E.M. (1996). The CLAVATA and SHOOT MERISTEMLESS loci competitively regulate meristem activity in *Arabidopsis*. Development **122,** 1567-1575.

Clayton, A.L., and Mahadevan, L.C. (2003). MAP kinase-mediated phosphoacetylation of histone H3 and inducible gene regulation. FEBS Lett **546,** 51-58.

Cleveland, D.W., Mao, Y., and Sullivan, K.F. (2003). Centromeres and kinetochores: from epigenetics to mitotic checkpoint signaling. Cell **112,** 407-421.

Craig, J.M., Earnshaw, W.C., and Vagnarelli, P. (1999). Mammalian centromeres: DNA sequence, protein composition, and role in cell cycle progression. Exp Cell Res **246,** 249-262.

Crosio, C., Fimia, G.M., Loury, R., Kimura, M., Okano, Y., Zhou, H., Sen, S., Allis, C.D., and Sassone-Corsi, P. (2002). Mitotic phosphorylation of histone H3: spatio-temporal regulation by mammalian Aurora kinases. Mol Cell Biol **22,** 874-885.

Czechowski, T., Bari, R.P., Stitt, M., Scheible, W.R., and Udvardi, M.K. (2004). Real-time RT-PCR profiling of over 1400 *Arabidopsis* transcription factors: unprecedented sensitivity reveals novel root- and shoot-specific genes. Plant J **38,** 366-379.

Dai, J., and Higgins, J.M. (2005). Haspin: a mitotic histone kinase required for metaphase chromosome alignment. Cell Cycle **4,** 665-668.

Dai, J., Sultan, S., Taylor, S.S., and Higgins, J.M. (2005). The kinase haspin is required for mitotic histone H3 Thr 3 phosphorylation and normal metaphase chromosome alignment. Genes Dev **19,** 472-488.

Dawe, R.K., and Henikoff, S. (2006). Centromeres put epigenetics in the driver's seat. Trends Biochem Sci **31,** 662-669.

Day, R.C., Grossniklaus, U., and Macknight, R.C. (2005). Be more specific! Laser-assisted microdissection of plant cells. Trends Plant Sci **10,** 397-406.

de la Barre, A.E., Gerson, V., Gout, S., Creaven, M., Allis, C.D., and Dimitrov, S. (2000). Core histone N-termini play an essential role in mitotic chromosome condensation. Embo J **19,** 379-391.

DeManno, D.A., Cottom, J.E., Kline, M.P., Peters, C.A., Maizels, E.T., and Hunzicker-Dunn, M. (1999). Follicle-stimulating hormone promotes histone H3 phosphorylation on serine-10. Mol Endocrinol **13,** 91-105.

Demidov, D., Van Damme, D., Geelen, D., Blattner, F.R., and Houben, A. (2005). Identification and dynamics of two classes of aurora-like kinases in *Arabidopsis* and other plants. Plant Cell **17,** 836-848.

Draghici, S., Khatri, P., Eklund, A.C., and Szallasi, Z. (2006). Reliability and reproducibility issues in DNA microarray measurements. Trends Genet **22,** 101-109.

Draviam, V.M., Xie, S., and Sorger, P.K. (2004). Chromosome segregation and genomic stability. Curr Opin Genet Dev **14,** 120-125.

Duggan, D.J., Bittner, M., Chen, Y., Meltzer, P., and Trent, J.M. (1999). Expression profiling using cDNA microarrays. Nat Genet **21,** 10-14.

Emerson, R.A. (1912). The inheritance of the ligule and auricles of corn leaves. *Nebraska Agricultural Experimental Station Annual Report* **25,** 81-88.

Emery, J.F., Floyd, S.K., Alvarez, J., Eshed, Y., Hawker, N.P., Izhaki, A., Baum, S.F., and Bowman, J.L. (2003). Radial patterning of *Arabidopsis* shoots by class III HD-ZIP and KANADI genes. Curr Biol **13,** 1768-1774.

Emmert-Buck, M.R., Bonner, R.F., Smith, P.D., Chuaqui, R.F., Zhuang, Z., Goldstein, S.R., Weiss, R.A., and Liotta, L.A. (1996). Laser capture microdissection. Science **274,** 998-1001.

Eshed, Y., Baum, S.F., Perea, J.V., and Bowman, J.L. (2001). Establishment of polarity in lateral organs of plants. Curr Biol **11,** 1251-1260.

Eshed, Y., Izhaki, A., Baum, S.F., Floyd, S.K., and Bowman, J.L. (2004). Asymmetric leaf development and blade expansion in *Arabidopsis* are mediated by KANADI and YABBY activities. Development **131,** 2997-3006.

Fahlgren, N., Montgomery, T.A., Howell, M.D., Allen, E., Dvorak, S.K., Alexander, A.L., and Carrington, J.C. (2006). Regulation of AUXIN RESPONSE FACTOR3 by TAS3 ta-siRNA affects developmental timing and patterning in *Arabidopsis*. Curr Biol **16,** 939-944.

Farrona, S., Hurtado, L., Bowman, J.L., and Reyes, J.C. (2004). The *Arabidopsis thaliana* SNF2 homolog AtBRM controls shoot development and flowering. Development **131,** 4965-4975.

Fischle, W., Wang, Y., and Allis, C.D. (2003). Binary switches and modification cassettes in histone biology and beyond. Nature **425,** 475-479.

Fleming, A.J. (2006). Leaf initiation: the integration of growth and cell division. Plant Mol Biol **60,** 905-914.

Forster, T., Roy, D., and Ghazal, P. (2003). Experiments using microarray technology: limitations and standard operating procedures. J Endocrinol **178,** 195-204.

Foster, T., Hay, A., Johnston, R., and Hake, S. (2004). The establishment of axial patterning in the maize leaf. Development **131,** 3921-3929.

Foster, T., Yamaguchi, J., Wong, B.C., Veit, B., and Hake, S. (1999). Gnarley1 is a dominant mutation in the knox4 homeobox gene affecting cell shape and identity. Plant Cell **11,** 1239-1252.

Francis, D., and Halford, N.G. (2006). Nutrient sensing in plant meristems. Plant Mol Biol **60,** 981-993.

Fuchs, J., Demidov, D., Houben, A., and Schubert, I. (2006). Chromosomal histone modification patterns--from conservation to diversity. Trends Plant Sci **11,** 199-208.

Fukagawa, T. (2004). Centromere DNA, proteins and kinetochore assembly in vertebrate cells. Chromosome Res **12,** 557-567.

Fukagawa, T., Pendon, C., Morris, J., and Brown, W. (1999). CENP-C is necessary but not sufficient to induce formation of a functional centromere. Embo J **18,** 4196-4209.

Fukagawa, T., Mikami, Y., Nishihashi, A., Regnier, V., Haraguchi, T., Hiraoka, Y., Sugata, N., Todokoro, K., Brown, W., and Ikemura, T. (2001). CENP-H, a constitutive centromere component, is required for centromere targeting of CENP-C in vertebrate cells. Embo J **20,** 4603-4617.

Galbraith, D.W., and Birnbaum, K. (2006). Global studies of cell type-specific gene expression in plants. Annu Rev Plant Biol **57,** 451-475.

Gallois, J.L., Woodward, C., Reddy, G.V., and Sablowski, R. (2002). Combined SHOOT MERISTEMLESS and WUSCHEL trigger ectopic organogenesis in *Arabidopsis*. Development **129,** 3207-3217.

Gasciolli, V., Mallory, A.C., Bartel, D.P., and Vaucheret, H. (2005). Partially redundant functions of *Arabidopsis* DICER-like enzymes and a role for DCL4 in producing trans-acting siRNAs. Curr Biol **15,** 1494-1500.

Gernand, D., Demidov, D., and Houben, A. (2003). The temporal and spatial pattern of histone H3 phosphorylation at serine 28 and serine 10 is similar in plants but differs between mono- and polycentric chromosomes. Cytogenet Genome Res **101,** 172-176.

Giet, R., and Glover, D.M. (2001). Drosophila aurora B kinase is required for histone H3 phosphorylation and condensin recruitment during chromosome condensation and to organize the central spindle during cytokinesis. J Cell Biol **152,** 669-682.

Giulini, A., Wang, J., and Jackson, D. (2004). Control of phyllotaxy by the cytokinin-inducible response regulator homologue ABPHYL1. Nature **430,** 1031-1034.

Golz, J.F., Roccaro, M., Kuzoff, R., and Hudson, A. (2004). GRAMINIFOLIA promotes growth and polarity of Antirrhinum leaves. Development **131,** 3661-3670.

Goto, H., Yasui, Y., Nigg, E.A., and Inagaki, M. (2002). Aurora-B phosphorylates Histone H3 at serine28 with regard to the mitotic chromosome condensation. Genes Cells **7,** 11-17.

Goto, H., Tomono, Y., Ajiro, K., Kosako, H., Fujita, M., Sakurai, M., Okawa, K., Iwamatsu, A., Okigaki, T., Takahashi, T., and Inagaki, M. (1999). Identification of a novel phosphorylation site on histone H3 coupled with mitotic chromosome condensation. J Biol Chem **274,** 25543-25549.

Grigg, S.P., Canales, C., Hay, A., and Tsiantis, M. (2005). SERRATE coordinates shoot meristem function and leaf axial patterning in *Arabidopsis*. Nature **437,** 1022-1026.

Handley, D., Serban, N., Peters, D.G., and Glymour, C. (2004). Concerns about unreliable data from spotted cDNA microarrays due to cross-hybridization and sequence errors. Stat Appl Genet Mol Biol **3,** Article25.

Hardiman, G. (2004). Microarray platforms--comparisons and contrasts. Pharmacogenomics **5,** 487-502.

Harper, L., and Freeling, M. (1996). Interactions of liguleless1 and liguleless2 function during ligule induction in maize. Genetics **144,** 1871-1882.

Hay, A., Kaur, H., Phillips, A., Hedden, P., Hake, S., and Tsiantis, M. (2002). The gibberellin pathway mediates KNOTTED1-type homeobox function in plants with different body plans. Curr Biol **12,** 1557-1565.

Heit, R., Underhill, D.A., Chan, G., and Hendzel, M.J. (2006). Epigenetic regulation of centromere formation and kinetochore function. Biochem Cell Biol **84,** 605-618.

Heller, M.J. (2002). DNA microarray technology: devices, systems, and applications. Annu Rev Biomed Eng **4,** 129-153.

Hendzel, M.J., Wei, Y., Mancini, M.A., Van Hooser, A., Ranalli, T., Brinkley, B.R., Bazett-Jones, D.P., and Allis, C.D. (1997). Mitosis-specific phosphorylation of histone H3 initiates primarily within pericentromeric heterochromatin during G2 and spreads in an ordered fashion coincident with mitotic chromosome condensation. Chromosoma **106,** 348-360.

Henikoff, S., Ahmad, K., and Malik, H.S. (2001). The centromere paradox: stable inheritance with rapidly evolving DNA. Science **293,** 1098-1102.

Henikoff, S., Ahmad, K., Platero, J.S., and van Steensel, B. (2000). Heterochromatic deposition of centromeric histone H3-like proteins. Proc Natl Acad Sci U S A **97,** 716-721.

Heslop-Harrison, J.S., Brandes, A., and Schwarzacher, T. (2003). Tandemly repeated DNA sequences and centromeric chromosomal regions of *Arabidopsis* species. Chromosome Res **11,** 241-253.

Higgins, J.M. (2001). Haspin-like proteins: a new family of evolutionarily conserved putative eukaryotic protein kinases. Protein Sci **10,** 1677-1684.

Houben, A., Demidov, D., Rutten, T., and Scheidtmann, K.H. (2005). Novel phosphorylation of histone H3 at threonine 11 that temporally correlates with condensation of mitotic and meiotic chromosomes in plant cells. Cytogenet Genome Res **109,** 148-155.

Houben, A., Demidov, D., Caperta, A.D., Karimi, R., Agueci, F., and Vlasenko, L. (2007). Phosphorylation of histone H3 in plants-A dynamic affair. Biochim Biophys Acta.

Houben, A., Wako, T., Furushima-Shimogawara, R., Presting, G., Kunzel, G., Schubert, I.I., and Fukui, K. (1999). Short communication: the cell cycle dependent phosphorylation of histone H3 is correlated with the condensation of plant mitotic chromosomes. Plant J **18,** 675-679.

Howman, E.V., Fowler, K.J., Newson, A.J., Redward, S., MacDonald, A.C., Kalitsis, P., and Choo, K.H. (2000). Early disruption of centromeric chromatin organization in centromere protein A (Cenpa) null mice. Proc Natl Acad Sci U S A **97,** 1148-1153.

Hsu, J.Y., Sun, Z.W., Li, X., Reuben, M., Tatchell, K., Bishop, D.K., Grushcow, J.M., Brame, C.J., Caldwell, J.A., Hunt, D.F., Lin, R., Smith, M.M., and Allis, C.D. (2000). Mitotic phosphorylation of histone H3 is governed by Ipl1/aurora kinase and Glc7/PP1 phosphatase in budding yeast and nematodes. Cell **102,** 279-291.

Hudson, A. (2001). Plant development: Two sides to organ asymmetry. Curr Biol **11,** R756-758.

Hunter, C., Willmann, M.R., Wu, G., Yoshikawa, M., de la Luz Gutierrez-Nava, M., and Poethig, S.R. (2006). Trans-acting siRNA-mediated repression of ETTIN and ARF4 regulates heteroblasty in *Arabidopsis*. Development **133,** 2973-2981.

Imbeaud, S., and Auffray, C. (2005). 'The 39 steps' in gene expression profiling: critical issues and proposed best practices for microarray experiments. Drug Discov Today **10,** 1175-1182.

Irish, V.F., and Sussex, I.M. (1992). A fate map of the *Arabidopsis* embryonic shoot apical meristem. Development **115,** 745-753.

Iwakawa, H., Ueno, Y., Semiarti, E., Onouchi, H., Kojima, S., Tsukaya, H., Hasebe, M., Soma, T., Ikezaki, M., Machida, C., and Machida, Y. (2002). The ASYMMETRIC LEAVES2 gene of *Arabidopsis thaliana*, required for formation of a symmetric flat leaf lamina, encodes a member of a novel family of proteins characterized by cysteine repeats and a leucine zipper. Plant Cell Physiol **43,** 467-478.

Jackson, D., Veit, B., and Hake, S. (1994). Expression of the maize KNOTTED-1 related homeobox genes in the shoot apical meristem predicts patterns of morphogenesis in the vegetative shoot. Development**,** 405-413.

Jasinski, S., Piazza, P., Craft, J., Hay, A., Woolley, L., Rieu, I., Phillips, A., Hedden, P., and Tsiantis, M. (2005). KNOX action in *Arabidopsis* is mediated by coordinate regulation of cytokinin and gibberellin activities. Curr Biol **15,** 1560-1565.

Jenssen, T.K., Langaas, M., Kuo, W.P., Smith-Sorensen, B., Myklebost, O., and Hovig, E. (2002). Analysis of repeatability in spotted cDNA microarrays. Nucleic Acids Res **30,** 3235-3244.

Jenuwein, T., and Allis, C.D. (2001). Translating the histone code. Science **293,** 1074-1080.

Jeong, S., Trotochaud, A.E., and Clark, S.E. (1999). The *Arabidopsis* CLAVATA2 gene encodes a receptor-like protein required for the stability of the CLAVATA1 receptor-like kinase. Plant Cell **11,** 1925-1934.

Jin, W., Melo, J.R., Nagaki, K., Talbert, P.B., Henikoff, S., Dawe, R.K., and Jiang, J. (2004). Maize centromeres: organization and functional adaptation in the genetic background of oat. Plant Cell **16,** 571-581.

Juarez, M.T., Kui, J.S., Thomas, J., Heller, B.A., and Timmermans, M.C. (2004). microRNA-mediated repression of rolled leaf1 specifies maize leaf polarity. Nature **428,** 84-88.

Kamme, F., Zhu, J., Luo, L., Yu, J., Tran, D.T., Meurers, B., Bittner, A., Westlund, K., Carlton, S., and Wan, J. (2004). Single-cell laser-capture microdissection and RNA amplification. Methods Mol Med **99,** 215-223.

Kaszas, E., and Cande, W.Z. (2000). Phosphorylation of histone H3 is correlated with changes in the maintenance of sister chromatid cohesion during meiosis in maize, rather than the condensation of the chromatin. J Cell Sci **113 (Pt 18),** 3217-3226.

Kawabe, A., Matsunaga, S., Nakagawa, K., Kurihara, D., Yoneda, A., Hasezawa, S., Uchiyama, S., and Fukui, K. (2005). Characterization of plant Aurora kinases during mitosis. Plant Mol Biol **58,** 1-13.

Kaya, H., Shibahara, K.I., Taoka, K.I., Iwabuchi, M., Stillman, B., and Araki, T. (2001). FASCIATA genes for chromatin assembly factor-1 in *Arabidopsis* maintain the cellular organization of apical meristems. Cell **104,** 131-142.

Keeney, S. (2001). Mechanism and control of meiotic recombination initiation. Curr Top Dev Biol **52,** 1-53.

Kerk, N.M., Ceserani, T., Tausta, S.L., Sussex, I.M., and Nelson, T.M. (2003). Laser capture microdissection of cells from plant tissues. Plant Physiol **132,** 27-35.

Kerstetter, R.A., Bollman, K., Taylor, R.A., Bomblies, K., and Poethig, R.S. (2001). KANADI regulates organ polarity in *Arabidopsis*. Nature **411,** 706-709.

Kidner, C.A., and Martienssen, R.A. (2004). Spatially restricted microRNA directs leaf polarity through ARGONAUTE1. Nature **428,** 81-84.

Kidner, C.A., and Timmermans, M.C. (2007). Mixing and matching pathways in leaf polarity. Curr Opin Plant Biol **10,** 13-20.

Kitajima, T.S., Kawashima, S.A., and Watanabe, Y. (2004). The conserved kinetochore protein shugoshin protects centromeric cohesion during meiosis. Nature **427,** 510-517.

Kitajima, T.S., Yokobayashi, S., Yamamoto, M., and Watanabe, Y. (2003). Distinct cohesin complexes organize meiotic chromosome domains. Science **300,** 1152-1155.

Klink, V.P., Alkharouf, N., MacDonald, M., and Matthews, B. (2005). Laser capture microdissection (LCM) and expression analyses of Glycine max (soybean) syncytium containing root regions formed by the plant pathogen Heterodera glycines (soybean cyst nematode). Plant Mol Biol **59,** 965-979.

Kouzarides, T. (2007). Chromatin modifications and their function. Cell **128,** 693-705.

Kumaran, M.K., Bowman, J.L., and Sundaresan, V. (2002). YABBY polarity genes mediate the repression of KNOX homeobox genes in *Arabidopsis*. Plant Cell **14,** 2761-2770.

Kunitoku, N., Sasayama, T., Marumoto, T., Zhang, D., Honda, S., Kobayashi, O., Hatakeyama, K., Ushio, Y., Saya, H., and Hirota, T. (2003). CENP-A phosphorylation by Aurora-A in prophase is required for enrichment of Aurora-B at inner centromeres and for kinetochore function. Dev Cell **5,** 853-864.

Kurihara, D., Matsunaga, S., Kawabe, A., Fujimoto, S., Noda, M., Uchiyama, S., and Fukui, K. (2006). Aurora kinase is required for chromosome segregation in tobacco BY-2 cells. Plant J **48,** 572-580.

Kwon, C.S., Chen, C., and Wagner, D. (2005). WUSCHEL is a primary target for transcriptional regulation by SPLAYED in dynamic control of stem cell fate in *Arabidopsis*. Genes Dev **19,** 992-1003.

Laux, T., Mayer, K.F., Berger, J., and Jurgens, G. (1996). The WUSCHEL gene is required for shoot and floral meristem integrity in *Arabidopsis*. Development **122,** 87-96.

Lee, H.R., Neumann, P., Macas, J., and Jiang, J. (2006). Transcription and evolutionary dynamics of the centromeric satellite repeat CentO in rice. Mol Biol Evol **23,** 2505-2520.

Leibfried, A., To, J.P., Busch, W., Stehling, S., Kehle, A., Demar, M., Kieber, J.J., and Lohmann, J.U. (2005). WUSCHEL controls meristem function by direct regulation of cytokinin-inducible response regulators. Nature **438,** 1172-1175.

Lenhard, M., and Laux, T. (2003). Stem cell homeostasis in the *Arabidopsis* shoot meristem is regulated by intercellular movement of CLAVATA3 and its sequestration by CLAVATA1. Development **130,** 3163-3173.

Li, H., Xu, L., Wang, H., Yuan, Z., Cao, X., Yang, Z., Zhang, D., Xu, Y., and Huang, H. (2005). The Putative RNA-dependent RNA polymerase RDR6 acts synergistically with ASYMMETRIC LEAVES1 and 2 to repress BREVIPEDICELLUS and MicroRNA165/166 in *Arabidopsis* leaf development. Plant Cell **17,** 2157-2171.

Lin, W.C., Shuai, B., and Springer, P.S. (2003). The *Arabidopsis* LATERAL ORGAN BOUNDARIES-domain gene ASYMMETRIC LEAVES2 functions in the repression of KNOX gene expression and in adaxial-abaxial patterning. Plant Cell **15,** 2241-2252.

Lipshutz, R.J., Fodor, S.P., Gingeras, T.R., and Lockhart, D.J. (1999). High density synthetic oligonucleotide arrays. Nat Genet **21,** 20-24.

Long, J., and Barton, M.K. (2000). Initiation of axillary and floral meristems in *Arabidopsis*. Dev Biol **218,** 341-353.

Long, J.A., Moan, E.I., Medford, J.I., and Barton, M.K. (1996). A member of the KNOTTED class of homeodomain proteins encoded by the STM gene of *Arabidopsis*. Nature **379,** 66-69.

Loyola, A., and Almouzni, G. (2004). Histone chaperones, a supporting role in the limelight. Biochim Biophys Acta **1677,** 3-11.

Luger, K., Mader, A.W., Richmond, R.K., Sargent, D.F., and Richmond, T.J. (1997). Crystal structure of the nucleosome core particle at 2.8 A resolution. Nature **389,** 251-260.

MacCallum, D.E., Losada, A., Kobayashi, R., and Hirano, T. (2002). ISWI remodeling complexes in Xenopus egg extracts: identification as major chromosomal components that are regulated by INCENP-aurora B. Mol Biol Cell **13,** 25-39.

Mahadevan, L.C., Willis, A.C., and Barratt, M.J. (1991). Rapid histone H3 phosphorylation in response to growth factors, phorbol esters, okadaic acid, and protein synthesis inhibitors. Cell **65,** 775-783.

Maiato, H., DeLuca, J., Salmon, E.D., and Earnshaw, W.C. (2004). The dynamic kinetochore-microtubule interface. J Cell Sci **117,** 5461-5477.

Manzanero, S., Arana, P., Puertas, M.J., and Houben, A. (2000). The chromosomal distribution of phosphorylated histone H3 differs between plants and animals at meiosis. Chromosoma **109,** 308-317.

Matsumoto, N., and Okada, K. (2001). A homeobox gene, PRESSED FLOWER, regulates lateral axis-dependent development of *Arabidopsis* flowers. Genes Dev **15,** 3355-3364.

Mayer, K.F., Schoof, H., Haecker, A., Lenhard, M., Jurgens, G., and Laux, T. (1998). Role of WUSCHEL in regulating stem cell fate in the *Arabidopsis* shoot meristem. Cell **95,** 805-815.

McAinsh, A.D., Tytell, J.D., and Sorger, P.K. (2003). Structure, function, and regulation of budding yeast kinetochores. Annu Rev Cell Dev Biol **19,** 519-539.

McConnell, J.R., Emery, J., Eshed, Y., Bao, N., Bowman, J., and Barton, M.K. (2001). Role of PHABULOSA and PHAVOLUTA in determining radial patterning in shoots. Nature **411,** 709-713.

McSteen, P., and Leyser, O. (2005). Shoot branching. Annu Rev Plant Biol **56,** 353-374.

Minoshima, Y., Hori, T., Okada, M., Kimura, H., Haraguchi, T., Hiraoka, Y., Bao, Y.C., Kawashima, T., Kitamura, T., and Fukagawa, T. (2005). The constitutive centromere component CENP-50 is required for recovery from spindle damage. Mol Cell Biol **25,** 10315-10328.

Modrek, B., Resch, A., Grasso, C., and Lee, C. (2001). Genome-wide detection of alternative splicing in expressed sequences of human genes. Nucleic Acids Res **29,** 2850-2859.

Moreno, M.A., Harper, L.C., Krueger, R.W., Dellaporta, S.L., and Freeling, M. (1997). liguleless1 encodes a nuclear-localized protein required for induction of ligules and auricles during maize leaf organogenesis. Genes Dev **11,** 616-628.

Muehlbauer, G.J., Fowler, J.E., and Freeling, M. (1997). Sectors expressing the homeobox gene liguleless3 implicate a time-dependent mechanism for cell fate acquisition along the proximal-distal axis of the maize leaf. Development **124,** 5097-5106.

Muehlbauer, G.J., Fowler, J.E., Girard, L., Tyers, R., Harper, L., and Freeling, M. (1999). Ectopic expression of the maize homeobox gene liguleless3 alters cell fates in the leaf. Plant Physiol **119,** 651-662.

Nakazawa, Y., Hiraguri, A., Moriyama, H., and Fukuhara, T. (2007). The dsRNA-binding protein DRB4 interacts with the Dicer-like protein DCL4 in vivo and functions in the trans-acting siRNA pathway. Plant Mol Biol **63,** 777-785.

Nakazono, M., Qiu, F., Borsuk, L.A., and Schnable, P.S. (2003). Laser-capture microdissection, a tool for the global analysis of gene expression in specific plant cell types: identification of genes expressed differentially in epidermal cells or vascular tissues of maize. Plant Cell **15,** 583-596.

Nardmann, J., Ji, J., Werr, W., and Scanlon, M.J. (2004). The maize duplicate genes narrow sheath1 and narrow sheath2 encode a conserved homeobox gene function in a lateral domain of shoot apical meristems. Development **131,** 2827-2839.

Navarro, C., Efremova, N., Golz, J.F., Rubiera, R., Kuckenberg, M., Castillo, R., Tietz, O., Saedler, H., and Schwarz-Sommer, Z. (2004). Molecular and genetic interactions between STYLOSA and GRAMINIFOLIA in the control of Antirrhinum vegetative and reproductive development. Development **131,** 3649-3659.

Nelson, T., Tausta, S.L., Gandotra, N., and Liu, T. (2006a). Laser microdissection of plant tissue: what you see is what you get. Annu Rev Plant Biol **57,** 181-201.

Nelson, T., Tausta, S.L., Gandotra, N., and Liu, T. (2006b). Laser Microdissection of Plant Tissue: What You See Is What You Get. Annu Rev Plant Biol.

Nespoli, A., Vercillo, R., di Nola, L., Diani, L., Giannattasio, M., Plevani, P., and Muzi-Falconi, M. (2006). Alk1 and Alk2 are two new cell cycle-regulated haspin-like proteins in budding yeast. Cell Cycle **5,** 1464-1471.

Nishihashi, A., Haraguchi, T., Hiraoka, Y., Ikemura, T., Regnier, V., Dodson, H., Earnshaw, W.C., and Fukagawa, T. (2002). CENP-I is essential for centromere function in vertebrate cells. Dev Cell **2,** 463-476.

Nogueira, F.T., Madi, S., Chitwood, D.H., Juarez, M.T., and Timmermans, M.C. (2007). Two small regulatory RNAs establish opposing fates of a developmental axis. Genes Dev **21,** 750-755.

Nonaka, N., Kitajima, T., Yokobayashi, S., Xiao, G., Yamamoto, M., Grewal, S.I., and Watanabe, Y. (2002). Recruitment of cohesin to heterochromatic regions by Swi6/HP1 in fission yeast. Nat Cell Biol **4,** 89-93.

Nowak, S.J., and Corces, V.G. (2000). Phosphorylation of histone H3 correlates with transcriptionally active loci. Genes Dev **14,** 3003-3013.

Nowak, S.J., and Corces, V.G. (2004). Phosphorylation of histone H3: a balancing act between chromosome condensation and transcriptional activation. Trends Genet **20,** 214-220.

Otsuga, D., DeGuzman, B., Prigge, M.J., Drews, G.N., and Clark, S.E. (2001). REVOLUTA regulates meristem initiation at lateral positions. Plant J **25,** 223-236.

Pekker, I., Alvarez, J.P., and Eshed, Y. (2005). Auxin response factors mediate *Arabidopsis* organ asymmetry via modulation of KANADI activity. Plant Cell **17,** 2899-2910.

Peragine, A., Yoshikawa, M., Wu, G., Albrecht, H.L., and Poethig, R.S. (2004). SGS3 and SGS2/SDE1/RDR6 are required for juvenile development and the production of trans-acting siRNAs in *Arabidopsis*. Genes Dev **18,** 2368-2379.

Petersen, J., Paris, J., Willer, M., Philippe, M., and Hagan, I.M. (2001). The S. pombe aurora-related kinase Ark1 associates with mitotic structures in a stage dependent manner and is required for chromosome segregation. J Cell Sci **114,** 4371-4384.

Pidoux, A.L., and Allshire, R.C. (2004). Kinetochore and heterochromatin domains of the fission yeast centromere. Chromosome Res **12,** 521-534.

Pien, S., Wyrzykowska, J., McQueen-Mason, S., Smart, C., and Fleming, A. (2001). Local expression of expansin induces the entire process of leaf development and modifies leaf shape. Proc Natl Acad Sci U S A **98,** 11812-11817.

Pluta, A.F., Mackay, A.M., Ainsztein, A.M., Goldberg, I.G., and Earnshaw, W.C. (1995). The centromere: hub of chromosomal activities. Science **270,** 1591-1594.

Poethig, R.S. (1984). Cellular parameters of leaf morphogenesis in maize and tobacco. Contemporary Problems of Plant Anatomy (eds. R. A. White and W. C. Dickinson)**,** 235-238.

Poethig, R.S., and Szymkowiak, E.J. (1995). Clonal analysis of leaf development in maize. Maydica**,** 67-76.

Polioudaki, H., Markaki, Y., Kourmouli, N., Dialynas, G., Theodoropoulos, P.A., Singh, P.B., and Georgatos, S.D. (2004). Mitotic phosphorylation of histone H3 at threonine 3. FEBS Lett **560,** 39-44.

Preuss, U., Landsberg, G., and Scheidtmann, K.H. (2003). Novel mitosis-specific phosphorylation of histone H3 at Thr11 mediated by Dlk/ZIP kinase. Nucleic Acids Res **31,** 878-885.

Prigent, C., and Dimitrov, S. (2003). Phosphorylation of serine 10 in histone H3, what for? J Cell Sci **116,** 3677-3685.

Prigge, M.J., Otsuga, D., Alonso, J.M., Ecker, J.R., Drews, G.N., and Clark, S.E. (2005). Class III homeodomain-leucine zipper gene family members have overlapping, antagonistic, and distinct roles in *Arabidopsis* development. Plant Cell **17,** 61-76.

Putkey, F.R., Cramer, T., Morphew, M.K., Silk, A.D., Johnson, R.S., McIntosh, J.R., and Cleveland, D.W. (2002). Unstable kinetochore-microtubule capture and chromosomal instability following deletion of CENP-E. Dev Cell **3,** 351-365.

Reinhardt, D. (2005). Regulation of phyllotaxis. Int J Dev Biol **49,** 539-546.

Reinhardt, D., Wittwer, F., Mandel, T., and Kuhlemeier, C. (1998). Localized upregulation of a new expansin gene predicts the site of leaf formation in the tomato meristem. Plant Cell **10,** 1427-1437.

Reinhardt, D., Pesce, E.R., Stieger, P., Mandel, T., Baltensperger, K., Bennett, M., Traas, J., Friml, J., and Kuhlemeier, C. (2003). Regulation of phyllotaxis by polar auxin transport. Nature **426,** 255-260.

Rensink, W.A., and Buell, C.R. (2005). Microarray expression profiling resources for plant genomics. Trends Plant Sci **10,** 603-609.

Richmond, T., and Somerville, S. (2000). Chasing the dream: plant EST microarrays. Curr Opin Plant Biol **3,** 108-116.

Rieder, C.L. (1982). The formation, structure, and composition of the mammalian kinetochore and kinetochore fiber. Int Rev Cytol **79,** 1-58.

Rieder, C.L., Cole, R.W., Khodjakov, A., and Sluder, G. (1995). The checkpoint delaying anaphase in response to chromosome monoorientation is mediated by an inhibitory signal produced by unattached kinetochores. J Cell Biol **130,** 941-948.

Roeder, G.S. (1997). Meiotic chromosomes: it takes two to tango. Genes Dev **11,** 2600-2621.

Rojo, E., Sharma, V.K., Kovaleva, V., Raikhel, N.V., and Fletcher, J.C. (2002). CLV3 is localized to the extracellular space, where it activates the *Arabidopsis* CLAVATA stem cell signaling pathway. Plant Cell **14,** 969-977.

Salvador, L.M., Park, Y., Cottom, J., Maizels, E.T., Jones, J.C., Schillace, R.V., Carr, D.W., Cheung, P., Allis, C.D., Jameson, J.L., and Hunzicker-Dunn, M. (2001). Follicle-stimulating hormone stimulates protein kinase A-mediated histone H3 phosphorylation and acetylation leading to select gene activation in ovarian granulosa cells. J Biol Chem **276,** 40146-40155.

Scanlon, M.J. (2000). NARROW SHEATH1 functions from two meristematic foci during founder-cell recruitment in maize leaf development. Development **127,** 4573-4585.

Scanlon, M.J. (2003). The polar auxin transport inhibitor N-1-naphthylphthalamic acid disrupts leaf initiation, KNOX protein regulation, and formation of leaf margins in maize. Plant Physiol **133,** 597-605.

Scanlon, M.J., and Freeling, M. (1997). Clonal sectors reveal that a specific meristematic domain is not utilized in the maize mutant narrow sheath. Dev Biol **182,** 52-66.

Scanlon, M.J., Schneeberger, R.G., and Freeling, M. (1996). The maize mutant narrow sheath fails to establish leaf margin identity in a meristematic domain. Development **122,** 1683-1691.

Schad, M., Mungur, R., Fiehn, O., and Kehr, J. (2005a). Metabolic profiling of laser microdissected vascular bundles of *Arabidopsis thaliana*. Plant Methods **1,** 2.

Schad, M., Lipton, M.S., Giavalisco, P., Smith, R.D., and Kehr, J. (2005b). Evaluation of two-dimensional electrophoresis and liquid chromatography--tandem mass spectrometry

for tissue-specific protein profiling of laser-microdissected plant samples. Electrophoresis **26,** 2729-2738.

Schena, M., Shalon, D., Davis, R.W., and Brown, P.O. (1995). Quantitative monitoring of gene expression patterns with a complementary DNA microarray. Science **270,** 467-470.

Schnable, P.S., Hochholdinger, F., and Nakazono, M. (2004). Global expression profiling applied to plant development. Curr Opin Plant Biol **7,** 50-56.

Schneeberger, R., Tsiantis, M., Freeling, M., and Langdale, J.A. (1998). The rough sheath2 gene negatively regulates homeobox gene expression during maize leaf development. Development **125,** 2857-2865.

Schneeberger, R.G., Becraft, P.W., Hake, S., and Freeling, M. (1995). Ectopic expression of the knox homeo box gene rough sheath1 alters cell fate in the maize leaf. Genes Dev **9,** 2292-2304.

Schoof, H., Lenhard, M., Haecker, A., Mayer, K.F., Jurgens, G., and Laux, T. (2000). The stem cell population of *Arabidopsis* shoot meristems in maintained by a regulatory loop between the CLAVATA and WUSCHEL genes. Cell **100,** 635-644.

Schueler, M.G., Higgins, A.W., Rudd, M.K., Gustashaw, K., and Willard, H.F. (2001). Genomic and genetic definition of a functional human centromere. Science **294,** 109-115.

Schwacha, A., and Kleckner, N. (1994). Identification of joint molecules that form frequently between homologs but rarely between sister chromatids during yeast meiosis. Cell **76,** 51-63.

Schwacha, A., and Kleckner, N. (1997). Interhomolog bias during meiotic recombination: meiotic functions promote a highly differentiated interhomolog-only pathway. Cell **90,** 1123-1135.

Scutt, C.P., Kamisugi, Y., Sakai, F., and Gilmartin, P.M. (1997). Laser isolation of plant sex chromosomes: studies on the DNA composition of the X and Y sex chromosomes of Silene latifolia. Genome **40,** 705-715.

Shani, E., Yanai, O., and Ori, N. (2006). The role of hormones in shoot apical meristem function. Curr Opin Plant Biol **9,** 484-489.

Shippy, R., Sendera, T.J., Lockner, R., Palaniappan, C., Kaysser-Kranich, T., Watts, G., and Alsobrook, J. (2004). Performance evaluation of commercial short-oligonucleotide microarrays and the impact of noise in making cross-platform correlations. BMC Genomics **5,** 61.

Siegfried, K.R., Eshed, Y., Baum, S.F., Otsuga, D., Drews, G.N., and Bowman, J.L. (1999). Members of the YABBY gene family specify abaxial cell fate in *Arabidopsis*. Development **126,** 4117-4128.

Sinha, N.R., Williams, R.E., and Hake, S. (1993). Overexpression of the maize homeo box gene, KNOTTED-1, causes a switch from determinate to indeterminate cell fates. Genes Dev **7,** 787-795.

Smith, L.G., Greene, B., Veit, B., and Hake, S. (1992). A dominant mutation in the maize homeobox gene, Knotted-1, causes its ectopic expression in leaf cells with altered fates. Development **116,** 21-30.

Spence, J.M., Critcher, R., Ebersole, T.A., Valdivia, M.M., Earnshaw, W.C., Fukagawa, T., and Farr, C.J. (2002). Co-localization of centromere activity, proteins and topoisomerase II within a subdomain of the major human X alpha-satellite array. Embo J **21,** 5269-5280.

Spencer, M.W., Casson, S.A., and Lindsey, K. (2007). Transcriptional profiling of the *Arabidopsis* embryo. Plant Physiol **143,** 924-940.

Strahl, B.D., and Allis, C.D. (2000). The language of covalent histone modifications. Nature **403,** 41-45.

Strelkov, I.S., and Davie, J.R. (2002). Ser-10 phosphorylation of histone H3 and immediate early gene expression in oncogene-transformed mouse fibroblasts. Cancer Res **62,** 75-78.

Sullivan, K.F. (2001). A solid foundation: functional specialization of centromeric chromatin. Curr Opin Genet Dev **11,** 182-188.

Takeda, S., Tadele, Z., Hofmann, I., Probst, A.V., Angelis, K.J., Kaya, H., Araki, T., Mengiste, T., Mittelsten Scheid, O., Shibahara, K., Scheel, D., and Paszkowski, J. (2004). BRU1, a novel link between responses to DNA damage and epigenetic gene silencing in *Arabidopsis*. Genes Dev **18,** 782-793.

Tanaka-Ueguchi, M., Itoh, H., Oyama, N., Koshioka, M., and Matsuoka, M. (1998). Over-expression of a tobacco homeobox gene, NTH15, decreases the expression of a gibberellin biosynthetic gene encoding GA 20-oxidase. Plant J **15,** 391-400.

Tanaka, H., Dhonukshe, P., Brewer, P.B., and Friml, J. (2006). Spatiotemporal asymmetric auxin distribution: a means to coordinate plant development. Cell Mol Life Sci **63,** 2738-2754.

Theodoris, G., Inada, N., and Freeling, M. (2003). Conservation and molecular dissection of ROUGH SHEATH2 and ASYMMETRIC LEAVES1 function in leaf development. Proc Natl Acad Sci U S A **100,** 6837-6842.

Timmermans, M.C., Hudson, A., Becraft, P.W., and Nelson, T. (1999). ROUGH SHEATH2: a Myb protein that represses knox homeobox genes in maize lateral organ primordia. Science **284,** 151-153.

Trotochaud, A.E., Jeong, S., and Clark, S.E. (2000). CLAVATA3, a multimeric ligand for the CLAVATA1 receptor-kinase. Science **289,** 613-617.

Tsiantis, M., Schneeberger, R., Golz, J.F., Freeling, M., and Langdale, J.A. (1999). The maize rough sheath2 gene and leaf development programs in monocot and dicot plants. Science **284,** 154-156.

Vagnarelli, P., and Earnshaw, W.C. (2004). Chromosomal passengers: the four-dimensional regulation of mitotic events. Chromosoma **113,** 211-222.

Van Hooser, A., Goodrich, D.W., Allis, C.D., Brinkley, B.R., and Mancini, M.A. (1998). Histone H3 phosphorylation is required for the initiation, but not maintenance, of mammalian chromosome condensation. J Cell Sci **111 (Pt 23),** 3497-3506.

Vaucheret, H. (2005). MicroRNA-dependent trans-acting siRNA production. Sci STKE **2005,** pe43.

Vos, L.J., Famulski, J.K., and Chan, G.K. (2006). How to build a centromere: from centromeric and pericentromeric chromatin to kinetochore assembly. Biochem Cell Biol **84,** 619-639.

Waites, R., and Hudson, A. (1995). *phantastica*: a gene required for dorsoventrality of leaves in *Antirrhinum-majus*. Development **121,** 2143-2154.

Waites, R., Selvadurai, H.R., Oliver, I.R., and Hudson, A. (1998). The PHANTASTICA gene encodes a MYB transcription factor involved in growth and dorsoventrality of lateral organs in Antirrhinum. Cell **93,** 779-789.

Watanabe, Y. (2004). Modifying sister chromatid cohesion for meiosis. J Cell Sci **117,** 4017-4023.

Watanabe, Y. (2005). Sister chromatid cohesion along arms and at centromeres. Trends Genet **21,** 405-412.

Wei, Y., Mizzen, C.A., Cook, R.G., Gorovsky, M.A., and Allis, C.D. (1998). Phosphorylation of histone H3 at serine 10 is correlated with chromosome condensation during mitosis and meiosis in Tetrahymena. Proc Natl Acad Sci U S A **95,** 7480-7484.

Williams, L., Grigg, S.P., Xie, M., Christensen, S., and Fletcher, J.C. (2005). Regulation of *Arabidopsis* shoot apical meristem and lateral organ formation by microRNA miR166g and its AtHD-ZIP target genes. Development **132,** 3657-3668.

Wojcik, E., Basto, R., Serr, M., Scaerou, F., Karess, R., and Hays, T. (2001). Kinetochore dynein: its dynamics and role in the transport of the Rough deal checkpoint protein. Nat Cell Biol **3,** 1001-1007.

Woll, K., Borsuk, L.A., Stransky, H., Nettleton, D., Schnable, P.S., and Hochholdinger, F. (2005). Isolation, characterization, and pericycle-specific transcriptome analyses of the novel maize lateral and seminal root initiation mutant rum1. Plant Physiol **139,** 1255-1267.

Wondrak, G.T., Cervantes-Laurean, D., Jacobson, E.L., and Jacobson, M.K. (2000). Histone carbonylation in vivo and in vitro. Biochem J **351 Pt 3,** 769-777.

Wu, X., Dabi, T., and Weigel, D. (2005). Requirement of homeobox gene STIMPY/WOX9 for *Arabidopsis* meristem growth and maintenance. Curr Biol **15,** 436-440.

Xu, L., Xu, Y., Dong, A., Sun, Y., Pi, L., Xu, Y., and Huang, H. (2003). Novel as1 and as2 defects in leaf adaxial-abaxial polarity reveal the requirement for ASYMMETRIC

LEAVES1 and 2 and ERECTA functions in specifying leaf adaxial identity. Development **130,** 4097-4107.

Yanai, O., Shani, E., Dolezal, K., Tarkowski, P., Sablowski, R., Sandberg, G., Samach, A., and Ori, N. (2005). *Arabidopsis* KNOXI proteins activate cytokinin biosynthesis. Curr Biol **15,** 1566-1571.

Yang, L., Liu, Z., Lu, F., Dong, A., and Huang, H. (2006). SERRATE is a novel nuclear regulator in primary microRNA processing in *Arabidopsis*. Plant J **47,** 841-850.

Yoshikawa, M., Peragine, A., Park, M.Y., and Poethig, R.S. (2005). A pathway for the biogenesis of trans-acting siRNAs in *Arabidopsis*. Genes Dev **19,** 2164-2175.

Yu, H.G., Hiatt, E.N., and Dawe, R.K. (2000). The plant kinetochore. Trends Plant Sci **5,** 543-547.

Zeitlin, S.G., Shelby, R.D., and Sullivan, K.F. (2001a). CENP-A is phosphorylated by Aurora B kinase and plays an unexpected role in completion of cytokinesis. J Cell Biol **155,** 1147-1157.

Zeitlin, S.G., Barber, C.M., Allis, C.D., and Sullivan, K.F. (2001b). Differential regulation of CENP-A and histone H3 phosphorylation in G2/M. J Cell Sci **114,** 653-661.

Zhang, J., Finney, R.P., Clifford, R.J., Derr, L.K., and Buetow, K.H. (2005). Detecting false expression signals in high-density oligonucleotide arrays by an in silico approach. Genomics **85,** 297-308.

Zhao, S., and Bruce, W.B. (2003). Expression profiling using cDNA microarrays. Methods Mol Biol **236,** 365-380.

Zhao, Y., Medrano, L., Ohashi, K., Fletcher, J.C., Yu, H., Sakai, H., and Meyerowitz, E.M. (2004). HANABA TARANU is a GATA transcription factor that regulates shoot apical meristem and flower development in *Arabidopsis*. Plant Cell **16,** 2586-2600.

Zhong, C.X., Marshall, J.B., Topp, C., Mroczek, R., Kato, A., Nagaki, K., Birchler, J.A., Jiang, J., and Dawe, R.K. (2002). Centromeric retroelements and satellites interact with maize kinetochore protein CENH3. Plant Cell **14,** 2825-2836.

CHAPTER 2

PHOSPHORYLATION OF MAIZE CENH3 DEMARCATES THE ACTIVE CENTROMERE DURING CELL DIVISION[1]

[1]Zhang, X., Li, X., Marshall, J.B., Zhong, C.X., and Dawe, R.K. (2005). Phosphoserines on maize CENTROMERIC HISTONE H3 and histone H3 demarcate the centromere and pericentromere during chromosome segregation. Plant Cell 17**,** 572-583. The material is copyrighted by the American Society of Plant Biologists, reprinted here with permission of the publisher (See APPENDICES A).

ABSTRACT

Multiple phosphorylation events occur on histone H3 with controversial functions. CENH3 is a centromeric histone H3 variant characterized with a divergent N-terminal tail. CENH3 is phosphorylated at Ser7 in human mitotic cells, and this phosphorylation is required for proper chromosome alignment and cytokinesis. Here we have identified and characterized a 17-18 kD serine-50-phosphorylated form of maize CENH3 (phCENH3-Ser50). Immunostaining in meiosis indicates that CENH3-Ser50 phosphorylation begins in diplotene, increases to a maximum at prometaphase-metaphase, and drops during anaphase. Dephosphorylation is precipitous (~6-fold) at the metaphase-anaphase transition, suggesting a role in the spindle checkpoint. Our data suggest that phosphorylation of CENH3 at Ser50 demarcates the active centromere during cell cycle. Furthermore, we propose that the primary role of histone H3 phosphorylation is to demarcate distinct chromosomal domains (i.e. centromere, pericentromere, chromosome arm) so that chromosomes can align and segregate properly.

INTRODUCTION

Throughout the eukaryotes, a complex set of interacting posttranslational modifications is known to regulate the interaction of histones with transcription factors and other chromatin binding proteins. Histone modifications such as acetylation, methylation, and phosphorylation are so prevalent that Strahl and Allis (2002) envisioned a combinatorial histone code, which in principle could extend the effective coding capacity of the genome. A strength of the histone code hypothesis is that the major histones are well conserved across all eukaryotes, as are the locations of many known posttranslational modifications. The proposed histone code, however, is confounded by a divergent group of histone variants, many of which have important functions (Malik and Henikoff, 2003). Histone variants typically have strong homology to canonical histones within the C-terminal section that lies within nucleosomes, but lack homology in the flexible N-terminal tails that extend outside nucleosomes. As the N-terminal tails are where the most important posttranslational modifications occur, histone variants may have different but functionally similar codes (Strahl and Allis, 2000a), erase previously set histone codes (Ahmad and Henikoff, 2002b) or present altogether new codes (Smith, 2002).

On histone H3, four residues on the N-terminal tail are known to be phosphorylated: serine 10, serine 28, threonine 3 and threonine 11 (Hendzel et al., 1997; Gernand et al., 2003; Preuss et al., 2003; Polioudaki et al., 2004). At all four residues and in all species studied, the level of phosphorylation is low or undetectable at interphase, increases at prophase, and decreases during anaphase and telophase. Among these, Ser10 (phH3-Ser10) is the most extensively characterized (Prigent and Dimitrov, 2003). In mammalian cells, the phosphorylation of H3-Ser10 initiates in pericentric heterochromatin and spreads to chromosome

arms during mitotic and meiotic metaphase (Hendzel et al., 1997). These staining patterns and earlier biochemical studies (Gurley et al., 1978; Allis and Gorovsky, 1981) suggest that H3-Ser10 phosphorylation may have a role in chromosome condensation (Wei et al., 1998). However, in the mitotic cells of most plants, phH3-Ser10 phosphorylation never extends beyond pericentric regions. It is only in meiosis I that the entire plant chromosomes stain uniformly with anti-phH3-Ser10 antisera (Kaszas and Birchler, 1996; Houben et al., 1999; Manzanero et al., 2000). These staining patterns and the analyses of univalents suggests that phH3-Ser10 is involved in sister chromatid cohesion (Kaszas and Cande, 2000a; Gernand et al., 2003). In animals, phH3-Ser10 recruits Aurora B kinase (Crosio et al., 2002), suggesting that the phosphoserine residues may also function as docking sites for proteins involved in cytokinesis (Andrews et al., 2003). Finally, a variety of data indicate that phosphorylation is involved in transcriptional activation (Clayton and Mahadevan, 2003). Given the varied and often conflicting data, the conserved functions of histone phosphorylation remain controversial. The primary function of histone phosphorylation may be to identify different domains of the chromosome and mark their progress through the cell cycle (Prigent and Dimitrov, 2003).

A key histone variant is Centromeric Histone H3 (CENH3), the only universally conserved essential inner kinetochore protein (Choo, 2001). CENH3 is characterized (and usually identified) by remarkable sequence and length polymorphism in the N-terminal tail (Henikoff et al., 2000). In humans there is weak homology between histone H3 and CENH3 over a region containing H3-Ser10. The analogous serine in human CENH3 is found at position 7, and is phosphorylated in a temporal pattern that is similar to H3-Ser10 (Zeitlin et al., 2001b). Recent data suggest that phCENP-A-Ser7 is required for proper chromosome alignment (Kunitoku et al., 2003). However any model based on phCENP-A-Ser7 is difficult to reconcile

with the sequences of other CENH3s. As shown in Figure 2.1, residues that could be interpreted as Ser7 counterparts are entirely absent in most CENH3s. Although there is no Ser7 counterpart in maize CENH3, there are several serines in the core-proximal portion of the tail that could in principle correspond to histone H3 phospho-Ser28; namely CENH3 serines 25, 46, and 50 (Fig. 2.1). One of these, Ser50, is within a peptide that was previously used to generate antisera for maize CENH3 (Zhong et al., 2002).

Here we show that maize CENH3-Ser50 is efficiently phosphorylated. The excellent cytology of maize allowed us to extend the description of phCENH3-Ser50 in meiosis, to show that phosphorylation is a prophase-to-anaphase event, and that in meiosis II dephosphorylation is rapid and coincident with anaphase onset. These data suggest that the position of a phosphorylated residue, not necessarily its sequence context, may be a better predictor of which residues are phosphorylated on histone H3 variants. Further, we argue that the main function of phosphorylation is to epigenetically mark distinct chromosome regions to ensure proper cell division.

RESULTS

Weak CENH3 staining in meiotic metaphase is reversed by phosphatase

Using a well-characterized anti-maize CENH3 polyclonal antibody (Zhong et al., 2002), we immunolocalized CENH3 in both meiotic and mitotic cells. As shown in Figure 2.2, CENH3 is present at all prophase stages of meiosis I; from premeiotic interphase (not shown), to the synapsed chromosomes of pachytene (Fig. 2.2 A) and further condensed diplotene and diakinesis chromosomes (Figs. 2.2 B-C). Interestingly, CENH3 staining was weak or absent in

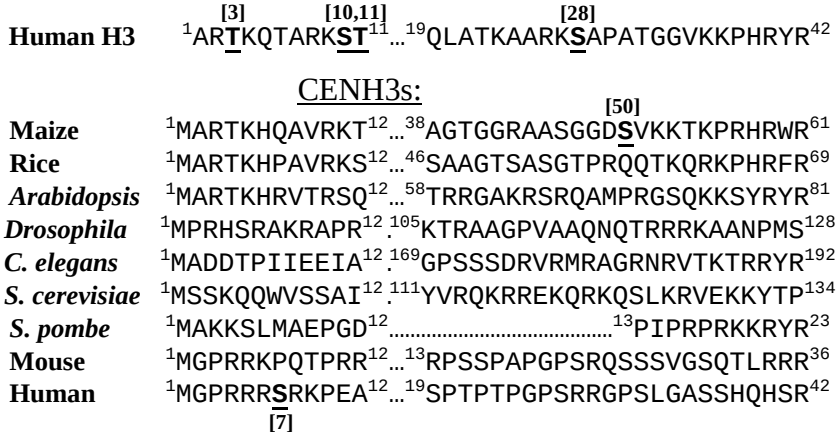

Figure 2.1 N-terminal tails of human histone H3 and nine CENH3s. Only the CENH3s with documented centromeric localization are listed. The first 12 and (no more than) the last 24 amino acids of the N-terminal tail region are shown (the N-terminus of *S. pombe* SpCENP-A contains only 23 amino acids). The residues known to be phosphorylated on human histone H3, human CENP-A, and maize CENH3 are indicated. The GenBank ID numbers for CENH3 homologs are as follows: Maize: AAM74226, Rice: AAR85315, *Arabidopsis*: NP_563627, *Drosophila*: AAF72652, *C. elegans*: NP_499128, *S. cerevisiae*: NP_012875, *S. pombe*: BAA94760, Mouse: NP_068686, and Human: NP_001800.

prometaphase and metaphase I and II (Figs. 2.2 D-E) but from the onset of anaphase CENH3 staining was again visible (Fig. 2.2F).

Blocking of the epitope by posttranslational modification seemed the most attractive explanation for the absence of staining in prometaphase and metaphase. Since histone H3 is phosphorylated during mitosis and meiosis in several organisms, including *Tetrahymena, Aspergillus, C. elegans*, plants and vertebrates (e.g. (Wei et al., 1999; Hsu et al., 2000; Souza et al., 2000; Crosio et al., 2002; Gernand et al., 2003), we theorized that Ser50, located within the peptide used to prepare antibodies, is phosphorylated.

As an initial test of the idea, we applied calf intestinal phosphatase (CIP) to fixed meiocytes and stained them with anti-CENH3 antisera. CIP preferentially releases phosphate groups from phosphoserine/threonine residues. As shown in Figure 2.3B and 2.3 C, the typically weak or absent CENH3 staining during meiotic metaphase was reversed by CIP treatment.

Anti-phCENH3-Ser50 antibodies recognize CENH3 on condensed chromosomes

To better understand the phosphorylation of CENH3, we raised rabbit antisera against a synthetic peptide corresponding to amino acids 46-54 (SGGDS[p]VKKT) with a phosphorylated serine at position 50 (Fig. 2.3A). The antisera were analyzed by ELISA, and the resulting data are shown in Figure 2.4. We found that both our original anti-CENH3 antibodies (Zhong et al., 2002) and the anti-phCENH3-Ser50 antibodies bound specifically to the peptides they were raised against (the CENH3 and phCENH3-Ser50 peptides, respectively), but showed no binding when incubated with the opposite peptides (the phCENH3-Ser50 and CENH3 peptides, respectively). In addition, my colleague Xuexian Li performed western blot and showed that anti-phCENH3-Ser50 recognized a 17-18kD protein (data not shown).

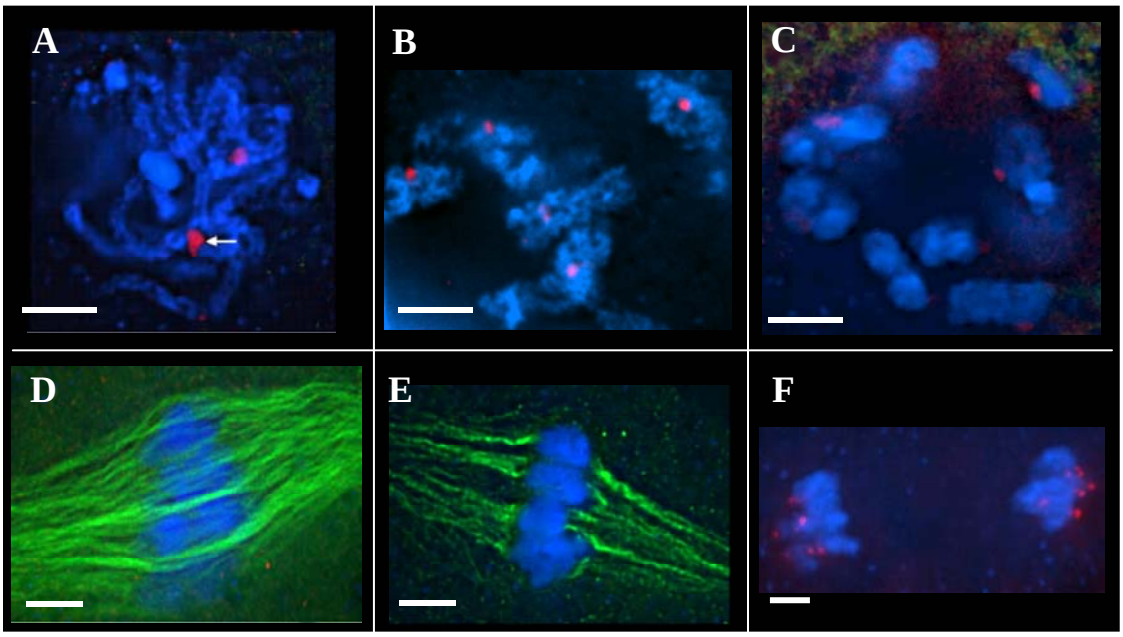

Figure 2.2 CENH3 localization in maize meiosis. All images are partial projections from 3D data sets. CENH3 staining is shown in red, microtubules in green, and chromosomes in blue. **A**) CENH3 at pachytene of meiosis I, when kinetochores are paired (arrow). **B**) CENH3 at diplotene. **C**) CENH3 at diakinesis. **D**) CENH3 at prometaphase I. **E**) CENH3 at prometaphase II. **F**) CENH3 at anaphase II. Bars (=5 μm) indicate the scale for all images in a given row.

Next we determined the distribution of phosphorylated CENH3 in meiotic cells. Staining of phCENH3-Ser50 was first detected in diplotene (Fig. 2.5B) and persisted through diakinesis and metaphase (Fig. 2.5 C-E). The staining then became weak in late anaphase (Fig. 2.5 F) and was lost in telophase (data not shown). Interestingly, maize H3-Ser28 was phosphorylated with the same temporal pattern but restricted to the pericentromeric region (Xuexian Li's work, data not shown). To confirm that the antisera recognize the phosphate moiety, alkaline phosphatase (CIP) was applied to meiocytes (Figs. 2.3D and 2.3E). CIP treatment reduced the intensity of anti-phCENH3-Ser50 immunostaining by approximately 90% ±2% (n =26 prior to, and 8 cells after CIP treatment).

CENH3 is rapidly dephosphorylated at meiotic anaphase, in a manner that is reminiscent of a role in the spindle checkpoint

In an effort to quantify the onset of CENH3 phosphorylation and dephosphorylation, we performed simultaneous immuno-detection of CENH3 and phCENH3-Ser50 at different meiotic stages. Representative microscope images and an analysis of the resulting data are shown in Figure 2.6. Consistent with the indirect immunolocalization data, only non-phosphorylated CENH3 was observed from the zygotene to pachytene stages of meiosis I, and only phCENH3-Ser50 was observed in metaphase. However, in diakinesis and anaphase I, both proteins were detectable. Over the diakinesis-anaphase I period, the percentage of kinetochore-localized phCENH3-Ser50 changed from 15% in diakinesis, to nearly 100% in late metaphase, and back to ~13% in anaphase I (Figs. 2.6A-E).

To further refine the stage at which CENH3 is dephosphorylated, we analyzed cells in meiosis II, where the distance between sister kinetochores can be used to predict anaphase with

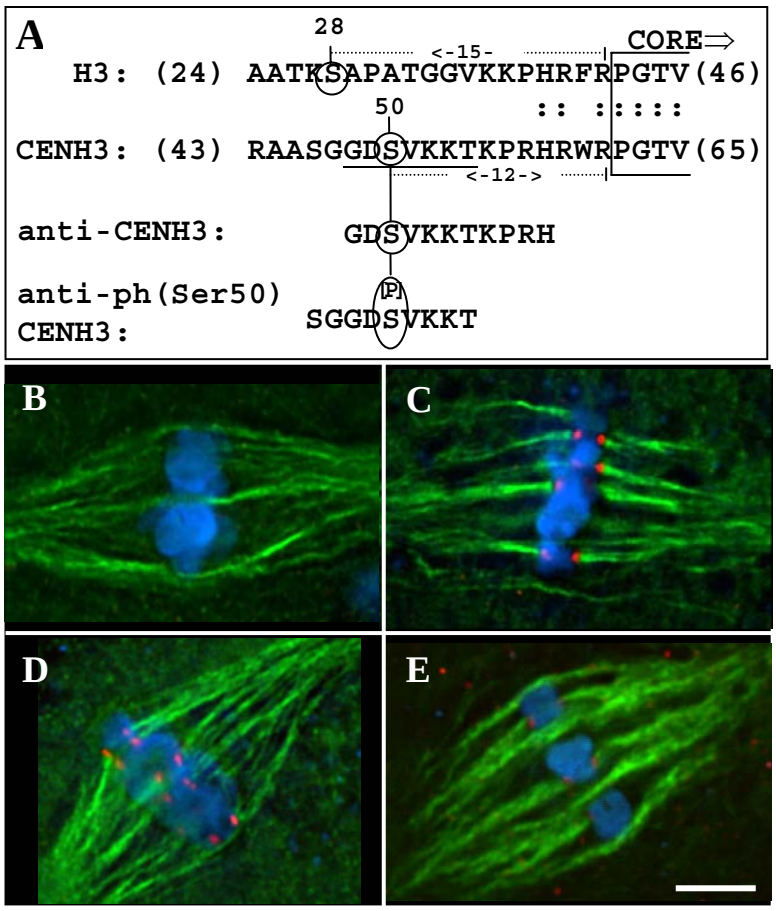

Figure 2.3 Descriptions of peptides used to develop antisera, and the reactivity of the antisera with metaphase chromosomes following phosphatase treatment. A) The locations of peptides used to prepare antisera. The top line shows a portion of histone H3, ranging from amino acids 24 to 46. Ser28 is indicated. The second line shows the corresponding region of maize CENH3 with Ser50 indicated. The two peptides used for antibody production are shown below. The CENH3 antiserum (Zhong et al., 2002) recognizes both of the non-phosphorylated peptides GDSVKKTKPRH and SGGDSVKKT with similar specificity (Fig. 4), indicating that the primary epitope for the CENH3 antibody (or antibodies) is the sequence GDSVKK. B) Image showing the characteristic absence of CENH3 staining at metaphase II.

(**Figure 2.3** legend continued) CENH3 staining is shown in red, microtubules in green, and chromosomes in blue. C) Bright CENH3 staining is revealed after alkaline phosphatase treatment. D) Image showing the characteristically strong phCENH3-Ser50 staining in untreated metaphase II cells. phCENH3-Ser50 is shown in red, microtubules in green, and chromosomes in blue. E) Alkaline phosphatase treatment reduces phCENH3-Ser50 staining by about 90%. Bars = 5μm.

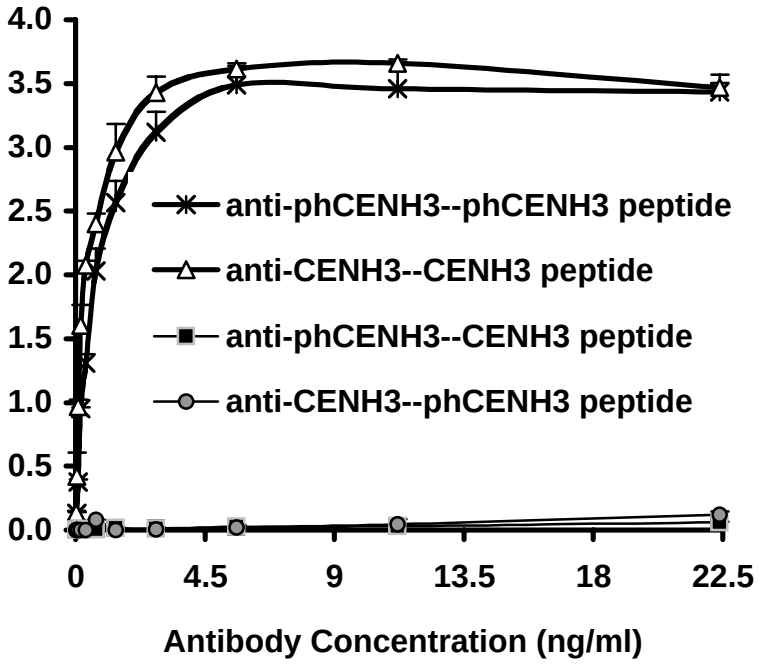

Figure 2.4 ELISA analyses. Anti-phCENH3-Ser50 antisera recognize the phCENH3-Ser50 peptide but not CENH3 peptide, while anti-CENH3 antisera recognize the CENH3 peptide but not phCENH3-Ser50 peptide.

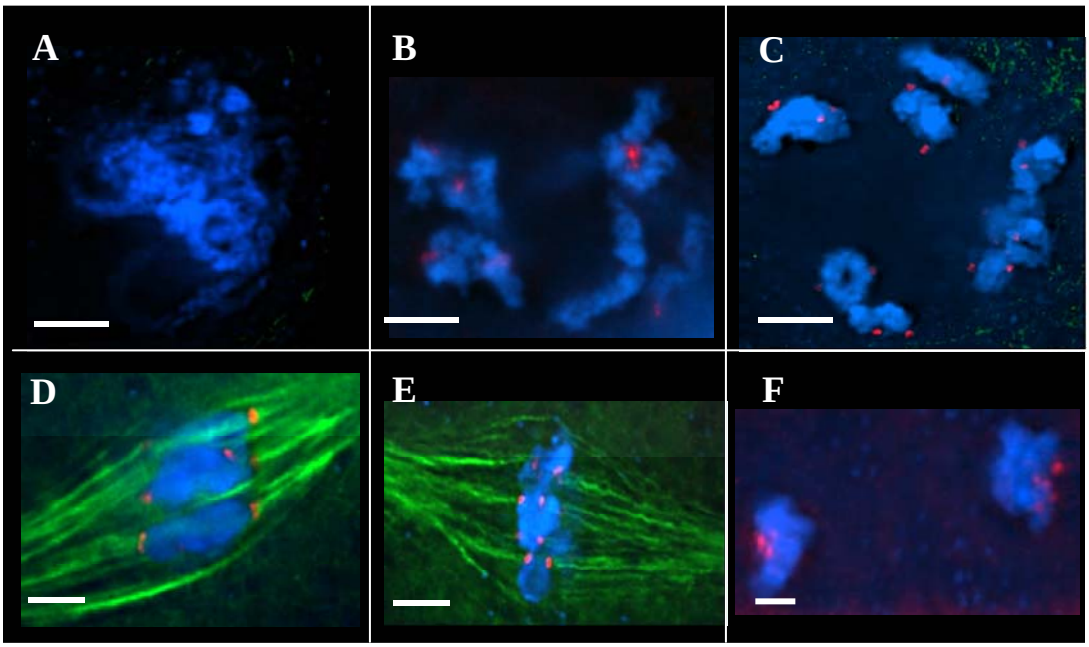

Figure 2.5 Localization of phCENH3-Ser50 in maize meiosis. All images are partial projections from 3D data sets. phCENH3-Ser50 staining is shown in red, microtubules in green, and chromosomes in blue. **A**) phCENH3-Ser50 at pachytene. **B**) phCENH3-Ser50 at diplotene. **C**) phCENH3-Ser50 at diakinesis. **D**) phCENH3-Ser50 at prometaphase I. **E**) phCENH3-Ser50 at prometaphase II. **F**) phCENH3-Ser50 at anaphase II. Bars (=5 μm) indicate the scale for all images in a given row.

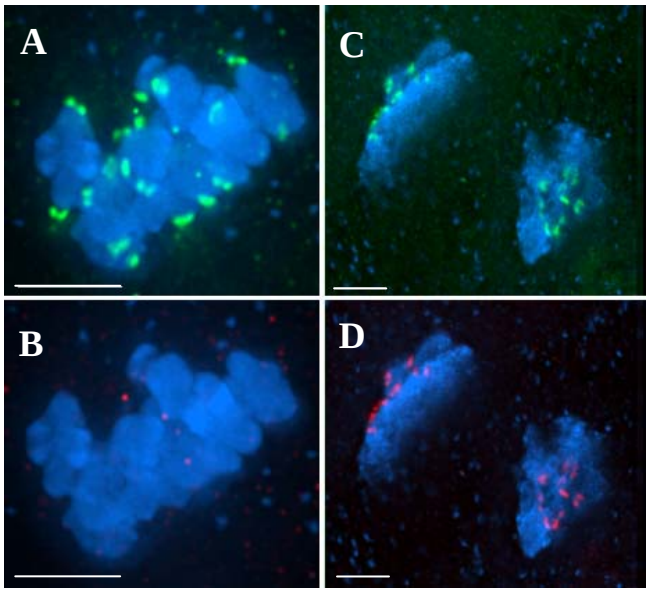
A
C
B
D

E

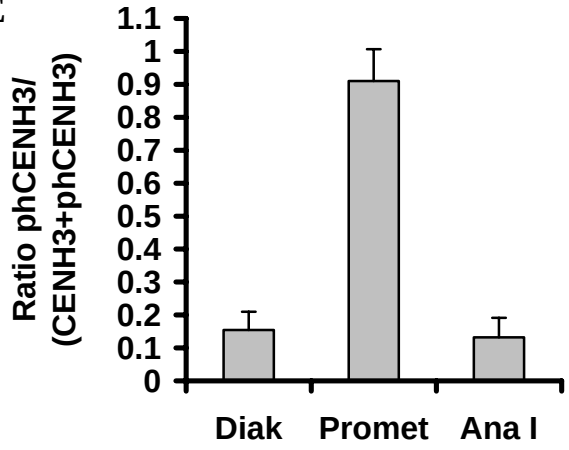
Ratio phCENH3/
(CENH3+phCENH3)
1.1
1
0.9
0.8
0.7
0.6
0.5
0.4
0.3
0.2
0.1
0
Diak
Promet
Ana I

F

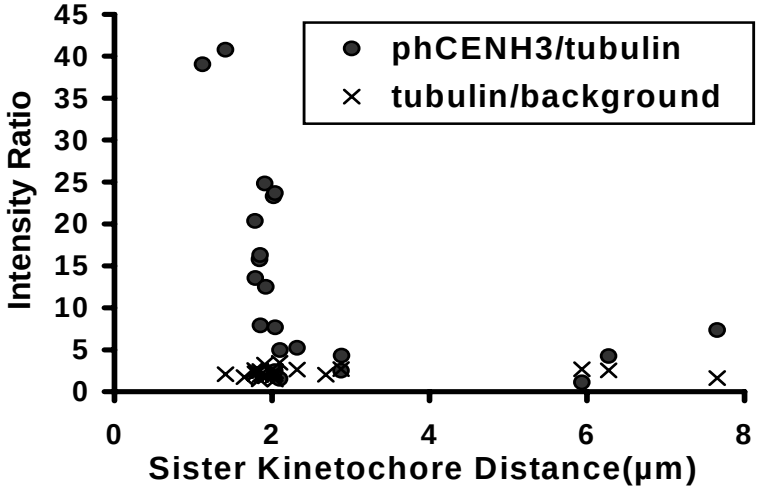
Intensity Ratio
45
40
35
30
25
20
15
10
5
0
0
2
4
6
8
Sister Kinetochore Distance(μm)
phCENH3/tubulin
tubulin/background

Figure 2.6 Quantitative analysis of phCENH3-Ser50 staining at various stages of meiosis. A-D show partial projections from 3D data sets, where phCENH3-Ser50 is shown in green, CENH3 in red, and chromosomes in blue. **A and B**) Co-labeling of phCENH3-Ser50 and CENH3 at prometaphase I. Nearly all of the staining is from anti-phCENH3-Ser50 antisera (A): only random background staining is visible in the CENH3 channel (B). **C and D**) Co-labeling of phCENH3-Ser50 and CENH3 at anaphase I. phCENH3-Ser50 staining is relatively weak (C; scaled up here to make it visible) while CENH3 staining is bright (D). **E**) The ratio of phCENH3-Ser50 to CENH3+phCENH3-Ser50 staining at three stages of meiosis I. Staining data were averaged from 3-5 cells at each stage, all from the same slide. **F**) CENH3 is rapidly dephosphorylated at anaphase onset. Data are expressed as tubulin S/N ratios (X's) or as phCENH3-Ser50 S/N divided by tubulin S/N (solid circles) plotted against the distance between sister kinetochores. Previous analysis of meiosis II in the W23 inbred (Yu et al., 1999) established that anaphase II commences when the kinetochores are roughly 1.8-2.1 μM apart. Bars = 5μm.

accuracy (Yu et al., 1999). Control experiments established that total tubulin staining intensity did not change appreciably from prometaphase II to anaphase II (Fig. 2.6F). Based on this observation, phCENH3-Ser50 staining was normalized to tubulin staining and plotted against the distance between sister kinetochores. As shown in Figure 2.6F, we found that phCENH3-Ser50 staining fell dramatically as the distance between sister kinetochores reached 2.0-2.1 microns. As prior data had established that anaphase commences when the kinetochores are 1.8-2.1 microns apart (in this same inbred line; (Yu et al., 1999), these data indicate that CENH3 is rapidly dephosphorylated at or near the metaphase-anaphase transition.

DISCUSSION

CENH3 is a highly conserved histone H3-like protein that is found uniquely at centromeres. Data from several organisms indicate that CENH3 is at the core of centromere/kinetochore complex, where it helps to establish a specialized chromatin environment and recruits a subset of kinetochore proteins (Hooser et al., 2001; Ando et al., 2002). Although CENH3 is an important histone H3 variant, little is known about its phosphorylation. The only known CENH3 phosphorylation event occurs on Ser7 of human CENP-A (Zeitlin et al., 2001a). Immunolocalization using anti-phCENP-A-Ser7 antisera revealed a pattern similar to what is observed with anti-phH3-Ser10 (Wei et al., 1998), except that phCENP-A-Ser7 is quickly dephosphorylated at anaphase (Zeitlin et al., 2001b). A Ser7-to-Ala7 substitution (Kunitoku et al., 2003) caused chromosome mis-segregation as well as cytokinesis defects (Zeitlin et al., 2001a), suggesting a dual role in chromosome alignment and cytokinesis.

In this study we raised antibodies that recognize Ser50-phosphorylated CENH3 and

confirmed the specificity of the antibodies by ELISA, western analysis, and alkaline phosphatase treatment (Figs. 2.3D, 2.3E, 2.4, data from Xuexian Li). Immunolocalization demonstrated that CENH3 phosphorylation is cell cycle dependent: phosphorylation initiates in diplotene, increases as the chromosomes condense, and at metaphase phosphorylation is almost complete (Figs. 2.5E, 2.6E). Following anaphase onset, CENH3 is dephosphorylated rapidly (Figs. 2.5F, 2.6E).

Histone H3 and CENH3 are phosphorylated with similar kinetics

In animals each of four different sites on the N-terminal tail of histone H3 — Thr3, Ser10, Thr11, and Ser28 — are phosphorylated in a similar prophase-telophase-specific pattern (Hendzel et al., 1997; Gernand et al., 2003; Preuss et al., 2003; Polioudaki et al., 2004). However, none of these residues are found on any known centromeric histone H3 variant (Fig. 2.1A). Indeed, a lack of homology in the N-terminus is a key identifier of histone variants (Henikoff et al., 2000), making the question of how the variants might fit into the proposed histone code a matter of speculation. Our data are the first to address this issue in earnest, since the previously characterized phCENP-A-Ser7 lies in a relatively well-conserved region of the protein (Zeitlin et al., 2001b; Fig. 2.1A). In the region of the N-terminal tail downstream of the first 12 amino acids (where H3-Ser28 and CENH3-Ser50 lie), there is a near complete absence of homology among the known CENH3s. Here the sequence data seem incompatible with idea of a strict combinatorial phosphorylation code, since the code would have to be effectively reinvented with the evolution of each new variant. Our data demonstrate that phosphorylation not only occurs in this region, but that it occurs in a temporal manner that mirrors other histone H3 phosphorylation events. Since both the location and context of the phosphorylation event are novel (relative to H3 and other CENH3s), the data support the view that presence or absence

phosphorylation, and/or the combined charges of the residues (Masayoshi and Smith, 2003) may be more important than their relative order or proximity to each other.

An issue of particular interest is whether a maize Aurora kinase is responsible for the phosphorylation of CENH3-Ser50. The Aurora kinases (A and B) belong to a conserved family of serine/threonine kinases with critical roles in centrosome separation, spindle assembly, chromosome alignment, and cytokinesis (Andrews et al., 2003; Pascreau et al., 2003). Human Aurora-B phosphorylates histone H3 at Ser10 and Ser28, and CENP-A at Ser7 (Giet and Glover, 2001; Zeitlin et al., 2001a; Crosio et al., 2002; Goto et al., 2002). More recent data suggest that CENP-A is initially phosphorylated by Aurora A, and that the completed reaction is required for the recruitment (i.e. docking) of Aurora-B at the inner centromere (Kunitoku et al., 2003).

Numerous Aurora kinase homologs exist in maize and other plants. Although no data are available on the localization or specificity of plant Aurora kinases, human and *S. cerevisiae* Aurora kinases have known consensus recognition sites. In humans there is a strong requirement for arginine at the -2 position relative to the phosphorylated serine, and evidence for binding preferences as far away as +4, while in *S. cerevisiae* the consensus site is {RK}X{ST}{LIV} (Cheeseman et al., 2002; Sugiyama et al., 2002). The evident differences between Aurora kinase recognition sites in these species (and the fact that deviations from a consensus generally reduce but do not abolish phosphorylation) make it difficult to predict whether CENH3-Ser50 is an Aurora kinase target. The involvement of Aurora kinase in maize CENH3 phosphorylation is nevertheless quite likely, given the strong conservation of function between the yeast and animal Aurora kinases (Pascreau et al., 2003). Should Aurora kinase prove to regulate maize CENH3-Ser50, the data will provide a strong endorsement of the idea that the presence and function of histone H3 phosphorylation events are broadly conserved (Strahl and Allis, 2000a).

The timing of CENH3 phosphorylation and dephosphorylation as it relates to anaphase onset

One of the most important functions of kinetochores is to facilitate the activities of the spindle checkpoint, a surveillance mechanism that regulates the timing and coordination of anaphase. After every kinetochore has attached to the spindle properly, a signal cascade is initiated (Lew and Burke, 2003) that results in the breakdown of cohesin, the protein complex responsible for holding chromatids together (Haering and Nasmyth, 2003). In maize, the spindle checkpoint proteins MAD2 and the 3F/2 antigen mark the progression of metaphase (Yu et al., 1999). Both proteins bind to outer kinetochores in early and mid metaphase, and are removed/degraded as opposing kinetochores are pulled to roughly 1.8-2.1 microns apart and anaphase begins (Yu et al., 1999). Similarly, we show here that phCENH3-Ser50 is rapidly dephosphorylated at the 2.0-2.1 micron mark that is indicative of anaphase (Fig. 2.6). Similar timing of phosphorylation and dephosphorylation was reported for phCENP-A-Ser7 (Zeitlin et al., 2001b).

Interestingly, recent data have established that spindle assembly is regulated in part by Aurora kinases (Kallio et al., 2002). Aurora B is a kinetochore 'passenger protein' that localizes to kinetochores only during chromosome alignment (in humans, by docking to phCENP-A-Ser7; (Kunitoku et al., 2003), and recruits MAD2 as well as other spindle checkpoint proteins (Ditchfield et al., 2003; Petersen and Hagan, 2003). Further, Aurora kinase is required to correct improper kinetochore microtubule attachments during chromosome alignment (Tanaka et al., 2002; Hauf et al., 2003). Without phCENP-A-Ser7 and Aurora kinase, the accuracy of chromosome segregation drops measurably (Tanaka et al., 2002; Hauf et al., 2003; Kunitoku et

al., 2003). Further studies will be required to determine if maize phCENH3-Ser50 recruits a similar kinase that functions in chromosome alignment and segregation.

CENH3 phosphorylation extends "histone code" to centromeres

The "histone code" refers to diverse posttranslational modifications imposed on histone amino termini and thereby conferred remarkable coding capability in mediating chromatin-templated biological processes (Strahl and Allis, 2000b; Barski et al., 2007; Kouzarides, 2007). As a reversible histone covalent modification, phosphorylation of histone H3 could occur at four different residues during cell division, Ser10, Ser28, Thr3 and Thr11(Hendzel et al., 1997; Gernand et al., 2003; Preuss et al., 2003; Polioudaki et al., 2004). These highly conserved phosphorylation events mainly occur on chromosome arms or pericentromeres in a cell-cycle dependent manner among higher eukaryotes. Here, we show that maize CENH3 is phosphorylated at Ser50 during meiosis (Fig 2.5). CENPA, the CENH3 orthologue in human, is also phosphorylated during mitosis in a similar pattern (Zeitlin et al., 2001b). Despite the different phosphoresidues, these two phosphorylation events precisely mark the active centromeres during cell division, suggesting that the "histone code" applies to centromeres as well.

Phosphorylation of histone H3 and its variant has been implicated in diverse biological processes such as chromosome condensation (Wei et al., 1998), sister chromatids cohesion (Kaszas and Cande, 2000a; Gernand et al., 2003), gene activation (Clayton and Mahadevan, 2003), and docking site for cytokinesis (Andrews et al., 2003). However, the primary function of histone H3 phosphoresidues may be to differentiate chromosome domains (i.e., centromere, pericentromere and chromosome arm), and to facilitate the transition of chromosome architecture

during cell cycle. For instance, phosphorylation of plant H3 at Thr11 marks chromosome arms and correlates with chromosome condensation (Houben et al., 2005). Phosphorylation of maize H3 at Ser10 marks pericentromeres during meiosis II, wherein correlates with the maintenance of sister chromatid cohesion (Kaszas and Cande, 2000b).

Maize CENH3 is a histone H3 variant that is present at centromeres throughout the cell cycle (Zhong et al., 2002). Phosphorylation of maize CENH3 at Ser50 initiates in prophase, increases to maximum in metaphase, decreases in anaphase and diminishes in telophase (Figure 2.5), thus demarcating the biologically active centromeres specifically during the cell cycle. Although the biological implication of CENH3 phosphorylation is uncertain, phosphorylation of CENH3 Ser50 may be involved in following processes. First, phosphorylation of CENH3 may function as a component or a part of the anaphase checkpoint. Our quantitative analysis shows that CENH3 phosphorylation at Ser50 drops dramatically (~6-fold) upon metaphase-anaphase transition (Figure 2.6), indicating that, like MAD2 checkpoint protein, CENH3 phosphorylation may play a role in the anaphase checkpoint to ensure proper chromosome alignment and bi-polar attachment. Alternatively, phosphorylation of CENH3 may facilitate kinetochore assembly and maturation during cell division. CENH3 is one of the kinetochore 'foundation' proteins that are essential for kinetochore assembly and function (Amor et al., 2004; Vos et al., 2006). The prophase-telophase pattern of phosphorylation at CENH3 Ser50 is synchronized with kinetochore maturation during the cell cycle, indicating that CENH3 phosphorylation may mediate kinetochore assembly and/or function as well, possibly by facilitating the recruitment of or interaction with other kinetochore proteins. Genetic, biochemical and cytological analyses will help to limit the options and perhaps suggest new hypotheses. To consolidate the "histone code"

in centromeres, it's necessary to identify and characterize other posttranslational modifications on CENH3s such as methylation, acetylation, and/or other phosphoresidues in diverse organisms.

MATERIALS AND METHODS

Antisera

A peptide was designed to correspond to residues 46-54 of maize CENH3 (Zhong et al., 2002), with a single phosphorylated serine at position 50 (SGGDS[p]VKKT). Anti-phCENH3-Ser50 antibodies were raised against the peptide conjugated to keyhole limpet hemocyanin. The preparation and affinity purification of antisera was performed by BioSource International, Inc. (Camarillo, CA).

ELISA assays

ELISA was performed according to a protocol provided by Biosource International. Plates were coated with 50 ml of phCENH3-Ser50 peptide (10mg/ml) or CENH3 peptide at 37°C overnight. After 3X washing with ddH_2O, the plates were blocked with 50 ml 0.3% BSA buffer (0.3% BSA, 0.3% Carnation non-fat milk, 0.0002% NaN_3, 0.03% Tween-20 in filtered TBS) at RT for 1 hour. Samples were washed 3X in ddH_2O and incubated for 2 hours at RT in 0.8% BSA buffer. Secondary antibodies were then applied at 1:2500 dilutions for 2 hrs at RT (diluted in 0.83% BSA buffer). Following a washing step (3X with ddH_2O), 75 ml of p-NPP substrate solution (6 mM p-nitrophenyl phosphate, 0.05M Na_2CO_3, 0.05 mM $MgCl_2$) was added to each well for 2 hours. The data were analyzed using a plate reader set at 405 nm.

Indirect immunolocalization in meiotic cells

Meiocytes were prepared from the W23 inbred line as described by Yu et al. (1999). Fixed samples were incubated with rabbit anti-CENH3 antibodies (1:25), rabbit anti-phCENH3-Ser50 antibodies (1:25), rabbit anti-phH3-Ser28 antibodies (1:25), chicken anti-CENPC antibodies (1:25) {Dawe, 1999 #84; Zhong, 2002 #1005} and/or mouse anti-tubulin antibodies (1:500) {Asai, 1982 #13} as appropriate. Rhodamine-conjugated goat anti-rabbit antibodies (1:25) (Jackson Immunoresearch, West Grove, PA) and/or FITC-conjugated goat anti-mouse or donkey anti-chicken (1:25) (14274020, Boehringer Mannheim) secondary antibodies were then applied for 2 hrs at RT. Procedures for the necessary washing steps, mounting, and 4,6-diamidino-2-phenylindole (DAPI) staining have been described previously (Yu et al., 1997). For alkaline phosphatase treatment, meiocytes were fixed, adhered to cover slips, and incubated with 10 units of calf intestinal phosphatase (p4252, Sigma**,** St. Louis, MO) diluted in AP buffer (100 mM NaCl, 5 mM $MgCl_2$, 100 mM Tris, pH 9.5) at 37°C overnight. Cells were then washed 3X in 1X PBS for 5 min each and processed for immunofluorescence.

Direct immunolocalization in meiotic cells

Anti-phCENH3-Ser50 antibodies were directly labeled with Alexa Fluor 488 (Molecular Probes, Eugene, OR) according to the manufacturer's instructions. Labeling efficiency was 3.2 moles Alexa Fluor 488/mole phCENH3-Ser50 antibody. For the double staining shown in Figure 2.6, meiocytes were first incubated with anti-CENH3 antibodies (overnight), then goat anti-rabbit secondary antibodies (3 hours), and finally 3.75 μg of direct-labeled phCENH3-Ser50 antisera (overnight). The protocol was finished in the same manner as a standard indirect immunofluorescence experiment.

Image analysis

Data were acquired and analyzed using a DeltaVision 3D light microscopy workstation and associated software (Applied Precision, Issaquah, WA). Staining intensity measurements were averaged from 4 X4 pixel boxes centered over 10 different kinetochores or spindle fibers (next to kinetochores) as appropriate. Intensity values were divided by background staining (calculated in the same way, from the cytoplasm) to obtain signal to noise (S/N) ratios. For the data in Figure 2.6E, the S/N ratios from phCENH3-Ser50 staining were divided by the sum of the S/N ratios from phCENH3-Ser50 and CENH3 staining. For Figures 2.3E and 2.6F, phCENH3-Ser50 S/N ratios were divided by the tubulin S/N ratios, in effect normalizing phCENH3-Ser50 staining to tubulin staining.

REFERENCES

Ahmad, K., and Henikoff, S. (2002b). Histone H3 variants specify modes of chromatin assembly. Proc. Nat. Acad. Sci. USA **99,** 6477-6484.

Allis, C.D., and Gorovsky, M.A. (1981). Histone phosphorylation in macro- and micronuclei of Tetrahymena thermophila. Biochemistry **20,** 3828-3833.

Amor, D.J., Kalitsis, P., Sumer, H., and Choo, K.H. (2004). Building the centromere: from foundation proteins to 3D organization. Trends Cell Biol **14,** 359-368.

Ando, S., Yang, H., Nozaki, N., Okazaki, T., and Yoda, K. (2002). CENP-A, -B, and -C chromatin complex that contains the I-type alpha-satellite array constitutes the prekinetochore in HeLa cells. Mol. Cell Biol. **22,** 2229-2241.

Andrews, P.D., Knatko, E., Moore, W.J., and Swedlow, J.R. (2003). Mitotic mechanics: the auroras come into view. Curr Opin Cell Biol **15,** 672-683.

Asai, D.J., Brokaw, C.J., Thompson, W.C., and Wilson, L. (1982). Two different monoclonal antibodies to tubulin inhibit the bending of reactivated sea urchin spermatozoa. Cell Motil. **2,** 599-614.

Barski, A., Cuddapah, S., Cui, K., Roh, T.Y., Schones, D.E., Wang, Z., Wei, G., Chepelev, I., and Zhao, K. (2007). High-resolution profiling of histone methylations in the human genome. Cell **129,** 823-837.

Cheeseman, I.M., Anderson, S., Jwa, M., Green, E.M., Kang, J., Yates, J.R., 3rd, Chan, C.S., Drubin, D.G., and Barnes, G. (2002). Phospho-regulation of kinetochore-microtubule attachments by the Aurora kinase Ipl1p. Cell **111,** 163-172.

Choo, K.H.A. (2001). Domain organization at the centromere and neocentromere. Dev. Cell **1,** 165-177.

Clayton, A.L., and Mahadevan, L.C. (2003). MAP kinase-mediated phosphoacetylation of histone H3 and inducible gene regulation. FEBS Lett **546,** 51-58.

Crosio, C., Fimia, G.M., Loury, R., Kimura, M., Okano, Y., Zhou, H., Sen, S., Allis, C.D., and Sassone-Corsi, P. (2002). Mitotic phosphorylation of histone H3: spatio-temporal regulation by mammalian Aurora kinases. Mol Cell Biol **22,** 874-885.

Dawe, R.K., Reed, L., Yu, H.-G., Muszynski, M.G., and Hiatt, E.N. (1999). A maize homolog of mammalian CENPC is a constitutive component of the inner kinetochore. Plant Cell **11,** 1227-1238.

Ditchfield, C., Johnson, V.L., Tighe, A., Ellston, R., Haworth, C., Johnson, T., Mortlock, A., Keen, N., and Taylor, S.S. (2003). Aurora B couples chromosome alignment with anaphase by targeting BubR1, Mad2, and Cenp-E to kinetochores. J Cell Biol **161,** 267-280.

Gernand, D., Demidov, D., and Houben, A. (2003). The temporal and spatial pattern of histone H3 phosphorylation at serine 28 and serine 10 is similar in plants but differs between mono- and polycentric chromosomes. Cytogenet. Genome Res. **101,** 172-176.

Giet, R., and Glover, D.M. (2001). Drosophila aurora B kinase is required for histone H3 phosphorylation and condensin recruitment during chromosome condensation and to organize the central spindle during cytokinesis. J Cell Biol **152,** 669-682.

Goto, H., Yasui, Y., Nigg, E.A., and Inagaki, M. (2002). Aurora-B phosphorylates histone H3 at serine 28 with regard to the mitotic chromosome condensation. Genes Cells **7,** 11-17.

Gurley, L.R., D'Anna, J.A., Barham, S.S., Deaven, L.L., and Tobey, R.A. (1978). Histone phosphorylation and chromatin structure during mitosis in Chinese hamster cells. Eur J Biochem **84,** 1-15.

Haering, C.H., and Nasmyth, K. (2003). Building and breaking bridges between sister chromatids. Bioessays **25,** 1178-1191.

Hauf, S., Cole, R.W., LaTerra, S., Zimmer, C., Schnapp, G., Walter, R., Heckel, A., van Meel, J., Rieder, C.L., and Peters, J.M. (2003). The small molecule Hesperadin reveals a role for Aurora B in correcting kinetochore-microtubule attachment and in maintaining the spindle assembly checkpoint. J Cell Biol **161,** 281-294.

Hendzel, M.J., Wei, Y., Mancini, M.A., Van Hooser, A., Ranalli, T., Brinkley, B.R., Bazett-Jones, D.P., and Allis, C.D. (1997). Mitosis-specific phosphorylation of histone H3 initiates primarily within pericentromeric heterochromatin during G2 and spreads in an ordered fashion coincident with mitotic chromosome condensation. Chromosoma **106,** 348-360.

Henikoff, S., Ahmad, K., Platero, J.S., and Steensel, B.V. (2000). Heterochromatic deposition of centromeric histone H3-like proteins. Proc. Natl. Acad. Sci. USA **97,** 716-721.

Hooser, A.V., Ouspensik, I., Gregson, H., starr, D., Yen, T., Goldberg, M., Yokomori, K., Earnshaw, W., Sullivan, K., and Brinkley, B. (2001). Specification of kinetochore-forming chromatin by the histone H3 variant CENP-A. J. Cell Sci. **114,** 3529-3542.

Houben, A., Demidov, D., Rutten, T., and Scheidtmann, K.H. (2005). Novel phosphorylation of histone H3 at threonine 11 that temporally correlates with condensation of mitotic and meiotic chromosomes in plant cells. Cytogenet Genome Res **109,** 148-155.

Houben, A., Wako, T., Furashima-Shimogawara, R., Presting, G., Kunzel, G., Schubert, I., and Fukui, K. (1999). The cell cycle dependent phosphorylation of histone H3 is correlated with the condensation of plant mitotic chromosomes. Plant J. **18,** 675-679.

Hsu, J.Y., Sun, Z.W., Li, X., Reuben, M., Tatchell, K., Bishop, D.K., Grushcow, J.M., Brame, C.J., Caldwell, J.A., Hunt, D.F., Lin, R., Smith, M.M., and Allis, C.D. (2000). Mitotic phosphorylation of histone H3 is governed by Ipl1/aurora kinase and Glc7/PP1 phosphatase in budding yeast and nematodes. Cell **102,** 279-291.

Kallio, M.J., McCleland, M.L., Stukenberg, P.T., and Gorbsky, G.J. (2002). Inhibition of aurora B kinase blocks chromosome segregation, overrides the spindle checkpoint, and perturbs microtubule dynamics in mitosis. Curr. Biol. **12,** 900-905.

Kaszas, E., and Birchler, J.A. (1996). Misdivision analysis of centromere structure in maize. EMBO J. **15,** 5246-5255.

Kaszas, E., and Cande, W.Z. (2000a). Phosphorylation of histone H3 is correlated with changes in the maintenance of sister chromatid cohesion during meiosis in maize, rather than the condensation of the chromatin. J. Cell Sci. **113,** 3217-3226.

Kaszas, E., and Cande, W.Z. (2000b). Phosphorylation of histone H3 is correlated with changes in the maintenance of sister chromatid cohesion during meiosis in maize, rather than the condensation of the chromatin. J Cell Sci **113 (Pt 18),** 3217-3226.

Kouzarides, T. (2007). Chromatin modifications and their function. Cell **128,** 693-705.

Kunitoku, N., Sasayama, T., T. Marumoto, D. Zhang, Honda, A., O. Kobayashi, Hatakeyama, K., Y. Ushio, Saya, H., and Hirota, T. (2003). CENP-A phosphorylation by Aurora-A in prophase is required for enrichment of Aurora-B at inner centromeres and for kinetochore function. Dev. Cell. **5,** 853-864.

Lew, D.J., and Burke, D.J. (2003). The spindle assembly and spindle position checkpoints. Annu Rev Genet **37,** 251-282.

Malik, M.S., and Henikoff, S. (2003). Phylogenomics of the nucleosome. Nat. Struct. Biol. **10,** 882-891.

Manzanero, S., Arana, P., Puertas, M.J., and Houben, A. (2000). The chromosomal distrubution of phosphorylated histone H3 differs between plants and animals at meiosis. Chromosoma **109,** 308-317.

Masayoshi, L., and Smith, M.M. (2003). Functional consequences of histone modifications. Curr. Opin. Genet. Dev. **13,** 154-160.

Pascreau, G., Arlot-Bonnemains, Y., and Prigent, C. (2003). Phosphorylation of histone and histone-like proteins by aurora kinases during mitosis. Prog Cell Cycle Res **5,** 369-374.

Petersen, J., and Hagan, I.M. (2003). S. pombe Aurora Kinase/Survivin Is Required for Chromosome Condensation and the Spindle Checkpoint Attachment Response. Curr. Biol. **13,** 590-597.

Polioudaki, H., Markaki, Y., Kourmouli, N., Dialynas, G., Theodoropoulos, P.A., Singh, P.B., and Georgatos, S.D. (2004). Mitotic phosphorylation of histone H3 at threonine 3. FEBS Lett **560,** 39-44.

Preuss, U., Landsberg, G., and Scheidtmann, K.H. (2003). Novel mitosis-specific phosphorylation of histone H3 at Thr11 mediated by Dlk/ZIP kinase. Nucleic Acids Res **31,** 878-885.

Prigent, C., and Dimitrov, S. (2003). Phosphorylation of serine 10 in histone H3, what for? J. Cell Sci. **116,** 3677-3685.

Smith, M. (2002). Centromeres and variant histones: what, where, when and why? Curr. Opin. Cell. Biol. **14,** 279-285.

Souza, C.P.D., Osmani, A.H., Wu, L.P., Spotts, J.L., and Osmani, S.A. (2000). Mitotic histone H3 phosphorylation by the NIMA kinase in *Aspergillus nidulans*. Cell **102,** 293-302.

Strahl, B.D., and Allis, C.D. (2000a). The language of covalent histone modifications. Nature **403,** 41-45.

Strahl, B.D., and Allis, C.D. (2000b). The language of covalent histone modifications. Nature **403,** 41-45.

Sugiyama, K., Sugiura, K., Hara, T., Sugimoto, K., Shima, H., Honda, K., Furukawa, K., Yamashita, S., and Urano, T. (2002). Aurora-B associated protein phosphatases as negative regulators of kinase activation. Oncogene **21,** 3103-3111.

Tanaka, T.U., Rachidi, N., Janke, C., Pereira, G., Galova, M., Schiebel, E., Stark, M.J., and Nasmyth, K. (2002). Evidence that the IpI1-Sli15 (Aurora kinase-INCENP) complex promotes chromosome biorientation by altering kinetochore-spindle pole connections. Cell **108,** 317-329.

Vos, L.J., Famulski, J.K., and Chan, G.K. (2006). How to build a centromere: from centromeric and pericentromeric chromatin to kinetochore assembly. Biochem Cell Biol **84,** 619-639.

Wei, Y., Mizzen, C.A., Cook, R.G., Gorovsky, M.A., and Allis, C.D. (1998). Phosphorylation of histone H3 at serine 10 is correlated with chromosome condensation during mitosis and meiosis in Tetrahymena. Proc Natl Acad Sci U S A **95,** 7480-7484.

Wei, Y., Yu, L., Bowen, J., Gorovsky, M.A., and Allis, C.D. (1999). Phosphorylation of histone H3 is required for proper chromosome condensation and segregation. Cell **97,** 99-109.

Yu, H.-G., Muszynski, M.G., and Dawe, R.K. (1999). The maize homologue of the cell cycle checkpoint protein MAD2 reveals kinetochore substructure and contrasting mitotic and meiotic localization patterns. J. Cell Biol. **145,** 425-435.

Zeitlin, S.G., Shelby, R.D., and Sullivan, K.F. (2001a). CENP-A is phosphorylated by Aurora B kinase and plays an unexpected role in completion of cytokinesis. J. Cell Biol. **155,** 1147-1157.

Zeitlin, S.G., Barber, C.M., Allis, C.D., and Sullivan, K.F. (2001b). Differential regulation of CENP-A and histone H3 phosphorylation in G2/M. J. Cell Sci. **114**.

Zhong, C.X., Marshall, J.B., Topp, C., Mroczek, R., Kato, A., Nagaki, K., Birchler, J.A., Jiang, J., and Dawe, R.K. (2002). Centromeric retroelements and satellites interact with maize kinetochore protein CENH3. Plant Cell **14,** 2825-2836.

CHAPTER 3

LASER MICRODISSECTION OF NARROW SHEATH MUTANT MAIZE UNCOVERS NOVEL GENE EXPRESSION IN THE SHOOT APICAL MERISTEM [1]

---

[1] Zhang, X., Madi, S., Borsuk, L., Nettleton, D., Elshire, R.J., Buckner, B., Janick-Buckner, D., Beck, J., Timmermans, M., Schnable, P.S., and Scanlon, M.J. (2007). Laser microdissection of narrow sheath mutant maize uncovers novel gene expression in the shoot apical meristem. PLoS Genet 3(6): e101. doi:10.1371/journal.pgen.0030101. The material is copyrighted and distributed under the terms of the Creative Commons Attribution Licenses, reprinted here with permission of the publisher (See APPENDICES B).

ABSTRACT

Microarrays enable comparative analyses of gene expression on a genomic scale, however these experiments frequently identify an abundance of differentially expressed genes such that it may be difficult to identify discrete functional networks that are hidden within large microarray datasets. Microarray analyses in which mutant organisms are compared to non-mutant siblings can be especially problematic, particularly when the gene of interest is expressed in relatively few cells. Here we describe the use of laser microdissection-microarray to perform transcriptional profiling of the maize shoot apical meristem (SAM), a ~ 100 μm pillar of organogenic cells that is required for leaf initiation. Microarray analyses compared differential gene expression within the SAM and incipient leaf primordium of non-mutant and narrow sheath mutant plants, which harbored mutations in the duplicate genes *narrow sheath1* (*ns1*) and *narrow sheath2* (*ns2*). Expressed in 8-10 cells within the SAM, *ns1* and *ns2* encode paralogous WUSCHEL1-like homeobOX (WOX) transcription factors required for recruitment of leaf initials that give rise to a large lateral domain within maize leaves. The data illustrate the utility of laser microdissection microarray analyses to identify a relatively small number of genes that are differentially expressed within the SAM. Moreover, these analyses reveal potentially conserved WOX gene functions, and implicate specific hormonal and signaling pathways during early events in maize leaf development.

INTRODUCTION

The paralogous *WUSCHEL*-like homeobOX (WOX) genes *narrow sheath1* (*ns1*) and *narrow sheath2* (*ns2*) function from two, lateral foci within the maize SAM (Figure 3.1) (Scanlon, 2000; Nardmann et al., 2004), which comprises a pool of over 1,200 pluripotent cells that ultimately generates all lateral organs of the vegetative shoot. Maize leaf development begins with the initialization of approximately 200 leaf founder-cells in the SAM, a recruitment process whereby cells occupying the periphery of the SAM are signaled to become founder-cells of the incipient leaf (Poethig, 1984; Poethig and Szymkowiak, 1995). The *ns1* and *ns2* duplicate genes encode redundant functions during maize leaf development. Single mutations in either *ns* gene are non-phenotypic (Scanlon et al., 1996; Scanlon and Freeling, 1997; Scanlon, 2000; Scanlon et al., 2000; Nardmann et al., 2004). Plants harboring recessive mutations in both of the *narrow sheath* genes fail to initialize founder-cells within a specific, lateral domain of the SAM; failure to transduce this founder-cell recruitment signal results in the pre-primordial deletion of an extensive lateral domain from the mutant maize leaf (Figure 3.1) (Scanlon et al., 1996; Scanlon and Freeling, 1997). Although redundantly expressed in two foci comprising only ~8-10 total cells (Nardmann et al., 2004), NS1 and NS2 propagate a founder-cell recruitment signal throughout the lateral domain of the SAM from where much of the lower portion of the maize leaf is derived. The molecular nature of this recruitment signal and the mechanism of its transduction within the SAM are unknown.

The technique of laser microdissection (LM) permits the facile isolation of specific cells and tissues from plants (Nelson et al., 2006). Nanogram quantities of total RNA extracted from laser-microdissected tissues are linearly amplified by T7 RNA polymerase and used in

microarray analyses. The combined use of laser microdissection and microarray technologies enables comparative analyses of discrete developmental fields while eliminating the transcriptional noise contributed by multiple tissues and downstream developmental events (Schnable et al., 2004). Laser microdissection has been applied to global expression analyses of maize vascular and epidermal tissues, maize roots, as well as *Arabidopsis* embryos, and floral organs (Nakazono et al., 2003; Casson et al., 2005; Woll et al., 2005; Cai and Lashbrook, 2006; Spencer et al., 2007) The relatively large size of the maize SAM, approximately 200 founder-cells are recruited into the incipient maize leaf versus 25-30 in *Arabidopsis* (Poethig, 1984; Irish and Sussex, 1992), renders the maize plant especially tractable to laser microdissection strategies owing to the unique utility of this new technology to microdissect localized gene expression patterns within plant tissues. Here we describe analyses of differential gene expression in whole maize SAMs derived from ns mutants and non-mutant siblings, genetically nearly identical tissues whose differences stem solely from the loss of NS1 homeobox gene expression in approximately 8-10 cells in the lateral SAM domain.

In microarray analyses of more than 37,000 cDNAs representing approximately 21,721 maize genes, 66 genes are identified as differentially expressed in the ns mutant SAM, which demonstrates the power of laser microdissection-microarray to focus global analyses of gene expression to discrete, developmental domains. Quantitative RT-PCR corroborated the differential expression of 18 implicated genes and identified transcripts that are enriched in maize shoot meristematic tissues. *In situ* hybridization analyses revealed previously undescribed expression patterns for 10 genes, six of which exhibit differential expression within the NS lateral domain of the SAM. Genes predicted to be involved in hormonal transport and signaling, signal transduction, and growth are especially implicated during NS-mediated leaf induction, and

potentially conserved WOX gene functions during the regulation of two component response pathways and of jasmonate-induced gene expression are identified.

RESULTS

Sixty-six Genes are Differentially Expressed in the ns Mutant SAM

Whole SAMs, comprised of the meristem proper as well as the founder cells of the incipient leaf, were laser-microdissected (Figure 3.2) from serial sections of ns mutant (genotype *ns1-R; ns2-R*) and non-mutant (genotype *Ns1/ns1-R; ns2-R*) seedlings grown under controlled conditions (see Materials and methods). Although previous analyses revealed that NS1 and NS2 perform redundant functions during maize leaf development (Scanlon et al., 1996; Scanlon and Freeling, 1997; Scanlon, 2000; Scanlon et al., 2000; Nardmann et al., 2004), the microarray experiments described herein measured differential gene expression conferred by NS1 function, given that the ns mutant and non-mutant samples analyzed in this study were all homozygous for the ns2-R mutation.

Technical barriers (described in Materials and Methods) precluded the use of our laser-microdissected RNA together with maize oligonucleotide microarrays. Therefore, following extraction and linear amplification of SAM RNA (Nakazono et al., 2003), expression profiles were generated for a combined total of 37,662 maize cDNA sequences (including approximately 21,721 maize genes) spotted onto three different microarray chips (SAM 1.1, SAM 2.0 and SAM 3.0) that were generated specifically for use in microarray analyses of the maize SAM (see Materials and Methods for descriptions of SAM chip contents; further details are provided at http://www.plantgenomics.iastate.edu/maizechip). SAM 3.0 in particular contains 10,816

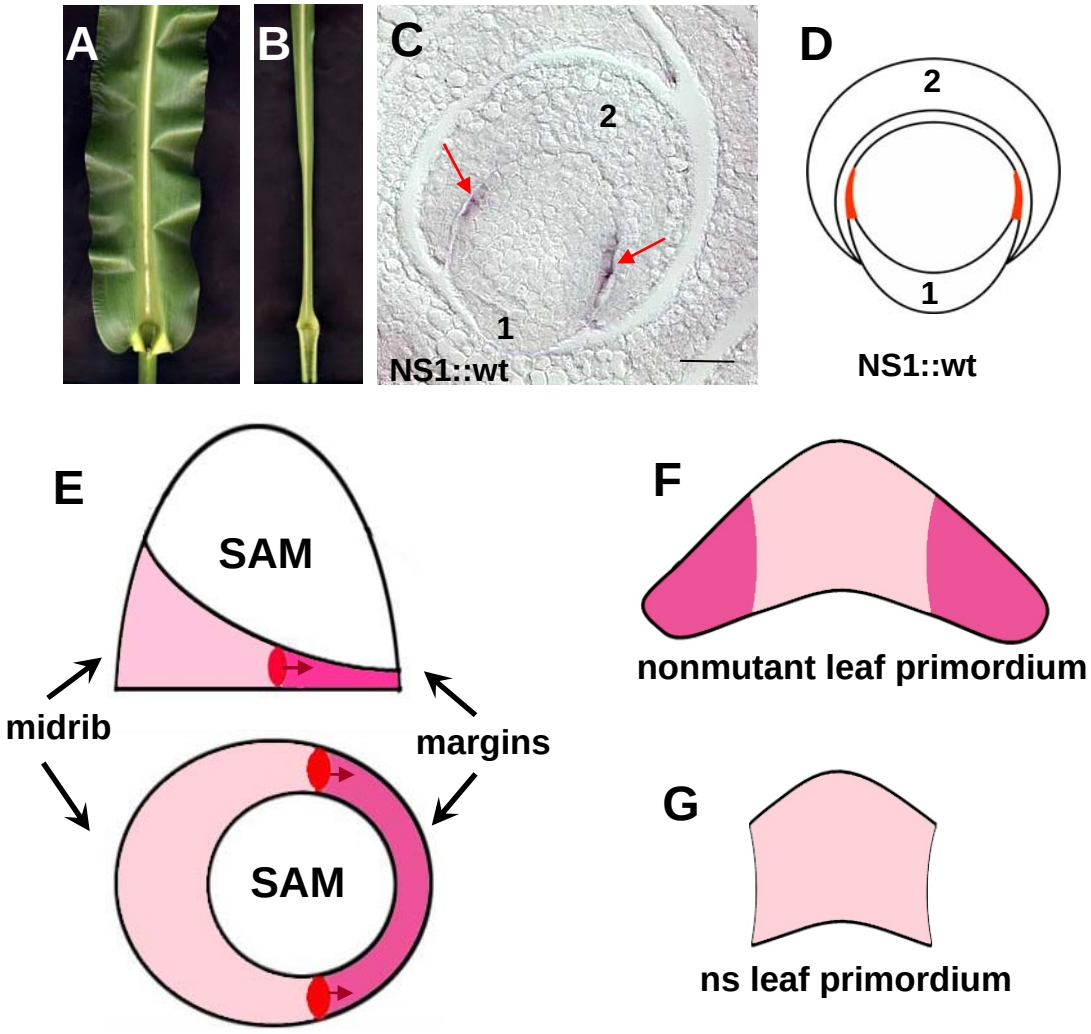

Figure 3.1 NS mutants delete lateral leaf domains due to loss of NS function in lateral foci of the SAM. (A-B) The narrow sheath mutant leaf (B) contains a developmental deletion of a large lateral domain present in non-mutant leaves (A). In situ hybridization reveals NS1 transcript accumulation (C and modeled in D) in two lateral foci during initiation of a new leaf primordium (1) from the SAM. (E) Cartoons of leaf initiation from the SAM are depicted in longitudinal (top) and transverse (bottom) sections. Leaf founder cell initiation begins on one SAM flank that gives rise to the midrib and central domain of the leaf primordium (faint pink in E-G). NS1 function (red arrows in E) is required to complete founder cell recruitment of lateral domains of the leaf

(**Figure 3.1** legend continued) that includes the margin (dark pink in E-F). Loss of the NS1 recruitment function results in failure to recruit this lateral leaf domain (G; B). Images in A-B and C are reproduced with permission from Nardmann et al., 2004.

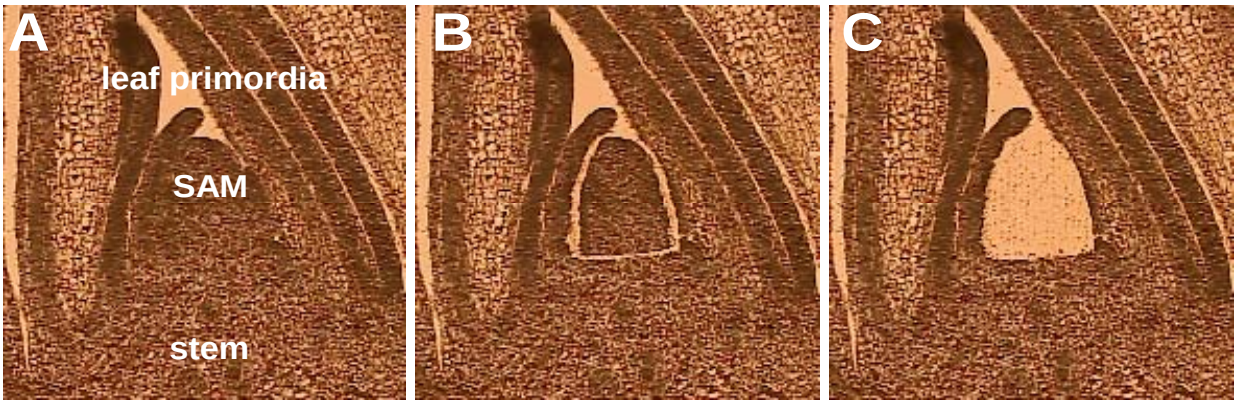

Figure 3.2 Laser microdissection of the SAM from paraffin sections of maize seedlings. (A) Apex before laser microdissection. (B) Laser ablation is used to isolate the SAM from surrounding leaf primordia and stem tissue, without heating or damaging adjacent SAM tissues. (C) SAM tissue is microdissected via laser pressure catapulting, in which the laser is focused beneath the targeted SAM tissue and a high photonic force catapults the tissue into a collection tube suspended above the sample.

sequences obtained from maize shoot apices (SAM plus four leaf primordia) as part of a SAM EST discovery program performed during this project (Emrich et al., 2007).

Six biological replicates were performed, each comprised of 10 laser-microdissected SAMs from mutant and non-mutant seedlings. For each array platform, three of the six pairs were measured with Cy3 from mutant SAMs and Cy5 dye for non-mutant. Dye assignments were reversed for the other three replications. Cy5 minus Cy3 differences were computed for each slide following normalization. The differences were used to test for evidence of differential expression between mutant and non-mutant SAMs using a linear model analysis for each gene (Nettleton, 2006) (see Material and Methods). With the intent of focusing on genes most likely to be differentially expressed, 56 genes with p-values < 0.001were selected; 10 additional genes were selected with p-values between 0.001 and 0.01 and fold changes greater than 1.5 or less than 0.67 (Table 3.1).

Bioinformatic predictions of function were performed for all genes differentially expressed in ns mutant apices and are presented at Gene Expression and Visualization Application (GENEVA:http://sam.truman.edu/), a SAM gene expression database created during this project (Buckner). Eleven functional categories are identified (Figure 3.3), including genes predicted to be involved in two-component signaling, auxin transport and signaling, jasmonate-induction/sugar signaling, intercellular transport, RNA processing, chromatin remodeling, transcription regulation, growth/cell division, ribosome structure, and general metabolism. Of the 66 genes identified in our microarray analyses, just one (DN233962) has been characterized biochemically (Asakura et al., 2003) and none have been subjected to genetic analysis in maize. In addition, nine genes of unknown function are differentially expressed in ns mutant SAMs (Table 3.1). Excluding unknowns and genes predicted to be involved in general metabolism or

Table 3.1 Genes differentially-expressed in the ns1 SAM

Accession No	Pvalue[a]	Fold change[b]	Putative Gene Identification[species]	E-Value[c]	Function[d]
CB816286	0.00015	0.61	putative jasmonate-induced protein-Ver2 lectin [H. vulgare]	9E-18	jasmonate
DN210415	8.2E-05	0.60	mannose-specific jacalin-related lectin (JAC1) [O. sativa]	3E-10	jasmonate
DN213521	0.00045	0.79	jasmonate-induced protein [T. aestivum]	4E-08	jasmonate
DN205423	0.00088	0.67	putative 32.7 kDa jasmonate-induced protein [H. vulgare]	2E-13	jasmonate
CB816294	0.00046	0.66	beta-glucosidase aggregating factor precursor-lectin [Z. mays]	3E-21	jasmonate
BQ778707	0.00036	0.66	putative jasmonate-induced protein [H. vulgare]	3E-05	jasmonate
CD001847	0.00045	0.79	Putative F-box containing protein TIR1 [O. sativa]	2E-70	auxin
DY402633	0.00084	0.79	putative ARF-GAP protein [O. sativa]	1E-65	auxin
DN233962	0.00020	1.21	histidine-containing phosphotransfer protein ZmHP1 [Z. mays]	0.00	signalling
BG840771	0.00112	1.61	response regulator-like [O. sativa]	6E-16	signalling
DN205777	6.7E-05	1.10	OsSERK1 mRNA for SERK-family receptor-like protein kinase [O. sativa]	1E-18	signalling
DN205805	0.00095	1.14	putative phosphoribosylanthranilate transferase [C. japonica]	2E-91	signalling
DN217728	0.00067	1.41	PREDICTED: similar to phosducin-like 3 [P. troglodytes]	1E-29	signaling
BM080009	8.7E-05	0.94	GTP-binding protein RAB1-like (rab1-1 gene) [P. pratensis]	3E-74	GTP-binding
DN221438	0.00060	1.15	Rab class GTP binding / guanyl nucleotide binding /signal transducer [A. thaliana]	7E-24	GTP-binding
DN206586	0.00033	0.85	GTP-binding protein [O. sativa]	2E-108	GTP-binding
DN215820	0.00061	0.90	guanyl nucleotide binding / signal transducer [A. thaliana]	1E-97	GTP-binding
DN232668	0.00074	1.29	putative GTP-binding protein ara-3 [A. thaliana]	9E-94	GTP-binding
DN211035	0.00014	0.83	putative GTP-binding protein [O. sativa]	4E-30	GTP-binding
BM078132	0.00077	0.89	partial CA8 gene for P-type ATPase [H. vulgare]	2E-44	transporter
DY400928	0.00764	0.42	putative sugar transporter protein [Z. mays]	7E-12	transporter
DN234152	0.00021	1.15	binding / transporter [A. thaliana]	3E-19	transporter
DV491557	0.00010	1.27	transporter-related [A. thaliana]	3E-75	transporter
DN225727	2.8E-05	1.11	H+-transporting two-sector ATPase [O. sativa]	5E-36	transporter
DN207731	0.00093	1.34	zinc transporter ZIP3 [O. sativa]	2E-85	transporter
BG841089	0.00010	0.86	putative nucleobase-ascorbate transporter [A. thaliana]	1E-82	transporter
DV621960	1.0E-05	0.72	DEAD BOX HELICASE [O. sativa]	3E-24	RNA biology
DV493987	4.7E-05	1.19	putative DNA-directed RNA polymerase [A. thaliana]	4E-26	RNA biology
BI361046	3.6E-05	1.55	RNA-directed DNA polymerase [M. truncatula]	2E-09	RNA biology
BG458643	0.00070	1.32	putative hUPF2 [O. sativa]	1E-62	RNA biology
BM080869	0.00065	0.85	putative splicing regulatory protein [O. sativa]	7E-41	RNA biology
AW066904	0.00030	1.26	RNA Recognition Motif (RRM) protein [O. sativa]	4E-110	RNA biology
DV942355	0.00080	1.51	maturase [Z. mays]	1E-04	RNA biology
AI820200	3.4E-06	1.23	putative amine oxidase 1 [A. thaliana]	8E-17	chromatin remodeling
DN224375	0.00080	0.90	Ohio43 HMG-like nucleosome/chromatin assembly factor D (nfd101) [Z. mays]	6E-135	chromatin remodeling
DV490133	0.00392	1.70	putative transcription factor (myb) [O. sativa]	3E-09	transcription factor

Table 3.1 (continued): Genes differentially-expressed in the ns1 SAM

Accession No	Pvalue	Fold change	Putative Gene Identification[species]	E-Value	Function
BM073866	0.00095	0.83	transcription factor (Rev136-2) [Vitis riparia]	2E-18	transcription factor
CD650947	0.00199	0.62	YABBY-related protein [T. aestivum]	1E-48	transcription factor
DN232259	0.00082	0.82	nucleoside diphosphate kinase (SoNDPK1) [S. officinarum]	1E-110	growth
CB381550	3.8E-05	0.74	cell division FtsZ protein [G. lutea]	3E-85	growth
DN228991	0.00093	0.69	structural constituent of ribosome GHS1 [A. thaliana]	2E-09	ribosome
DN231080	0.00055	0.85	60S ribosomal protein L34 [N. tabacum]	3E-52	ribosome
CB331743	0.00059	0.89	putative ribosomal protein L32 [O. sativa]	5E-56	ribosome
CB816451	0.00010	0.81	putative 40S ribosomal protein [O. sativa]	2E-76	ribosome
DN219087	0.00036	0.85	60S ribosomal protein L7A [A. thaliana]	2E-92	ribosome
DN204688	0.00074	0.82	acyltransferase/ dihydrolipoyllysine-residue acetyltransferase/ protein binding LTA3 [A. thaliana]	5E-40	metabolism
DN210237	1.5E-05	1.23	lysine ketoglutarate reductase/saccharopine dehydrogenase (LKRSDH) [Z. mays]	3E-108	metabolism
BM380298	0.00588	0.63	putative 2-oxoglutarate-dependent dioxygenase [O. sativa]	3E-30	metabolism
BM266800	0.00082	1.26	cinnamoyl-CoA reductase [Z. mays]	5E-59	metabolism
DN217167	0.00060	0.87	unknown protein [A. thaliana]	1E-25	unknown
DN232420	0.00079	0.90	unkown protein [Z. mays]	1E-13	unknown
BG946630	0.00927	1.54	no significance similarity found		unknown
BI096810	0.00258	1.60	no significance similarity found		unknown
DN207440	0.00016	1.40	no significance similarity found		unknown
DN207757	0.00097	1.25	no significance similarity found		unknown
DN224044	0.00031	0.87	no significance similarity found		unknown
DN233672	0.00084	1.18	no significance similarity found		unknown
DY576324	0.00143	0.08	no significance similarity found		unknown
BG462729	0.00088	0.52	nucellin-like aspartic protease [Z. mays]	1E-118	others
DV492114	0.00010	1.18	putative interferon-related protein [O. sativa]	7E-60	others
DN210635	0.00069	0.86	TPA_inf: prx3 gene for class III peroxidase 3 precursor [O. sativa]	1E-99	others
BI396270	0.00060	1.32	endonuclease V protein-like [O. sativa]	8E-23	others
DV551351	0.00020	1.49	translation initiation factor isopentenyl-diphosphate delta isomerase 2 [Z. mays]	1E-86	others
DV491384	0.00031	0.32	mitochondrial uncoupling protein 1 [Saccharum officinarum]	2E-09	others
BG518167	0.00836	0.62	putative proline-rich protein [O. sativa]	1E-21	others
BI359303	0.00771	1.52	cytochrome b6/f complex subunit V; petE [O. sativa]	1E-18	others

[a] p-Values calculated as described in Materials and Methods.

[b] Fold change presented as relative abundance of transcript in ns mutant SAM/nonmutant SAM.

[c] Expectation value for alignment of maize gene to putative gene identification.

[d] General category of predicted gene function in maize.

"housekeeping" function, 28 out of the remaining 40 genes are predicted to be involved in some aspect of signal transduction or cell differentiation/growth. In order to ensure that the cells comprising the SAM lateral domains were not injured or degraded due to proximity to the UV laser during microdissection, internal controls included comparisons of *ns2* transcript abundance in laser-microdissected SAMs versus whole seedlings. qRT-PCR and microarray data confirmed that *ns2* expression is indeed enriched in the laser-microdissected SAM samples (data not shown), suggesting that the SAM lateral domains are not compromised by the UV laser-microdissection procedure. The identification of additional, previously uncharacterized gene expression within the SAM lateral domain (described below) provides further proof that these SAM domains were not destroyed during microdissection.

qRT-PCR and *in situ* Hybridizations are Used to Corroborate Microarray Data and Identify SAM Domain-Specific Differential Expression

Quantitative RT-PCR (qRT-PCR) of cDNA prepared from RNA microdissected from ns and non-mutant SAMs corroborated the differential expression of 18 out of 22 genes tested, whose microarray fold changes were large enough to detect by qRT-PCR methodology (i.e. fold changes $\leq$ 0.67 and $\geq$ 1.5; Table 3.2). Overall, the qRT-PCR and microarray data exhibited remarkable agreement in quantitative fold change between ns mutant and non-mutant SAMs (Pearson correlation coefficient was 0.856, r^2=0.733, p=0.000006). Four genes originally detected as differentially expressed in ns apices by microarray analyses could not be verified by qRT-PCR and were removed from further consideration. One such false positive gene encoding a predicted F-Box protein (BM078718) may have been detected by cross-hybridization to a TIR1-like F-box gene (CD001847) that was later verified as differentially expressed via *in situ*

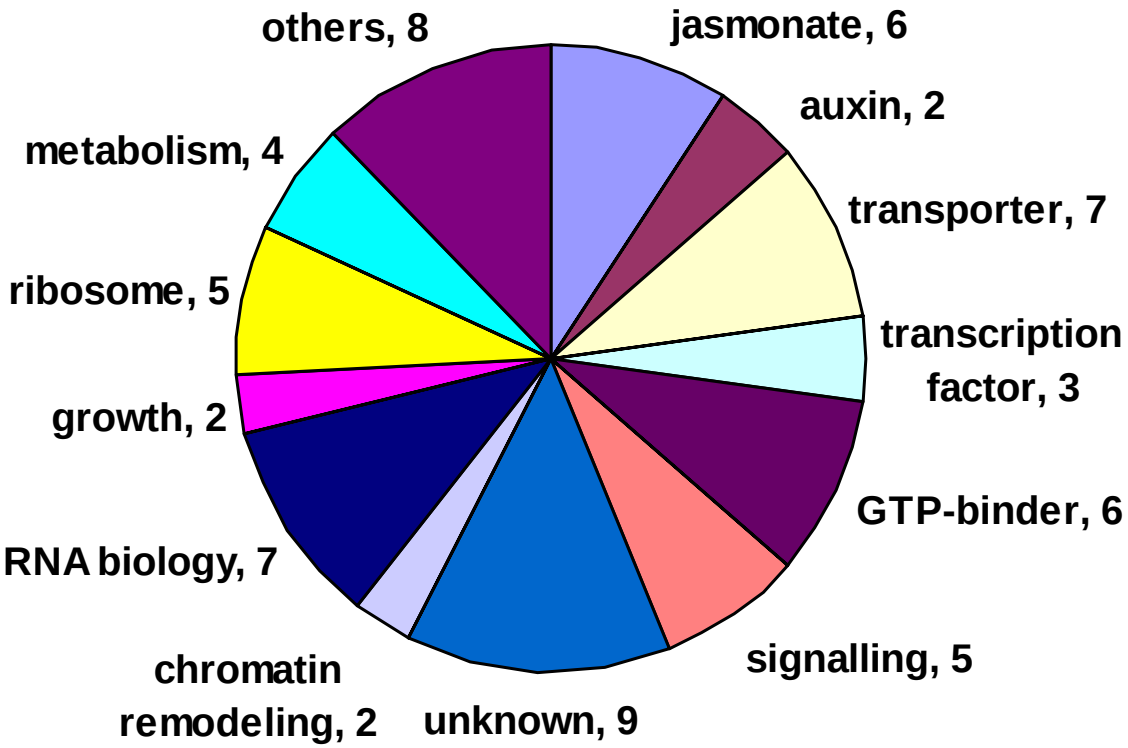

Figure 3.3 Predicted functions of 66 genes differentially expressed in the ns1-R mutant SAM. Excluding unknowns and housekeeping genes, 28/40 genes are predicted to function during hormonal-cellular signaling or growth and cell division.

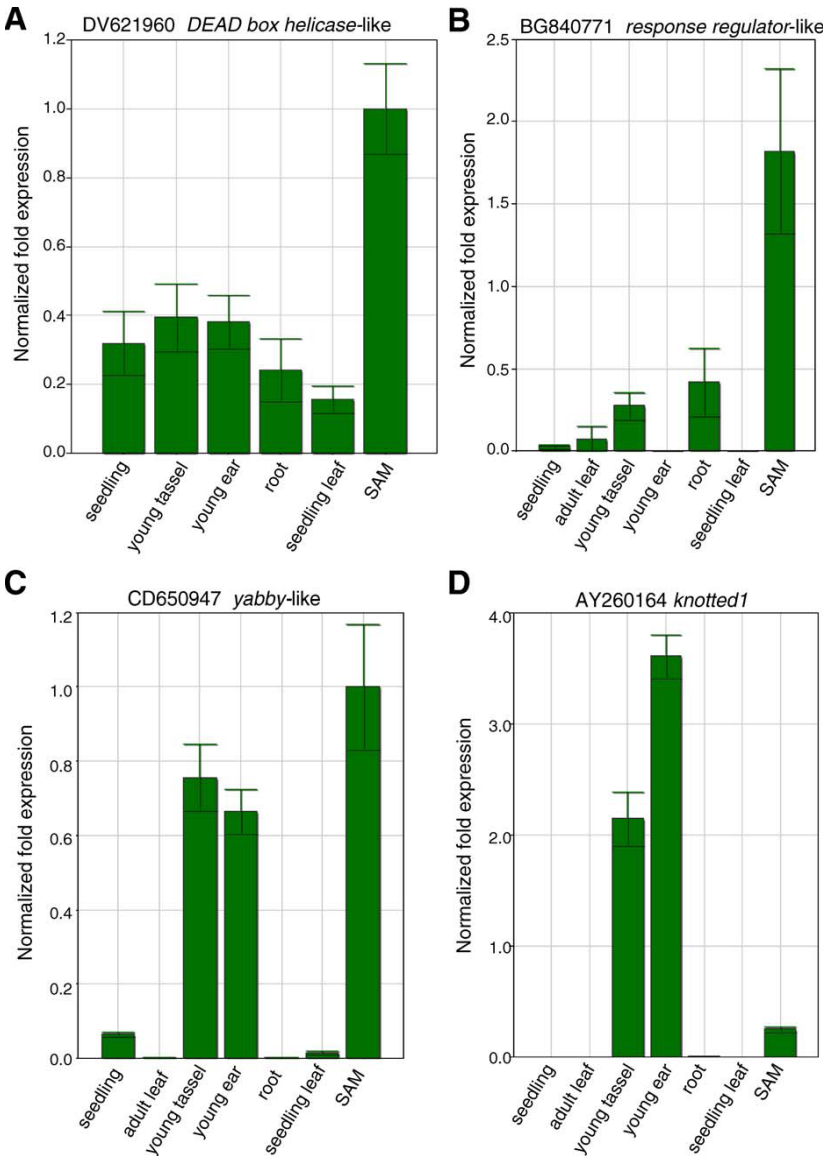

Figure 3.4 Identification of shoot meristem-enriched maize transcripts by qRT-PCR analyses of multiple maize tissues. (A) Transcripts of the *DEAD box helicase*-like gene DV621960 and the (B) *response regulator*-like gene BG840771 are enriched in the SAM, whereas (C) the *yabby*-like gene CD650947 is upregulated in inflorescence tissues bearing floral meristems as well as in the SAM. (D) Control expression pattern of *knotted1*(AY260164), which is enriched in shoot meristems.

hybridization (described below; Figure 3.5 I-L). This example illustrates one drawback to the use of long cDNA arrays in expression profiling, and underscore the importance of secondary verification of microarray data by qRT-PCR and *in situ* hybridization.

As part of a larger effort (http://maize-meristems.plantgenomics.iastate.edu/) to identify maize genes whose expression is enriched in shoot meristems, qRT-PCR analyses of transcript accumulation in a variety of maize tissues were performed for thirteen genes contained in Table 3.1 (Figure 3.4; data not shown). Maize tissues examined in these analyses included the vegetative SAM, immature tassel inflorescence, immature ear inflorescence, whole seedlings, expanded mature leaves, expanded seedling leaves, and seedling root (see Materials and Methods). In addition, *in situ* hybridization was used to characterize the expression patterns of fourteen differentially expressed maize genes, four of which exhibited weak or indiscernible staining and could not be interpreted. Ten genes examined via *in situ* hybridization of maize apices yielded interesting mRNA accumulation patterns (Figures 3.5-3.6); six of which exhibited lateral SAM domain-specific differential expression and are thereby predicted candidate genes functioning within or nearby the NS expression foci (Figure 3.1 C) during maize leaf initiation.

For example, a predicted *DEAD box helicase* gene (DV621960) is expressed in the lateral founder cell regions of the initiating nonmutant leaf primordium (red arrows in Figure 3.5 A), whereas no expression is noted in ns mutant sibling SAMs (Figure 3.5 A-D). These *in situ* hybridization data are in agreement with our microarray data (Table 3.1), which indicated that expression of DV621960 is significantly down-regulated in ns apices (p-value = 1.0E-05). Characterized by their shared ability to unwind RNA helices, the 32 DEAD box HELICASE proteins of *Arabidopsis* are implicated in a variety of RNA-metabolic processes (including transcription and pre-mRNA splicing, ribosome biogenesis and translation, gene expression and

meristematic cell division) although their functions as yet described are specific and non-interchangeable (Aubourg et al., 1999; Linder, 2006). Indeed, qRT-PCR analyses of DV621960 transcript accumulation in various maize tissues reveal that expression of this maize *DEAD box helicase*-like gene is enriched in the SAM (Figure 3.4A). Moreover, the lateral SAM domain-specific differential accumulation of DV621960 suggests that its expression is activated by NS function and is related to founder-cell recruitment. As described below, the lateral domain-specific differential expression of five additional maize genes (CD001847; DN210415; DN233962; DN221438; DN232668) in the ns mutant SAM implies that domain-specific hormonal and signaling mechanisms are important during maize leaf initiation.

Two-Component Signaling Pathway(s) Implicated in NS Function: SAM-Enriched and Domain-Specific Differential Expression

Two-component response regulators comprise an evolutionarily conserved signal transduction pathway involving the transfer of phosphate from a sensor HISTIDINE KINASE (HK) to a RESPONSE REGULATOR (ARR) effector molecule (Mizuno, 2005). HISTIDINE PHOSPHOTRANSFER (HP) proteins mediate these exchanges, whereupon the phosphorylated ARR regulates the activation of specific cellular responses. In plants the two-component system is implicated in numerous developmental functions including responses to ethylene and cytokinin (Hass et al., 2004; To et al., 2004), whereas pseudo-response regulators function to control circadian rhythms (Strayer et al., 2000). Previously, microarray analyses of WUS1 induction revealed that four *Arabidopsis arr* genes are direct targets of WUS1 transcriptional repression (Leibfried et al., 2005).

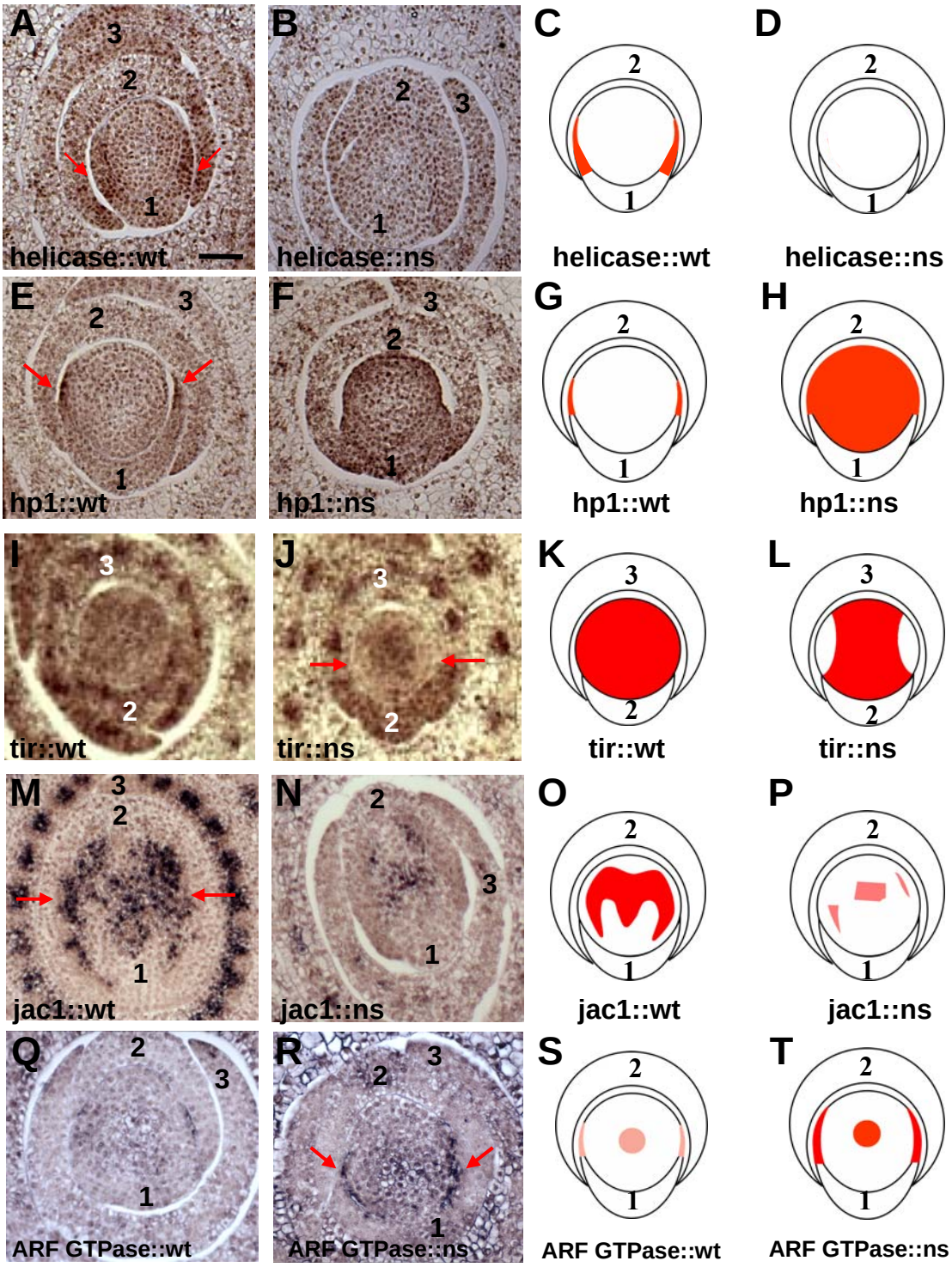

Figure 3.5 *In situ* hybridization reveals domain-specific expression of differentially expressed maize genes in non-mutant (wt:A;E;I;M;Q) and ns1-R mutant (ns:B;F;J;N;R) shoot apices, part I.

(**Figure 3.5** legend continued) Cartoons of SAM expression patterns are modeled in (C-D;G-H; K-L; O-P;S-T). No expression in leaf primordia is portrayed in cartoons, since transcripts accumulating in leaves were not LM sampled or reflected in microarray data. Probes were made from maize ESTs: DV621960; A-B) ; CD001847 (E-F); DN210415 (I-J); DN233962 (M-N) and DN221438 (Q-R). Predicted functions are abbreviated as: helicase (DEAD BOX HELICASE); hp1 (HISTIDINE PHOSPHOTRANSFER PROTEIN1); tir1 (TRANSPORT INHIBITOR RESPONSE F-BOX protein); jac1 (JACALIN-related LECTIN); and GTPase (Rab class GTP-BINDING SIGNAL TRANSDUCER). Numbers denote leaf primordia. Analyses of expression patterns are provided in the text.

Table 3. 2 qRT-PCR corroboration of ns1-R differentially expressed genes

Accession No	P-Value[a]	Putative Gene Identification [species]	E-Value[b]	microarray foldchange[c]	qRT-PCR foldchange[d]	ΔCt±std in qRT-PCR
DY400928	0.00800	putative sugar transporter protein [Z. mays]	7E-12	0.42	0.11	3.18±0.11
CB816294	0.00046	beta-glucosidase aggregating factor precursor-lectin [Z mays]	3E-21	0.66	0.28	1.83±0.49
BQ778707	0.00036	putative jasmonate-induced protein [H. vulgare]	3E-05	0.66	0.43	1.22±0.51
CB816286	0.00014	putative jasmonate-induced protein-Ver2 lectin [H.vulgare]	9E-18	0.61	0.66	0.59±0.19
DN205423	0.00088	beta-glucosidase aggregating factor precursor [Z. mays]	2E-13	0.67	0.60	0.75±0.55
CD650947	0.00199	YABBY-related protein [T. aestivum]	1E-48	0.62	0.65	0.62±0.23
BG840771	0.00112	response regulator-like [O. sativa]	6E-16	1.61	4.05	-2.02±0.25
DV490133	0.00400	putative transcription factor (myb) [O. sativa]	3E-09	1.70	1.66	-0.73±0.12
BI361046	3.6E-05	RNA-directed DNA polymerase [M. truncatula]	2E-09	1.55	2.77	-1.47±0.14
BG462729	0.00088	nucellin-like aspartic protease [Z. mays]	1E-118	0.52	0.04	4.61±0.58
BG518167	0.00836	putative proline-rich protein [O. sativa]	1E-21	0.62	0.33	1.59±0.68
BM380298	0.00588	putative 2-oxoglutarate-dependent dioxygenase [O. sativa]	3E-30	0.63	0.63	0.67±0.31
BI359303	0.00771	cytochrome b6/f complex subunit V; petE [O. sativa]	1E-18	1.52	3.20	-1.68±0.46
DV491384	0.00031	mitochondrial uncoupling protein 1 [S. officinarum]	2E-09	0.32	0.15	2.70±0.16
DY576324	0.00143	no significance similarity found		0.08	0.06	4.16±0.24
BG946630	0.00927	no significance similarity found		1.54	1.72	-0.78±0.17
BI096810	0.00258	no significance similarity found		1.60	1.99	-0.99±0.32
DV942355	0.00080	maturase [Z. mays]	1E-04	1.51	1.74	-0.80±0.26

[a] p-Values calculated as described in Materials and Methods.

[b] Expectation value for alignment of maize gene to putative gene identification.

[c] Fold change presented as relative abundance of transcript in ns mutant SAM/nonmutant SAM.

[d] Fold change presented as relative abundance of transcript.

Both the predicted maize response regulator gene BG840771 and the maize phosphotransfer gene Zm*hp1* (DN233962) are upregulated in the ns mutant SAM (Table 3.1). qRT-PCR reveals that transcripts from the predicted response regulator gene BG840771 accumulate to 4.05 fold higher in the ns SAM (Table 3.2), which is consistent with our microarray data (Table 3.1). In addition, tissue-specific qRT-PCR revealed that transcripts of BG840771 are especially abundant in the vegetative SAM as compared to other maize tissues (Figure 3.4 B). These data further illustrate the utility of laser microdissection-microarray analyses to identify new genes whose expression, and implicated function, is likely to be enriched in the SAM.

ZmHP1 has been shown to function *in vitro* as a phospho-donor for the maize response regulators ZmRR1, ZmRR4, ZmRR8 and ZmRR9, whereas accumulation of ZmHP1 in both the cytoplasm and nucleus is consistent with its predicted function during two-component signaling (Asakura et al., 2003). *In situ* hybridization of *Zmhp1* reveals transcript accumulation at two lateral foci within the non-mutant SAM (red arrows in Figure 3.5 E,G), which mimics the *ns* expression domain (Figure 3.2 C) (Nardmann et al., 2004). In contrast, *Zmhp1* transcripts accumulate throughout the ns mutant SAM (Figure 3.5 F, H); this upregulated mutant expression is consistent with our microarray data (Table 3.1).

Auxin Transport and Response Genes are Differentially Expressed in the narrow sheath1-R SAM

Polar auxin transport (PAT) is required for leaf initiation and lateral margin development in plants (Reinhardt et al., 2000; Scanlon, 2003). Auxin is transported to sites of leaf initiation via the PINFORMED1 (PIN) family of efflux proteins (Benkova et al., 2003; Friml et al., 2003;

Reinhardt et al., 2003; Heisler et al., 2005), a process that requires ARF-GAP-mediated vesicular cycling of PIN proteins (Geldner et al., 2003; Sieburth et al., 2006). Auxin signaling involves targeted proteolysis of transcriptional regulators wherein the F-box protein TIR1 functions as an auxin receptor (Dharmasiri et al., 2005; Kepinski and Leyser, 2005).

Two genes predicted to be involved in auxin biology are down-regulated in our analyses of ns mutant SAMs (Table 3.1), including a putative ARF-GAP encoding gene (DY402633) with predicted orthology to the *Arabidopsis van3/scf1* gene required for vesicle trafficking and PIN recycling (Koizumi et al., 2005; Sieburth et al., 2006) and the predicted maize orthologue of the *tir1* auxin receptor (CD001847). Whereas *in situ* hybridizations reveal that *Zm*tir1* is expressed throughout the non-mutant SAM as well as in the margins and vasculature of leaf primordia (Figure 3.5 I, K), *Zm*tir1* transcript abundance is diminished specifically in the lateral domain of the ns mutant SAM (red arrows in Figure 3.5 J, L). These data suggest that auxin transport and auxin signaling are correlated with NS-mediated recruitment of leaf founder cells within this lateral SAM domain.

Jasmonate-Induced Sugar-Binding Genes Upregulated by NS Function

Six genes predicted to be induced by jasmonate, a phytohormone functioning during plant development and defense (Lorenzo and Solano, 2005), are down-regulated in the ns mutant SAM (Table 3.1). Auxin signaling induces jasmonate responses and both hormones share common downstream signaling pathways (Tiryaki and Staswick, 2002; Grossmann et al., 2004; Nagpal et al., 2005), suggesting that down-regulation of jasmonate responses in ns apices might be related to defects in auxin signaling. Notably, all the jasmonate-induced genes identified herein encode putative lectins, carbohydrate-binding receptor proteins that are implicated during

sugar transport in plants (Van Damme et al., 2004). qRT-PCR corroborated the differential expression of four jasmonate-induced genes (Table 3.2), and *in situ* hybridization of a putative jacalin-related LECTIN encoding gene (DN210415) reveals a butterfly-shaped expression pattern at the insertion of the leaf primordium into the apex (Figure 3.5 M, O). The "wings" of this expression pattern (red arrows in Figure 3.5 M) are diminished or absent in ns mutants (Figure 3.5 N, P), revealing down-regulated *lectin* mRNA accumulation in lateral domains of the mutant apex. Although transcript accumulation in leaf primordia was not measured in our microarray analyses, DN21415 transcripts are also detected in the vasculature of non-mutant leaves and are not detected in ns mutant leaf primordia. Notably, the apparent *Arabidopsis* orthologue of this particular jacalin-related *lectin* gene is known to be a direct target of the NS-related WOX protein WUS1 (Leibfried et al., 2005). Furthermore, a putative sugar transporter encoding gene (DY400928) was qRT-PCR-verified as down-regulated (0.11 fold compared to non-mutant) in the ns mutant SAM (Table 3.2), implying further that sugar transport and/or sugar signaling is required for NS function. *In situ* hybridization reveals accumulation of this putative *sugar-transporter* transcript in initiating leaf primordia, and in leaf vascular traces within the non-mutant apex (Figure 3.6 E-H).

Differential Expression of GTP-Binding Proteins Suggests that Multiple Signaling Networks are Operating During NS-Mediated Recruitment of Leaf Founder Cells

Transcriptome analyses of ns mutant SAMs suggest that numerous GTP-binding proteins are involved during NARROW SHEATH1 signaling within the initiating maize leaf. Six genes predicted to encode GTP-binding proteins are significantly mis-expressed in the ns mutant (Table 3.1), including genes predicted to be involved in vesicle trafficking (three Rab GTPases

and an ADP-ribosylation factor (ARF) GTPase), signal transduction (a heterotrimeric G protein), and cell growth and division (a GTP1/OBG family GTPase) (Jones and Assmann, 2004).

In the non-mutant SAM, transcripts encoding a putative Rab-class ARF-GTPase (DN221438) are detected in the meristem center, as well as in lateral stripes overlapping the NS functional domain (red arrows in Figure 3.5 Q, S). In the ns mutant SAM, the lateral expression of DN221438 is wider and more pronounced (Figure 3.5 R, T), consistent with the upregulation observed in microarray hybridizations and implicating NS during negative regulation of this putative ARF-GTPase encoding gene. Likewise, a second predicted Rab-class GTPase encoding gene (DN232668) homologous to the *Arabidopsis* GTP-binding protein gene *ara3* (Moshkov et al., 2003) is also upregulated in the ns mutant SAM (Table 3.1). *In situ* hybridization reveals that the *ara3*-like GTPase (DN232668) gene is expressed in the midrib/central founder-cell domain of the non-mutant SAM (red arrows in Figure 3.6 A, C), whereas in mutant apices loss of NS function results in the expansion of this expression domain into the lateral SAM domain and thereby encompasses the entire founder-cell ribbon (Figure 3.6 B, D).

New Maize Genes Predicted to be Involved in Chromatin Remodeling, Cell Division, and Growth are Differentially Expressed in the ns Mutant SAM

Two maize genes with predicted functions in chromatin remodeling (AI820200 and DN224375) are significantly differentially expressed in ns mutant apices (Table 3.2). *In situ* hybridizations reveal that one such gene, encoding a predicted *amine oxidase* implicated in histone modification (Shi et al., 2004), is unexpectedly upregulated in the midrib/central domain as well as in the lateral domain of ns mutant founder cells (Figure 3.6 I-L).

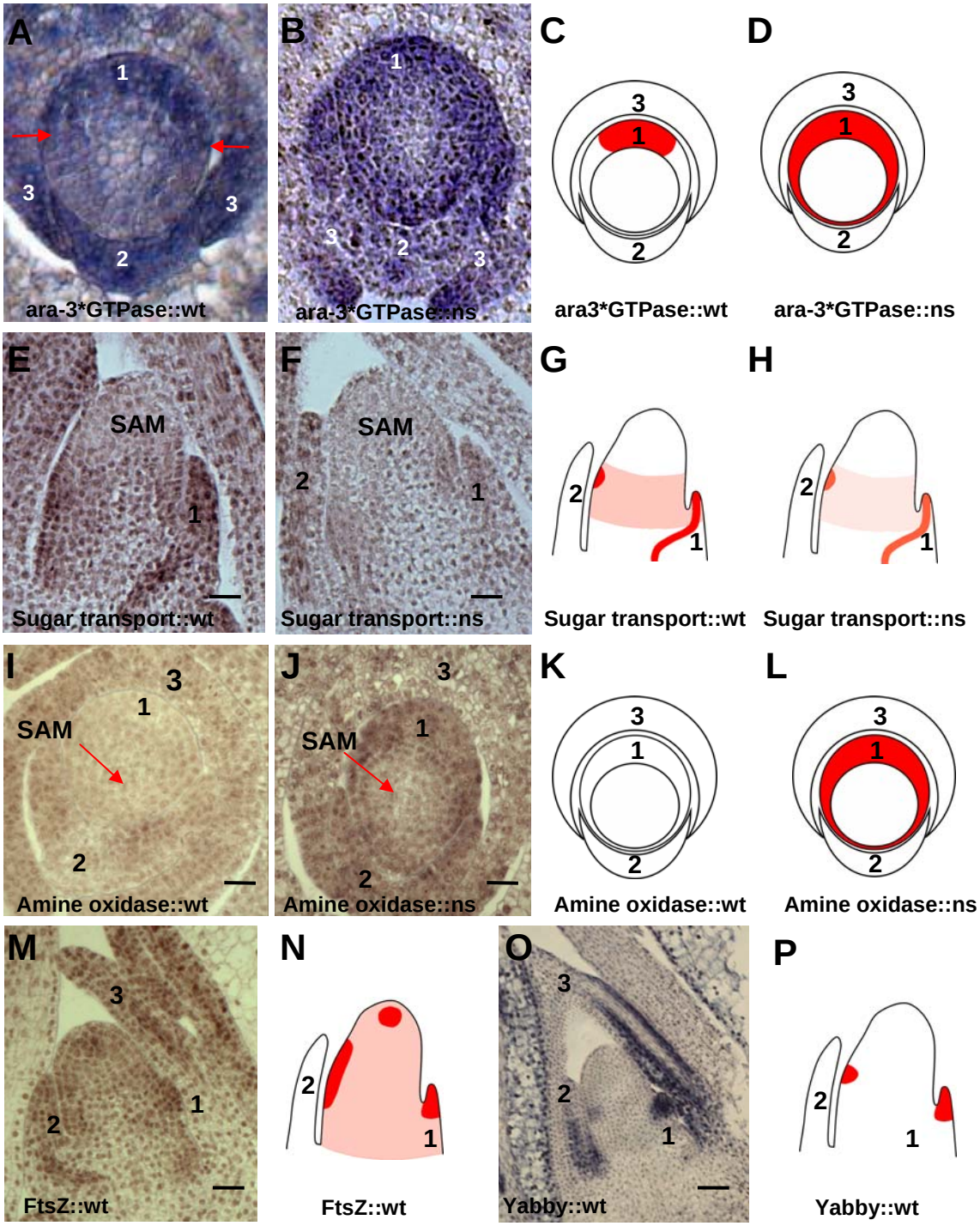

Figure 3.6 *In situ* hybridization reveals domain-specific expression of differentially expressed maize genes in non-mutant (wt:A;E;I;M;O)and ns1-R mutant (ns:B;F;J) shoot apices, part II.

(**Figure 3.6** legend continued) Cartoons of SAM expression patterns are modeled in (C-D;G-H; K-L; N and P). No expression in leaf primordia is portrayed in cartoons, since transcripts accumulating in leaves were not LM sampled or reflected in microarray data. Probes were made from maize ESTs: DN232668 (A-B); DY400928 (E-F); AI820200 (I-J); CB381550 (M) and CD650947 (O). Predicted functions are abbreviated as: ara GTPase (GTP-BINDING PROTEIN ARA-3); sugar trans (SUGAR TRANSPORTER PROTEIN); amine oxidase (AMINE OXIDASE1); FtsZ (CELL DIVISION FTSZ PROTEIN); and Yabby (YABBY-RELATED PROTEIN). Numbers denote leaf primordia. Analyses of expression patterns are provided in the text.

A maize *ftsZ*-related gene (CB381550) is significantly down-regulated in the ns mutant SAM (Table 3.1), and shares homology with *Arabidopsis* genes encoding tubulin-like, structural proteins required for cell division in chloroplasts (Osteryoung et al., 1998). *In situ* hybridizations of non-chlorophyllic maize apices reveal *ftsZ*-like transcript accumulation in actively dividing tissues including young leaf primordia and leaf founder cells, as well as in the SAM apical tip (Figure 3.6 M-N). Although statistical parameters suggest robust support for differential expression of this gene in each of our six biological replicate samples (p-value = 3.8E-05), no domain-specific differences in CB381550 expression are observed *in situ* hybridizations of ns samples. It is likely that in the absence of domain-specific changes in mRNA localization, our *in situ* hybridization protocols are unable to discriminate a 0.72 fold quantitative change in transcript accumulation.

Lastly, a previously undescribed maize *yabby*-like gene (CD650947), the putative orthologue of the *drooping leaf* gene of rice (Yamaguchi et al., 2004), is also down-regulated in our analyses of ns mutants. In non-mutant apices *yabby*-like transcripts accumulate in newly initiating leaf primordia (Figure 3.6 O-P), an expression pattern that is consistent with the predicted role of YABBY proteins during initiation and expansion of lateral organ primordia (Eshed et al., 2004; Juarez et al., 2004; Yamaguchi et al., 2004). No domain-specific changes in mRNA accumulation are noted in ns apices, however qRT-PCR corroborates the down-regulation of this maize *yabby*-like gene in the ns mutant SAM that was observed in microarray analyses (Table 3.2). Furthermore, tissue specific qRT-PCR reveals that transcripts of the *yabby*-like gene CD650947 accumulate in the SAM as well as in shoot meristem-enriched tissues such as the young tassel and young ear, each of which bears numerous spikelet and spikelet pair meristems (Figure 3.4 C).

DISCUSSION

Laser Microdissection-Microarray is a Useful Technology to Identify Genes Expressed in Micro-Domains of Plant Tissues

The power of laser microdissection to focus microarray comparisons to small developmental fields is demonstrated in these analyses of ns mutant and non-mutant SAMs. Among the genes represented in this relatively small dataset are a number of likely candidates implicated during NS-mediated leaf initiation and predicted to function in hormonal signaling, signal transduction, or growth (discussed below). Although the primary developmental function of NS is shown to be localized in the shoot apex during recruitment of leaf founder cells in a lateral domain of the SAM (Scanlon et al., 1996; Scanlon and Freeling, 1997; Scanlon, 2000), loss of NS function is predicted to cause widespread changes in gene expression in the growing seedling owing to enormous differences in the differentiation and expansion of marginal/lateral leaf tissues that happens during normal leaf development downstream of NS function. The differential gene expression that ensues in mutant leaves following the ns-induced leaf domain deletion event is unlikely to address our experimental question, namely, the mechanisms of founder cell recruitment.

Microarray analyses of the ns SAM provide a resource for new gene discovery; of the 66 differentially expressed genes identified in these analyses, all but one are previously undescribed maize genes and at least three exhibit enriched transcription in maize shoot meristematic tissues (Figure 3.4). In addition, six candidate genes chosen for *in situ* hybridization analyses exhibited differential expression within or overlapping the SAM lateral domain of NS function and expression (Figure 3.5-3.6; Figure 3.1) (Scanlon, 2000; Nardmann et al., 2004). Our data illustrate the combined utility of *in situ* hybridization and LM technology to focus microarray

comparisons to a discrete developmental field, thereby limiting the number of identified differentially expressed genes to those transcribed in close vicinity to the domain of NS function.

Although the use of six biological replicates enabled the selection of ns differentially expressed genes, it is noted that the majority of the candidate genes represented in Table 3.1 exhibit relatively modest fold-changes in expression level. This result was expected, considering that the NS micro-domain of expression and function comprises a relatively small number of cells in the lower lateral region of the maize shoot apex (Figure 3.1 C) (Scanlon, 2000; Nardmann et al., 2004). During SAM laser microdissection (Figure 3.2) the RNA contribution of cells comprising the NS lateral domain is diluted by RNA collected from the rest of maize SAM, which may explain the relatively low fold changes observed in our microarray analyses. Unfortunately, without the use of technically prohibitive NS expression markers during laser microdissection of the SAM, reliable microdissection of the NS lateral micro-domain away from the rest of the SAM proper is not feasible.

Analyses of NS Function Suggest that Multiple Hormonal and Signaling Pathways are Involved in the Recruitment of Maize Leaf Founder Cells

Excluding genes of unpredicted function, the majority of transcripts differentially expressed in the ns SAM (28/40) are putatively involved in some aspect of developmental signaling or growth regulation (Table 3.1). These include genes involved in two-component response pathways, auxin signaling, jasmonate-induced pathways, as well as GTP-binding proteins implicated during signal transduction or cellular trafficking. These results are consistent with previous models for NS function during transduction of a cell-autonomous, founder-cell recruitment signal required for maize leaf initiation. Especially intriguing are those genes whose

expression domains mirror or overlap the NS lateral foci (Figure 3.5; Figure 3.6 A-D). We hypothesize that these co-expressed genes may function closely downstream of NS. Subsequent reverse genetic and molecular/biochemical analyses of these implicated genes will test this hypothesis and help to elucidate the NS signaling pathway.

Our microarray data and *in situ* hybridization analyses of the maize *tir1*-like gene (CD001847; Figure 3.5 I-L) suggest that auxin activity is involved in NS-mediated recruitment of leaf founder-cells in the lateral domain of the maize SAM. Previous analyses among multiple laboratories implicate PIN-mediated auxin transport during leaf initiation, and leaf initiation correlates with *knox* gene down regulation within the SAM (Smith et al., 1992; Jackson et al., 1994; Long et al., 1996). More recent studies established a mechanistic link between these two correlated phenomena, illustrating that *knox* down regulation requires auxin (Scanlon, 2003; Hay et al., 2006). Initial analyses of NS function revealed that ns mutants fail to down-regulate KNOX accumulation in the lateral domain of the SAM, which correlates with the failure to recruit founder-cells from this meristem domain (Scanlon et al., 1996; Scanlon and Freeling, 1997). In light of the recently established links between *knox* down-regulation, leaf initiation and auxin activity, our microarray analyses and *Zm*tir1* expression data suggest that NS-mediated founder cell recruitment and KNOX down-regulation require TIR-mediated auxin signaling within the SAM lateral domain.

In addition, the expression of six genes predicted to encode jasmonate-induced lectins is consistently down regulated in the ns mutant SAM (Table 3.1). Lectins are carbohydrate-binding proteins that function to facilitate the intercellular transport of sugars (Van Damme et al., 2004). *In situ* hybridization of a jacalin-related *lectin* gene (DN210415) reveals a pattern of transcript accumulation that spreads laterally at the insertion site of the newly-initiated leaf

primordium into the shoot (Figure 3.5 M-P). The decreased lateral accumulation of DN210415 transcripts in ns mutant shoots suggests that NS promotes the novel expression pattern of this jasmonate-induced gene.

Likewise, a predicted sugar transporter gene (DY400928) is under expressed in ns 1-R mutants (Table 3.1; Table 3.2; Figure 3.6 E-H), which further implicates a role for carbohydrate transport during NS function. Numerous studies reveal a hormone-like role for sugar signaling in plants, in which carbohydrate transport regulates gene transcription (Rolland et al., 2006). Subsequent analyses are required to determine if this putative sugar transporter and the jasmonate-induced lectins perform metabolic functions or signaling functions during NS-mediated founder-cell recruitment.

Conserved WOX Gene Functions Suggested by Microarray Analyses of ns Mutant Apices

At present, *ns1* and its duplicated paralogue *ns2* are the only maize *wox* genes for which genetic analyses of function are described. *Arabidopsis* includes 15 WOX family members (Haecker et al., 2004), seven of which have been subjected to genetic analyses (WUS1 (Mayer et al., 1998); PRESSED FLOWER/WOX3 (Matsumoto and Okada, 2001); WOX2 (Haecker et al., 2004); PRETTY FEW SEEDS2/WOX6 (Park et al., 2005); STIMPY/WOX9 (Wu et al., 2005); WOX5 (Gonzali et al., 2005); WOX4:Ji and Scanlon, unpublished data). Although the phenotypes of individual WOX mutants are varied (affecting shoot and root meristems, embryogenesis, organogenesis of lateral organs and the vascular procambium), the combined genetic and molecular expression data suggest that an evolutionarily-conserved general function of WOX proteins is to promote the organization of embryonic/meristematic cells or lateral organ initials. For example, WUS1 organizes proliferation in the central zone of *Arabidopsis* shoot

meristems via repressing the transcription of several two-component response regulator genes (ARR5, ARR6, ARR7 and ARR15), which function to reduce SAM size (Leibfried et al., 2005).

Meanwhile, our analyses demonstrate that NS is required to repress the expression of two maize genes predicted to function in two-component signaling pathways that operate within the maize SAM (Table 3.1; Figure 3.4 A; Figure 3.5 E-H). These include a SAM-enriched response regulator-like gene (BG840771) as well as the maize histidine phosphotransfer gene *Zmhp1*, whose non-mutant RNA accumulation pattern (Figure 3.5 E, G) mirrors that of the *ns* duplicate genes (Figure 3.1 C). Taken together, these data suggests that transcriptional repression of specific, two-component signaling pathways may be conserved functions of WUS1 and NS. As likewise observed in our studies of ns meristems (Table 3.1; Figure 3.5 M-P), microarray analyses of WUS-induced gene expression also revealed the upregulation of numerous jasmonate-induced *lectin* genes (Leibfried et al., 2005), including an apparent homolog of the maize jacalin-related *lectin* gene (DN210415) that is down-regulated in the ns mutant SAM. Although preliminary, these analyses suggest that NS and WUS1 may share a conserved WOX function to activate the expression of specific *lectin* genes during plant development. The laser microdissection-microarray analyses described herein provide a starting point toward reverse genetic and biochemical analyses of the mechanisms of NS-mediated founder cell recruitment during maize leaf initiation.

MATERIALS AND METHODS

Plant materials

The ns 1:1 line was propagated by crossing ns mutant plants (genotype *ns1-R; ns2-R*) onto non-mutant siblings (genotype *Ns1/ns1-R; ns2-R*) for over twenty successive generations as described (Scanlon and Freeling, 1997; Scanlon et al., 2000). Seedlings of this near-isogenic ns 1:1 line were grown in an environmentally controlled chamber with light intensity 220-250 $\mu ES^{-1}M^{-2}$; 25°C for 15-hours of light; 20°C for 9-hours of dark; 50% for humidity, and harvested for laser microdissection at two weeks after germination.

Laser microdissection of maize SAMs

Seedlings were fixed in acetone and paraffin-embedded as described (Emrich et al., 2007). SAM cells were laser microdissected from 10 μm sections (10-12 sections per SAM) using the P.A.L.M. Laser Microbeam (Bernried, Germany). Expression of the lateral SAM domain control gene *ns2* was highly enriched in our laser-dissected SAM samples compared to that of the whole seedlings, as monitored by RT-PCR and microarray (data not shown). Six biological replicates, each comprised of 10-12 whole ns or non-mutant laser microdissected SAMs (ranging from 2.4 mm^2 to 4.2 mm^2 of tissue) were used in these experiments (Supplementary Table 3.1). RNA was isolated using the PicoPure™ RNA extraction kit (Arcturus Molecular Devices, Sunnyvale, CA) and two rounds of RNA amplification were performed using T7-RNA polymerase as described (Nakazono et al., 2003) with changes described in (Moll et al., 2004). Yields of amplified SAM RNA ranged from 16.7 μg to 57.6 μg quantities.

Two μg of amplified SAM RNA were reverse transcribed with Superscript II (Invitrogen, Carlsbad, CA) and 0.5 μg of random primers (Roche Diagnostics, Indianapolis, IN). The resultant cDNA were indirectly labeled with Cy dyes assisted by amino allyl incorporation as described (Nakazono et al., 2003); dye bias was removed by swapping Cy dyes between the RNA samples. Microarray hybridizations were performed as described (Nakazono et al., 2003).

SAM microarrays

Two technical problems prevented our use of laser microdissected, amplified RNA in hybridizations with the maize oligo arrays that are currently in production at the University of Arizona (http://www.maizearray.org). First, amplified RNA prepared as described above is antisense-orientated and therefore unusable with sense-directed oligo arrays. Although, linear RNA amplification protocols that generate sense-oriented RNA are available, these truncate the 3' ends of the amplified RNA product. Because the majority of the maize oligo array sequences are generated from 3' ends of maize ESTs, sense amplified RNA generated by these protocols is also suboptimal. A second caveat is that the maize EST sequences that were used to design the maize oligo microarrays are under-represented for sequences derived from the vegetative maize SAM; SAM-specific cDNA libraries were not deeply sequenced in previous maize EST projects. Therefore, we initiated a SAM EST discovery project in which cDNA was prepared from hand-dissected maize apices (SAM plus P1-P4) and 31,036 apex ESTs were generated (Emrich et al., 2007) and submitted to GenBank. These include 3,503 SAM ESTs that are not found among EST libraries from any other maize tissues (Emrich et al., 2007); these SAM EST sequences are also not represented on the current maize oligo arrays.

In light of the obstacles preventing our use of the maize oligo arrays, three microarrays (SAM 1.1; SAM 2.0 SAM 3.0) containing a combined total of 37,662 informative cDNAs including approximately 21,721 maize genes were constructed. SAM 1.1 contains 14,401 informative spots corresponding to ~9,423 maize cDNAs; SAM 2.0 contains 8,991 informative spots representing ~7,599 maize genes. Whereas SAM 1.1 and SAM 2.0 contain maize UniGenes (Lunde et al., 2003) as well as cDNAs derived from maize inflorescences, the SAM 3.0 chip is particularly enriched for cDNAs derived from the maize SAM. Gene chip SAM 3.0 contains 14,270 informative spots and approximately 12,257 new genes, including more than 10,800 cDNAs derived from dissected maize apices and identified during this project (described above and in (Emrich et al., 2007)). All three SAM microarrays contain 45 control genes that are known to be expressed in the maize SAM and/or young leaf primordia. SAM chips may be ordered online (http://www.plantgenomics. iastate.edu/maizechip/) and their gene content may be searched via the online tool MADI (MicroArray Data Interface; http://schnablelab.plantgenomics.iastate.edu:8080/madi/).

Microarray analyses

Hybridized arrays were scanned using a ScanArray 5000™ (GSI Lumonics, Billerica, MA) at 10 μm resolution. Image processing utilized Digital Genome System™ software (MolecularWare, Irvine, CA). Signals were background corrected and LOWESS normalized within each slide to remove intensity-dependent dye bias (Dudoit et al., 2002). Normalization across slides was accomplished by median centering data from each channel (Yang et al., 2002). Our model for the normalized log-scale signal intensities for any given gene is as follows:

$$y_{ijk}=\mu + \tau_i + \delta_j + s_k + e_{ijk}, \quad (1)$$

where y_{ijk} denotes the normalized log-scale signal intensity from SAM type i (i=1,2 for mutant and non-mutant SAMs, respectively), dye j (j=3,5 for Cy3 and Cy5 dyes, respectively), and slide k (k=1,2,3,4,5,6); μ is an intercept term; τ_i denotes the effect of SAM type i; δ_j denotes the effect of dye j; s_k denotes the random effect of slide k; and e_{ijk} denotes a random residual term. The slide and residual random effects are assumed to be independent and normally distributed with a single variance for slides and a single variance for residuals. All parameters are allowed to vary from gene to gene though we have suppressed a gene specific subscript to simplify notation.

To obtain tests of SAM type effects ($H_0 : \tau_1=\tau_2$), the difference between normalized signals (Cy5 minus Cy3) was computed for each spot. Based on our model (1) above, the six differences (denoted $d_1,...,d_6$) can be modeled as $d_k = \beta_0 + \beta_1 x_k + \varepsilon_k$, where $\beta_0 = \delta_5 - \delta_3$, $\beta_1 = \tau_1 - \tau_2$, ε_k is a difference of the form $e_{ijk} - e_{i'j'k}$, and $x_1 , ..., x_6$ are -1,-1,-1,1,1,1 to correspond to our design in which three of the slides have Cy3 and Cy5 assigned to mutant and non-mutant SAMs, respectively, and three have the opposite assignment. In this simple linear regression model, the intercept term accounts for gene-specific dye effects not removed in normalization ($\delta_5 - \delta_3$) and the slope term accounts for the SAM type effect of interest ($\tau_1 - \tau_2$) which corresponds to the mean difference in normalized log-scale expression between mutant and non-mutant SAMs. The resulting p-values from the tests for SAM type effects were converted to q-values using the method of Storey and Tibshirani (Storey and Tibshirani, 2003) to estimate the false discovery rate (FDR) associated with any p-value threshold for significance. Functional annotation of differentially expressed genes was performed as described (Buckner). MIAME guidelines utilized in these experiments are described in Text SI; all microarray data is available at Gene Expression Omnibus (GEO; http://www.ncbi.nlm.nih.gov/geo/), accession number GSE7248.

Quantitative real time RT-PCR and *in situ* hybridization

qRT-PCR analyses were performed on cDNA synthesized from the identical SAM amplified RNA samples used in our analyses, using either Taq-Man or SYBR-Green probes (Gomes-Ruiz et al., 2006) (Supplemental Table 3.2). Three biological replicates were used, upon which three technical replicates were performed. Reactions were normalized to control *ubiquitin* expression as described (Livak and Schmittgen, 2001).

Tissue-specific qRT-PCR analyses were performed as above using the SYBR-Green methodology and gene-specific probes (Supplemental Table 3.1); three technical replicates were performed. Expression of each transcript was normalized to the level of ubiquitin controls; relative gene expression values were graphed using the iQ5 Optical System Software version 1.0 (Bio-Rad), wherein no expression was assigned a value of zero. All tissues were derived from the maize inbred B73. Tissues included the laser microdissected SAM from 14 day-old seedlings; fully expanded mature leaf (leaf 10); fully expanded leaf from 14 day-old seedlings (leaf 4); seedling roots; immature ears (6 mm long) containing multiple spikelet meristems and spikelet pair meristems with glume primordia; and immature tassels (8 mm) containing branch primordia, multiple spikelet meristems and spikelet pair meristems with glume primordia. Except for LM derived SAM tissues (RNA extracted and amplified as above), all RNA extractions of maize tissues were performed using the Trizol™ method, as described (Nardmann et al., 2004).

Maize 14 day-old seedlings were grown in controlled conditions (above) and processed for *in situ* hybridization as described (Juarez et al., 2004). For each gene-specific probe analyzed, at least six replicate samples each of ns1-R mutant and non-mutant sibling were analyzed. Cartoons of transcript accumulation patterns modeled in Figure 3.5 and Figure 3.6 depict SAM

expression only. Expression in leaf primordia, which was not measured in our microarray analyses, is not depicted in cartoons.

ACKNOWLEDGEMENTS

The authors thank L. Brooks for technical assistance; J. Nardmann and W. Werr for the image reproduced in Figure 3.1C; K. Browning, A. Fritz, E. Hoxha and Z. Kamvar for assistance in data annotation; and K. Dawe for stimulating discussions of the data.

Supplemental table 3.1 LMM samples used in this study

Sample Information	ns1	wt1	ns2	wt2	ns3	wt3	ns4	wt4	ns5	wt5	ns6	wt6
mm^2 captured[i]	4.1	4.2	3.3	3.2	4.2	3.3	2.8	2.4	2.5	2.8	2.2	2.4
aRNA yield (µg)	47.3	41.2	31.4	28.9	16.7	31.6	55.3	21.6	57.6	22.1	30.8	17.1
Labeling for SAM1	Cy3	Cy5	Cy5	Cy3	Cy3	Cy5	Cy5	Cy3	Cy3	Cy5	Cy5	Cy3
Labeling for SAM2	Cy5	Cy3	Cy3	Cy5	Cy5	Cy3	Cy3	Cy5	Cy5	Cy3	Cy3	Cy5
Labeling for SAM3	Cy3	Cy5	Cy5	Cy3	Cy3	Cy5	Cy5	Cy3	Cy5	Cy3	Cy3	Cy5

[i] square surface area of SAM tissue isolated by laser microdissection

Supplemental table 3.2 Primer information used for quantitative real time RT-PCR

Accession No	Forward primer 5'-3'	Reverse primer 5'-3'
DY576324	ATTGGGGAAGGTGCAGAAG	CACTTCAGTGACGGCTTCAA
DV491384	TCTCCTCCAATCCAGCTCTC	TGCACTGCAAGTAGGGATTG
DY400928	CGTACTTATTCAAGCCCTTCAGCAAGTA[FAM]G	AACTGAACTCCATGCTGAACTGAA
BG462729	ACTCTGCCTCTGTGCTGGAA	ATTCTTGGCACTGGCAAAGC
CB816286	CCCTGTCGGCGAGATACCTTC	CGTAGACTGACGAGTGGGCGATCTA[FAM]G
CD650947	GAGCTGATGGTACTCGAAATGG	CGCTCAGACATCTTCAAGCAGATTGAG[FAM]G
BG518167	AACACGATTTCGGTAAGCAGTT	CGGCAGGCTTCTGTTAGTTATT
BM380298	CGTGTTCAAACCAATAGTCGAG	ACGCTCAGCTATCTGCCTATCT
CB816294	ACCGGTGTCATGAAGAGAAGAA	GATCTTGGTGACGGAGGAGAT
DN205423	CAGCGCTGTCAGTATAGGTGAA	CTCACAGTCAGAGCTGCAAGAT
DV942355	GCCTAATGTGGGGAAAGGTT	GCCAATCGCTCTTTTGACTT
BI359303	ATCCTACAGAGCGTGATTCCAT	TTTAGCGGGATTATTCGTGACT
BG946630	ATCCTACAGAGCGTGATTCCAT	CTCTCTGGTCTGGAGGAGGTC
BI361046	AAAATTCTCCCGAAAATCCAAT	GAGAAAATCGATTCATCAGACG
BI096810	CATCTATGTCAATTAAAGGGACTAAAA	AGAGTATCGGCAAGGAATCTCG
BG840771	TTTTTCTTAACTGGCCTGCATT	CATACGCTTAGGTGTTTGTGGA
DV490133	CACAGATCATAGCCTTCAAATGAATCTG[FAM]G	TGCAGGGAACAGAGAAATAGCA
DV621960	TTTTTCAAAATCCCATACTCATCC	TGACGATCGTTCGCATCC
DY402633	GAGCCGCTGAACTTTACAGG	GAGTAGCGCCCTTTGTGAAC
DN210415	GCTGTCAGTATAGGTGAACTC	GGACAAGAGATACGTGAGTG
CB381550	TGCTACAGGAAAGTCAAGAG	CATTCACCTCAAACAAAGTCAG
AY260164	GGCACTGGCTGAGTCTAC	CTCCTCGGATGGCTTCCAGT

REFERENCES

Asakura, Y., Hagino, T., Ohta, Y., Aoki, K., Yonekura-Sakakibara, K., Deji, A., Yamaya, T., Sugiyama, T., and Sakakibara, H. (2003). Molecular characterization of His-Asp phosphorelay signaling factors in maize leaves: implications of the signal divergence by cytokinin-inducible response regulators in the cytosol and the nuclei. Plant Mol Biol **52,** 331-341.

Aubourg, S., Kreis, M., and Lecharny, A. (1999). The DEAD box RNA helicase family in *Arabidopsis thaliana*. Nucleic Acids Res **27,** 628-636.

Benkova, E., Michniewicz, M., Sauer, M., Teichmann, T., Seifertova, D., Jurgens, G., and Friml, J. (2003). Local, efflux-dependent auxin gradients as a common module for plant organ formation. Cell **115,** 591-602.

Buckner, B., Beck, J., Browning, K. F., Fritz, A. E., Hoxha, A., Grantham, L. D., Kamvar, Z. N., Lough, A. N., Nikolova, O., Schnable, P. S., Scanlon, M. J and Janick-Buckner, D. Involving undergraduates in the annotation and analysis of global gene expression studies: creation of a maize shoot apical meristem expression database. Genetics (*in press)*

Cai, S., and Lashbrook, C.C. (2006). Laser capture microdissection of plant cells from tape-transferred paraffin sections promotes recovery of structurally intact RNA for global gene profiling. Plant J **48,** 628-637.

Casson, S., Spencer, M., Walker, K., and Lindsey, K. (2005). Laser capture microdissection for the analysis of gene expression during embryogenesis of *Arabidopsis*. Plant J **42,** 111-123.

Dharmasiri, N., Dharmasiri, S., and Estelle, M. (2005). The F-box protein TIR1 is an auxin receptor. Nature **435,** 441-445.

Dudoit, S., Yang, Y.H., Callow, M.J., and Speed, T.P. (2002). Statistical methods for identifying genes with differential expression in replicated cDNA microarray experiments. Statistical Sinica**,** 111-139.

Emrich, S.J., Barbazuk, W.B., Li, L., and Schnable, P.S. (2007). Gene discovery and annotation using LCM-454 transcriptome sequencing. Genome Res **17,** 69-73.

Eshed, Y., Izhaki, A., Baum, S.F., Floyd, S.K., and Bowman, J.L. (2004). Asymmetric leaf development and blade expansion in *Arabidopsis* are mediated by KANADI and YABBY activities. Development **131,** 2997-3006.

Friml, J., Vieten, A., Sauer, M., Weijers, D., Schwarz, H., Hamann, T., Offringa, R., and Jurgens, G. (2003). Efflux-dependent auxin gradients establish the apical-basal axis of *Arabidopsis*. Nature **426,** 147-153.

Geldner, N., Anders, N., Wolters, H., Keicher, J., Kornberger, W., Muller, P., Delbarre, A., Ueda, T., Nakano, A., and Jurgens, G. (2003). The *Arabidopsis* GNOM ARF-GEF mediates endosomal recycling, auxin transport, and auxin-dependent plant growth. Cell **112,** 219-230.

Gomes-Ruiz, A.C., Nascimento, R.T., de Paula, S.O., and da Fonseca, B.A. (2006). SYBR green and TaqMan real-time PCR assays are equivalent for the diagnosis of dengue virus type 3 infections. J Med Virol **78,** 760-763.

Gonzali, S., Novi, G., Loreti, E., Paolicchi, F., Poggi, A., Alpi, A., and Perata, P. (2005). A turanose-insensitive mutant suggests a role for WOX5 in auxin homeostasis in *Arabidopsis thaliana*. Plant J **44,** 633-645.

Grossmann, K., Rosenthal, C., and Kwiatkowski, J. (2004). Increases in jasmonic acid caused by indole-3-acetic acid and auxin herbicides in cleavers (Galium aparine). J Plant Physiol **161,** 809-814.

Haecker, A., Gross-Hardt, R., Geiges, B., Sarkar, A., Breuninger, H., Herrmann, M., and Laux, T. (2004). Expression dynamics of WOX genes mark cell fate decisions during early embryonic patterning in *Arabidopsis thaliana*. Development **131,** 657-668.

Hass, C., Lohrmann, J., Albrecht, V., Sweere, U., Hummel, F., Yoo, S.D., Hwang, I., Zhu, T., Schafer, E., Kudla, J., and Harter, K. (2004). The response regulator 2 mediates ethylene signalling and hormone signal integration in *Arabidopsis*. Embo J **23,** 3290-3302.

Hay, A., Barkoulas, M., and Tsiantis, M. (2006). ASYMMETRIC LEAVES1 and auxin activities converge to repress BREVIPEDICELLUS expression and promote leaf development in *Arabidopsis*. Development **133,** 3955-3961.

Heisler, M.G., Ohno, C., Das, P., Sieber, P., Reddy, G.V., Long, J.A., and Meyerowitz, E.M. (2005). Patterns of auxin transport and gene expression during primordium development revealed by live imaging of the *Arabidopsis* inflorescence meristem. Curr Biol **15,** 1899-1911.

Irish, V.F., and Sussex, I.M. (1992). A fate map of the *Arabidopsis* embryonic shoot apical meristem. Development **115,** 745-753.

Jackson, D., Veit, B., and Hake, S. (1994). Expression of the maize KNOTTED-1 related homeobox genes in the shoot apical meristem predicts patterns of morphogenesis in the vegetative shoot. Development**,** 405-413.

Jones, A.M., and Assmann, S.M. (2004). Plants: the latest model system for G-protein research. EMBO Rep **5,** 572-578.

Juarez, M.T., Kui, J.S., Thomas, J., Heller, B.A., and Timmermans, M.C. (2004). microRNA-mediated repression of rolled leaf1 specifies maize leaf polarity. Nature **428,** 84-88.

Kepinski, S., and Leyser, O. (2005). The *Arabidopsis* F-box protein TIR1 is an auxin receptor. Nature **435,** 446-451.

Koizumi, K., Naramoto, S., Sawa, S., Yahara, N., Ueda, T., Nakano, A., Sugiyama, M., and Fukuda, H. (2005). VAN3 ARF-GAP-mediated vesicle transport is involved in leaf vascular network formation. Development **132,** 1699-1711.

Leibfried, A., To, J.P., Busch, W., Stehling, S., Kehle, A., Demar, M., Kieber, J.J., and Lohmann, J.U. (2005). WUSCHEL controls meristem function by direct regulation of cytokinin-inducible response regulators. Nature **438,** 1172-1175.

Linder, P. (2006). Dead-box proteins: a family affair--active and passive players in RNP-remodeling. Nucleic Acids Res **34,** 4168-4180.

Livak, K.J., and Schmittgen, T.D. (2001). Analysis of relative gene expression data using real-time quantitative PCR and the 2(-Delta Delta C(T)) Method. Methods **25,** 402-408.

Long, J.A., Moan, E.I., Medford, J.I., and Barton, M.K. (1996). A member of the KNOTTED class of homeodomain proteins encoded by the STM gene of *Arabidopsis*. Nature **379,** 66-69.

Lorenzo, O., and Solano, R. (2005). Molecular players regulating the jasmonate signalling network. Curr Opin Plant Biol **8,** 532-540.

Lunde, C.F., Morrow, D.J., Roy, L.M., and Walbot, V. (2003). Progress in maize gene discovery: a project update. Funct Integr Genomics **3,** 25-32.

Matsumoto, N., and Okada, K. (2001). A homeobox gene, PRESSED FLOWER, regulates lateral axis-dependent development of *Arabidopsis* flowers. Genes Dev **15,** 3355-3364.

Mayer, K.F., Schoof, H., Haecker, A., Lenhard, M., Jurgens, G., and Laux, T. (1998). Role of WUSCHEL in regulating stem cell fate in the *Arabidopsis* shoot meristem. Cell **95,** 805-815.

Mizuno, T. (2005). Two-component phosphorelay signal transduction systems in plants: from hormone responses to circadian rhythms. Biosci Biotechnol Biochem **69,** 2263-2276.

Moll, P.R., Duschl, J., and Richter, K. (2004). Optimized RNA amplification using T7-RNA-polymerase based in vitro transcription. Anal Biochem **334,** 164-174.

Moshkov, I.E., Mur, L.A., Novikova, G.V., Smith, A.R., and Hall, M.A. (2003). Ethylene regulates monomeric GTP-binding protein gene expression and activity in *Arabidopsis*. Plant Physiol **131,** 1705-1717.

Nagpal, P., Ellis, C.M., Weber, H., Ploense, S.E., Barkawi, L.S., Guilfoyle, T.J., Hagen, G., Alonso, J.M., Cohen, J.D., Farmer, E.E., Ecker, J.R., and Reed, J.W. (2005). Auxin response factors ARF6 and ARF8 promote jasmonic acid production and flower maturation. Development **132,** 4107-4118.

Nakazono, M., Qiu, F., Borsuk, L.A., and Schnable, P.S. (2003). Laser-capture microdissection, a tool for the global analysis of gene expression in specific plant cell types: identification of genes expressed differentially in epidermal cells or vascular tissues of maize. Plant Cell **15,** 583-596.

Nardmann, J., Ji, J., Werr, W., and Scanlon, M.J. (2004). The maize duplicate genes narrow sheath1 and narrow sheath2 encode a conserved homeobox gene function in a lateral domain of shoot apical meristems. Development **131,** 2827-2839.

Nelson, T., Tausta, S.L., Gandotra, N., and Liu, T. (2006). Laser microdissection of plant tissue: what you see is what you get. Annu Rev Plant Biol **57,** 181-201.

Nettleton, D. (2006). A discussion of statistical methods for design and analysis of microarray experiments for plant scientists. Plant Cell **18,** 2112-2121.

Osteryoung, K.W., Stokes, K.D., Rutherford, S.M., Percival, A.L., and Lee, W.Y. (1998). Chloroplast division in higher plants requires members of two functionally divergent gene families with homology to bacterial ftsZ. Plant Cell **10,** 1991-2004.

Park, S.O., Zheng, Z., Oppenheimer, D.G., and Hauser, B.A. (2005). The PRETTY FEW SEEDS2 gene encodes an *Arabidopsis* homeodomain protein that regulates ovule development. Development **132,** 841-849.

Poethig, R.S. (1984). Cellular parameters of leaf morphogenesis in maize and tobacco. Contemporary Problems of Plant Anatomy (eds. R. A. White and W. C. Dickinson)**,** 235-238.

Poethig, R.S., and Szymkowiak, E.J. (1995). Clonal analysis of leaf development in maize. Maydica**,** 67-76.

Reinhardt, D., Mandel, T., and Kuhlemeier, C. (2000). Auxin regulates the initiation and radial position of plant lateral organs. Plant Cell **12,** 507-518.

Reinhardt, D., Pesce, E.R., Stieger, P., Mandel, T., Baltensperger, K., Bennett, M., Traas, J., Friml, J., and Kuhlemeier, C. (2003). Regulation of phyllotaxis by polar auxin transport. Nature **426,** 255-260.

Rolland, F., Baena-Gonzalez, E., and Sheen, J. (2006). Sugar sensing and signaling in plants: conserved and novel mechanisms. Annu Rev Plant Biol **57,** 675-709.

Scanlon, M.J. (2000). NARROW SHEATH1 functions from two meristematic foci during founder-cell recruitment in maize leaf development. Development **127,** 4573-4585.

Scanlon, M.J. (2003). The polar auxin transport inhibitor N-1-naphthylphthalamic acid disrupts leaf initiation, KNOX protein regulation, and formation of leaf margins in maize. Plant Physiol **133,** 597-605.

Scanlon, M.J., and Freeling, M. (1997). Clonal sectors reveal that a specific meristematic domain is not utilized in the maize mutant narrow sheath. Dev Biol **182,** 52-66.

Scanlon, M.J., Schneeberger, R.G., and Freeling, M. (1996). The maize mutant narrow sheath fails to establish leaf margin identity in a meristematic domain. Development **122,** 1683-1691.

Scanlon, M.J., Chen, K.D., and McKnight, C.I. (2000). The narrow sheath duplicate genes: sectors of dual aneuploidy reveal ancestrally conserved gene functions during maize leaf development. Genetics **155,** 1379-1389.

Schnable, P.S., Hochholdinger, F., and Nakazono, M. (2004). Global expression profiling applied to plant development. Curr Opin Plant Biol **7,** 50-56.

Shi, Y., Lan, F., Matson, C., Mulligan, P., Whetstine, J.R., Cole, P.A., Casero, R.A., and Shi, Y. (2004). Histone demethylation mediated by the nuclear amine oxidase homolog LSD1. Cell **119,** 941-953.

Sieburth, L.E., Muday, G.K., King, E.J., Benton, G., Kim, S., Metcalf, K.E., Meyers, L., Seamen, E., and Van Norman, J.M. (2006). SCARFACE encodes an ARF-GAP that is

required for normal auxin efflux and vein patterning in *Arabidopsis*. Plant Cell **18,** 1396-1411.

Smith, L.G., Greene, B., Veit, B., and Hake, S. (1992). A dominant mutation in the maize homeobox gene, Knotted-1, causes its ectopic expression in leaf cells with altered fates. Development **116,** 21-30.

Spencer, M.W., Casson, S.A., and Lindsey, K. (2007). Transcriptional profiling of the *Arabidopsis* embryo. Plant Physiol **143,** 924-940.

Storey, J.D., and Tibshirani, R. (2003). Statistical methods for identifying differentially expressed genes in DNA microarrays. Methods Mol Biol **224,** 149-157.

Strayer, C., Oyama, T., Schultz, T.F., Raman, R., Somers, D.E., Mas, P., Panda, S., Kreps, J.A., and Kay, S.A. (2000). Cloning of the *Arabidopsis* clock gene TOC1, an autoregulatory response regulator homolog. Science **289,** 768-771.

Tiryaki, I., and Staswick, P.E. (2002). An *Arabidopsis* mutant defective in jasmonate response is allelic to the auxin-signaling mutant axr1. Plant Physiol **130,** 887-894.

To, J.P., Haberer, G., Ferreira, F.J., Deruere, J., Mason, M.G., Schaller, G.E., Alonso, J.M., Ecker, J.R., and Kieber, J.J. (2004). Type-A *Arabidopsis* response regulators are partially redundant negative regulators of cytokinin signaling. Plant Cell **16,** 658-671.

Van Damme, E.J., Lannoo, N., Fouquaert, E., and Peumans, W.J. (2004). The identification of inducible cytoplasmic/nuclear carbohydrate-binding proteins urges to develop novel concepts about the role of plant lectins. Glycoconj J **20,** 449-460.

Woll, K., Borsuk, L.A., Stransky, H., Nettleton, D., Schnable, P.S., and Hochholdinger, F. (2005). Isolation, characterization, and pericycle-specific transcriptome analyses of the

novel maize lateral and seminal root initiation mutant rum1. Plant Physiol **139,** 1255-1267.

Wu, X., Dabi, T., and Weigel, D. (2005). Requirement of homeobox gene STIMPY/WOX9 for *Arabidopsis* meristem growth and maintenance. Curr Biol **15,** 436-440.

Yamaguchi, T., Nagasawa, N., Kawasaki, S., Matsuoka, M., Nagato, Y., and Hirano, H.Y. (2004). The YABBY gene DROOPING LEAF regulates carpel specification and midrib development in *Oryza sativa*. Plant Cell **16,** 500-509.

Yang, Y.H., Dudoit, S., Luu, P., Lin, D.M., Peng, V., Ngai, J., and Speed, T.P. (2002). Normalization for cDNA microarray data: a robust composite method addressing single and multiple slide systematic variation. Nucleic Acids Res **30,** e15.

CHAPTER 4

LASER MICRODISSECTION-MICROARRAY ANALYSES OF RAGGED SEEDLING2, A GENE REQUIRED FOR MAIZE LEAF PATTERNING[1]

[1] Zhang, X., Borsuk, L., Nettleton, D., Buckner, B., Janick-Buckner, D., Beck, J., Timmermans, M., Schnable, P.S., and Scanlon, M.J. Laser microdissection-microarray analyses of ragged seedling2, a gene required for maize leaf patterning. To be submitted to Current Biology.

ABSTRACT

The recessive mutation *ragged seedling2-R* (*rgd2-R*) conditions defective lateral development of maize leaves. Although dorsiventral patterning is established in rgd2-R mutant leaves, some swapping of adaxial/abaxial epidermal identity may occur. Molecular analyses indicate that RGD2 is required for normal transcript levels of multiple leaf developmental markers (including NS1, YABBY14, Zm*KANADI2 and ROLLED1), although the domain-specificity and expression patterns of these transcripts are normal. These data suggest that RGD2 is required for the coordination of dorsiventral and lateral patterning during maize leaf development. The RGD2 gene product and the mechanisms of RGD2 function are unknown. Here we investigate the genetic mechanisms downstream of RGD2 gene function using SAM-specific transcript profiling via laser microdissection-microarray analyses. Out of 28,671 maize cDNAs examined, 202 genes are identified as differentially expressed in rgd2-R mutant meristems. Quantitative RT-PCR corroborated the differential expression of 21 genes, and *in situ* hybridization reveals the previously undescribed expression patterns of eight novel maize genes. Genes predicted to be involved in transcriptional regulation, chromatin remodeling, signal transduction, and proteolysis/protein fate are especially misexpressed in the rgd2-R mutant apex. Our data suggest that RGD2 may function through the previously-described ARP (ASYMMETRIC LEAVES 1/ROUGH SHEATH2/PHANTASTICA) pathway, or via a novel proteolytic pathway, to coordinate dorsiventral patterning and mediolateral growth during maize leaf development.

INTRODUCTION

Leaves are produced sequentially and reiteratively from the shoot apical meristem (SAM), a specialized pluripotent pool of stem cells located at the summit of plant shoots. Maize leaf development initiates by recruitment of about 200 leaf founder cells from the flank of the SAM, a process that is visualized by the downregulation of KNOX (KNOTTED1-like homeobox) protein accumulation in the apex (Poethig, 1984; Smith et al., 1992; Jackson et al., 1994; Poethig and Szymkowiak, 1995). Subsequent leaf patterning occurs along the proximodistal (base-tip), mediolateral (midrib-margin) and dorsiventral (top-bottom) axes to establish a fully differentiated, three-dimensional leaf primordium.

Mutant studies in multiple species including maize, *Arabidopsis*, snapdragon and tomato have contributed to a model (Waites and Hudson, 1995) wherein juxtaposition of adaxial and abaxial developmental fields generates a positional signal that specifies patterning and expansive growth along the mediolateral and proximodistal axes of the leaf (Waites and Hudson, 1995; Eshed et al., 2001; Hudson, 2001; Bowman et al., 2002). Loss of either adaxial or abaxial identity causes a partial or completely radial leaf that fails to expand laterally (Waites and Hudson, 1995; Waites et al., 1998; Siegfried et al., 1999; Timmermans et al., 1999; Tsiantis et al., 1999; Eshed et al., 2001; Kerstetter et al., 2001; McConnell et al., 2001).

In support of the Waites-Hudson model, class III HOMEODOMAIN-LEUCINE ZIPPER (HD ZIPIII) genes such as PHABULOSA (PHB), PHAVOLUTA (PHV) and REVOLUTA (REV) in *Arabidopsis* and the REV orthologue ROLLED LEAF1(RLD1) in maize are required for adaxial identity. HD-ZIPIII genes are expressed in the adaxial side of leaf primordia and in the central zone of the SAM (McConnell et al., 2001; Otsuga et al., 2001; Emery et al., 2003).

Gain-of-function mutations in PHB, PHV or REV in *Arabidopsis* causes narrow or radial adaxialized leaves, whereas recessive double and triple mutations in *phb, phv,* and *rev* result in abaxialized leaves. These data are consistent with the hypothesis that HD-ZIP III genes function redundantly to promote adaxial cell fate in the *Arabidopsis* leaf (McConnell and Barton, 1998; McConnell et al., 2001; Otsuga et al., 2001; Bowman et al., 2002; Emery et al., 2003; Prigge et al., 2005).

Transcripts of HD-ZIPIII class genes are targeted for destruction by miR165 and miR166, microRNAs that accumulate in the abaxial domain of leaf primordia (Juarez et al., 2004; Kidner and Martienssen, 2004). Genes involved in microRNA biogenesis, such as DICER-LIKE1 (DCL1), SERRATE (SE) and ARGONAUTE1 (AGO1), regulate leaf dorsiventrality via their effects on miR166/5 accumulation (Kidner and Martienssen, 2004; Baumberger and Baulcombe, 2005; Grigg et al., 2005; Williams et al., 2005)

HD-ZIPIII genes are mutually antagonistic to members of the KANADI (KAN) gene family, GARP transcription factors that are expressed abaxially in developing leaf primordia to promote abaxial identity (Kerstetter et al., 2001; Kidner and Timmermans, 2007). Overexpressions of *KAN* genes yield abaxialized radial leaves, a phenotype that mimics that of *phb phv rev* triple mutants. Conversely, loss of KAN function result in the expansion of PHB, PHV and REV expression domain and loss of abaxial identity (Kerstetter et al., 2001; Emery et al., 2003; Eshed et al., 2004).

Recent evidence reveals that the ARP pathway and a trans-acting small interfering RNA (ta-siRNA) pathway function redundantly to regulate dorsiventral patterning in leaves. ARP designates a group of orthologous MYB transcription factor genes that negatively regulate *KNOX* gene expression in leaf primordia (AS1 in *Arabidopsis*, RS2 in maize and PHAN in

Antirrhinum). The ARP genes are expressed uniformly within the developing leaf primordia and P0, but are excluded from the SAM proper (Waites and Hudson, 1995; Waites et al., 1998; Timmermans et al., 1999; Tsiantis et al., 1999; Byrne et al., 2000; Xu et al., 2003). Solo mutations in ARP genes exhibit pronounced abaxialized leaf phenotypes in *Antirrhinum* and tomato. Although orthologous mutations in maize and *Arabidopsis* exhibit defects along the proximodistal axis, dorsiventral patterning is unaffected (Schneeberger et al., 1998; Waites et al., 1998; Byrne et al., 2000; Kim et al., 2003; Theodoris et al., 2003; Xu et al., 2003). The reasons for these species-specific phenotype discrepancies observed in ARP mutants are unclear. However, variations in the level of functional redundancy during dorsiventral patterning may explain these disparate phenotypes.

A separate genetic mechanism controlling dorsiventrality in plant organs is the recently discovered trans-acting silencing RNA pathway (ta-siRNA), which mediates leaf adaxial/abaxial pattering by targeted-cleavage of mRNA from the abaxial determinants AUXIN RESPONSE FACTOR 3 (ARF3) and ARF4 (Pekker et al., 2005). Thus, genes involved in ta-siRNA biogenesis or function, including SUPPRESSOR OF GENE SILENCING3 (SGS3), RNA-dependent RNA polymerase (RDR6), dsRNA-BINDING PROTEIN4 (DRB4), DICER-LIKE4 (DCL4) and ARGONAUTE7 (AGO7), affect adaxial /abaxial cell fate indirectly (Peragine et al., 2004; Allen et al., 2005; Gasciolli et al., 2005; Vaucheret, 2005; Yoshikawa et al., 2005; Adenot et al., 2006; Hunter et al., 2006; Nakazawa et al., 2007; Nogueira et al., 2007). The maize gene LEAFBLADELESS1 (LBL1) encodes an SGS3 orthologue required for tas3-siRNA biogenesis; lbll mutant leaves are abaxialized, a phenotype that correlates with the over-accumulation of maize ARF3 and ARF4 transcripts (Nogueira et al., 2007).

The leaf patterning mutants described above display narrow and radial leaf phenotypes, accompanied with a loss or reduction in adaxial or abaxial identity. In contrast, the maize mutant *ragged seedling2-R* (*rgd2-R*) displays a narrow/filamentous leaf phenotype (Henderson et al., 2005), but no net loss of adaxial or abaxial identity (Henderson et al., 2005; Henderson et al., 2006). Molecular analyses indicate that RGD2 is required for normal transcript levels of multiple genes required for leaf development, including NARROW SHEATH1 (NS1), YABBY14, Zm*KAN2 and RLD1. Although these transcripts are greatly reduced in rgd2 shoots, the domain-specific expression patterns of these genes remain intact. These data contribute to a model proposing that RGD2 functions to maintain the normal expression level of multiple leaf patterning genes required to coordinate dorsiventral and mediolateral patterning during maize leaf development (Henderson et al., 2005; Henderson et al., 2006). In this view and in keeping with the Waites-Hudson model (1995), RGD2 is required to translate the juxtaposition of adaxial and abaxial leaf polarity into expansion along the mediolateral axis. The RGD2 gene product is unknown, although double mutants combining rgd2-R with the macroscopically similar leaf mutant lbl1 are shootless and embryo-lethal. This synergistic double-mutant phenotype indicates that RGD2 functions redundantly with, but in a separate genetic pathway than, the ta3-siRNA regulator LBL1.

Here we investigate the genetic mechanisms downstream of RGD2 gene function using SAM-specific transcript profiling of 28,671 maize cDNAs via laser microdissection-microarray analyses. Compared to non-mutant siblings, 202 genes are differentially expressed in rgd2-R mutant SAMs. Quantitative RT-PCR verified the differential expression of 21 genes, and *in situ* hybridization characterized the tissue-specific expression patterns of eight novel maize genes. Genes predicted to be involved in transcription regulation, chromatin remodeling, signal

transduction and proteolysis/protein fate are especially misexpressed in the rgd2-R mutant SAMs. Our data suggest two hypothetical genetic pathways through which RGD2 may function to coordinate leaf dorsiventrality and lateral expansion in maize. Cloning of the RGD2 locus, combined with reverse genetic analyses of genes differentially expressed in the rgd2-R mutant SAM, will help determine the precise role of RGD2 during maize leaf development.

RESULTS

Transcripts of 202 Genes are Differentially Accumulated in the rgd2-R Mutant SAM

Maize SAM cells, including the meristem proper and the leaf founder cells were harvested from 14-day-old rgd2-R mutant and non-mutant seedlings by laser-microdissection as described (Zhang et al., 2007; Figure 4.1). Six biological replicates, each comprised of 3-5 whole SAMs from either mutant or non-mutant plants, were laser microdissected; RNA extracted from the captured SAM cells was linearly amplified to yield sufficient quantities for microarray hybridizations (see Materials and Methods). Two maize gene chips, SAM1.1 and SAM3.0, which contain a combined total of maize 28,671 cDNAs sequences (approximately 17,472 maize genes, Zhang et al., 2007; see Materials and methods), were used for SAM-specific transcript profiling. SAM1.1 is enriched for cDNAs derived from maize inflorescences, whereas SAM3.0 contains over 10,000 cDNAs expressed in the maize SAM (Zhang et al., 2007). Following reverse transcription of the amplified RNA, the resultant cDNA was labeled with Cy fluorescent dyes as described (Nakazono et al., 2003). For each array platform, three of the six pairs were measured with Cy3 for mutant SAMs and Cy5 dye for nonmutant. Dye assignments were

reversed for the other three replications. Cy5 minus Cy3 differences were computed for each slide following normalization as described (Nettleton, 2006; Zhang et al., 2007; see Material and Methods)**.**

Utilizing a p value cutoff of $p < 0.001$ or $0.001 < p < 0.01$ in combination with fold change > 2.0, 202 genes were identified as differentially expressed in the rgd2-R mutant SAMs (Table 4.1). Functional annotation of the 202 differentially expressed genes was performed as described (Buckner et al., 2007); these annotations are publicly available at the database Gene Expression and Visualization Application (GENEVA:http://sam.truman.edu/; Buckner et al., 2007). The 202 differentially expressed genes were subdivided into fourteen functional categories (Figure 4.2), comprised of genes predicted to be involved in transcriptional regulation, chromatin remodeling, signal transduction, proteolysis/protein fate, cytoskeletal structure, general metabolism, protein translation, RNA binding or processing, DNA replication, vesicle trafficking, stress-response and intercellular transport. Moreover, 57 maize genes of unknown function are differentially accumulated in the rgd2-R mutant SAMs (Table 4.1). Excluding unknowns and genes putatively involved in general metabolism or translation, genes predicted to be involved in transcriptional regulation, proteolysis, signal transduction and chromatin remodeling are highly enriched (47/74) in this RGD2 dataset (Figure 4.2).

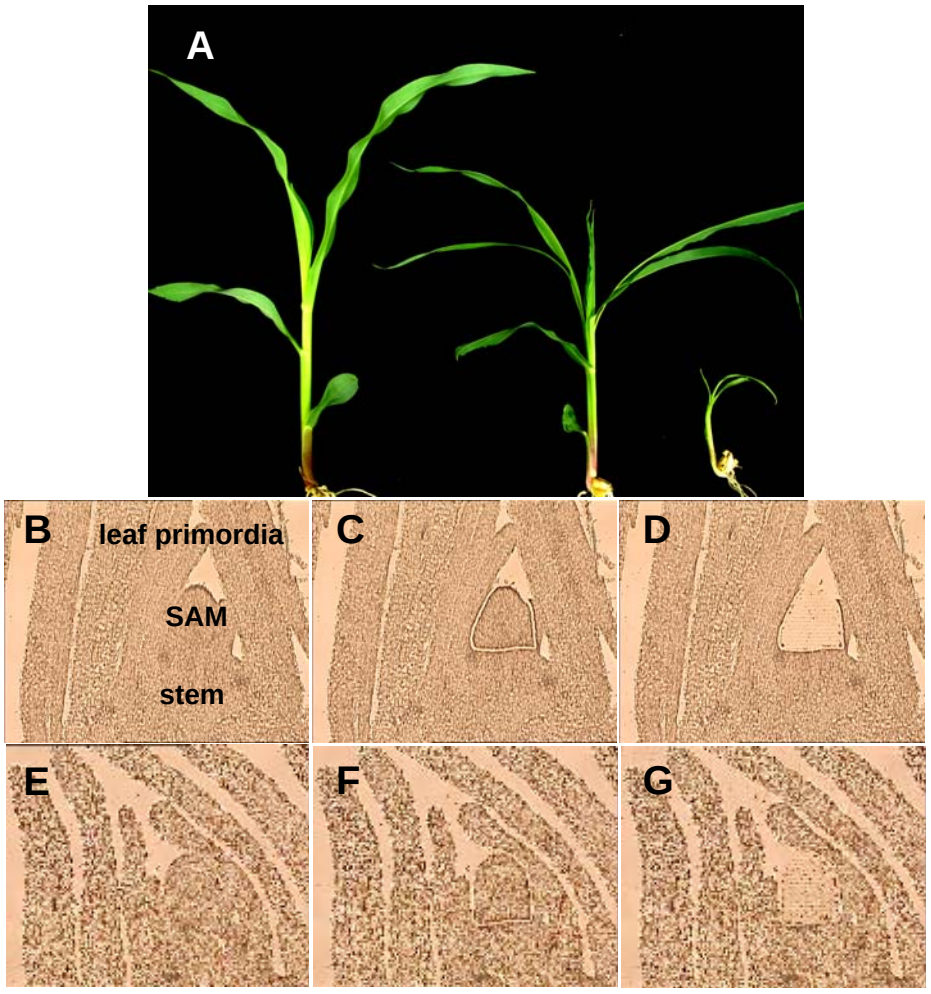

Figure 4.1 Laser microdissection of the maize SAM cells from non-mutant and rgd2-R mutants siblings. (A) Variable leaf morphology in the rgd2-R mutant seedlings. Non-mutant seedling (left) next to the moderate (middle) or severe (right) rgd2-R mutant seedlings. (B-G) Light micrograph of a 10 µm longitudinal section of a maize shoot apex shows the laser capture of cells from the entire SAM of non-mutant (B-D) and rgd2-R mutant (E-G). (B, E) SAMs before laser capture. (C, F) Laser ablation cuts and destroys tissues surrounding the SAM cells. (D, G) SAM cells are removed by laser pressure catapulting into collection caps suspended above the samples.

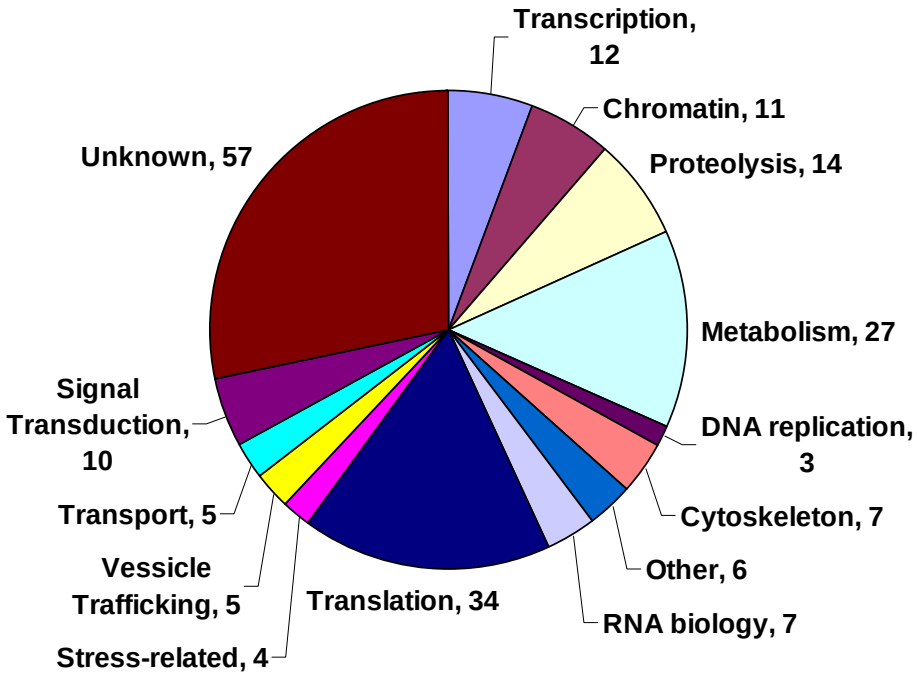

Figure 4.2 Putative functional annotation of 202 genes differentially expressed in the rgd2-R mutant SAMs. Excluding genes involved in general metabolism, translation and unknown function, genes predicted to be involved in transcription, proteolysis, chromatin remodeling and signal transduction are highly enriched (47/85) in the differentially expressed genes.

Table 4.1 Genes differentially-expressed in the rgd2-R mutant SAM

Accession #	p value	Fold change	Putative Gene Identification
Transcription			
DN224320	0.00001	0.28	Maize DNA-binding WRKY
CB381425	0.00053	0.90	Cold-shock protein, DNA-binding/ CCHC-type Zinc finger protein
CD058851	0.00051	0.75	Putative zinc finger homeodomain protein
DN222016	0.00424	0.42	Putative DP transcription factor
DY397856	0.00125	3.37	Maize MADS box transcription factor
CB381167	0.00002	1.44	Possible transcription factor
DN222770	0.00311	0.42	Transcription factor BTF3-like
CD661731	0.00041	0.64	Helix-loop-helix DNA-binding domain, sterol regulatory element-binding protein-like
DN210718	0.00082	1.17	Transcriptional adaptor 2 (ADA2)
DV621143	0.01077	0.45	Member of the HIR1 family of WD-repeat proteins
DV621732	0.00004	1.21	Possible C2H2-type Zinc finger transcription factor
BM267520	0.00023	1.21	Zinc finger, B-box domain containing protein
Chromatin			
CD651386	0.00006	0.68	Nucleosome/chromatin assembly factor group D protein
CB816664	0.00084	1.22	HMG1/2 (high mobility group) box-protein
CB380544	0.00075	0.90	Putative high mobility group box protein
CB885544	0.00096	0.75	Putative Histone H2A
DN229198	0.00004	1.10	Maize histone H2A
CD484720	0.00044	1.31	Maize Histone H2B
DN221834	0.00048	0.75	Maize histone H2B
CB617087	0.00092	0.72	Putative Histone H2B5
CB885370	0.00081	0.76	Maize histone H2B.5
CB280768	0.00070	1.19	Putative histone H 4
CB834099	0.00064	1.30	Putative Histone H4
Signal transduction			
BM340951	0.00061	0.69	Serine-Threonine Protein Kinase, Plant-Type
DN225508	0.00031	3.56	Serine-Threonine Protein Kinase, Plant-Type
DN220529	0.00049	0.76	Putative Serine/Threonine protein kinase
DV622343	0.00026	0.76	Serine-Threonine Protein Kinase
DV491381	0.00087	1.41	Putative ERECTA receptor protein kinase
CB329429	0.00017	1.54	Putative receptor-like protein kinase
DN210188	0.00049	0.81	Putative wall-associated receptor protein kinase
DN204294	0.00008	1.27	ras-GTPase-activating protein SH3-domain binding protein-like
BM079608	0.00539	9.39	Putative p21-rho-binding domain containing
DN234378	0.00525	3.57	Leucine-rich repeat-containing protein
Proteolysis/Protein fate			
BG840965	0.00158	0.10	Ankyrin repeat-containing protein, putative ubiquitin ligase
DN232995	0.00556	3.51	Ubiquitin-specific protease-like
BQ279703	0.00018	7.52	Ubiquitin-like
CB331199	0.00027	1.53	putative ring-box protein
CD527256	0.00033	1.19	Putative ubiquitination factor E4
DN231478	0.00007	0.64	Cysteine protease Mir3-like
DV621524	0.00020	1.20	Putative Serine Endopeptidase DEGP2
DV490108	0.00018	1.28	Putative Proteasome subunit alpha type 2
BG840917	0.00064	0.89	Putative Proteinase inhibitor I12, Bowman-Birk type
DN227596	0.00011	1.38	Putative TCP-1/cpn60 chaperonin family protein

Table 4.1 (continued): Genes differentially-expressed in the rgd2-R mutant SAM			
Accession #	**p value**	**Fold change**	**Putative Gene Identification**
DN218224	0.00097	1.40	Heat shock 70 protein
BG841726	0.00448	7.74	putative HSP70, ARM repeat containing
CB331649	0.00038	1.38	per-1 family member
CB331278	0.00066	3.18	Maize cyclophilin, Peptidyl-prolyl cis-trans isomerase, cyclophilin type
Cytoskeleton			
CB331550	0.00022	1.42	Actin-binding, cofilin/tropomyosin type protein
CB604270	0.00074	1.29	Zea mays beta-7 tubulin
DN208851	0.00066	0.79	Putative unconventional myosin XI-like
BM340564	0.00052	0.52	Microtubule-associated protein 1 light chain 3-like protein
DN212951	0.00074	0.84	Putative myosin-like protein
BM347967	0.00378	2.13	Putative ARP2/3 complex 20 kDa subunit (ARPC4)
DN204110	0.00053	1.16	Elongation factor 1 alpha
DNA replication			
AI622063	0.00012	1.27	DNA replication licensing factor MCM7-like
DN209850	0.00053	0.64	Single-strand binding protein family
DV621454	0.00081	0.69	Maize Origin Recognition Complex Subunit 1
Metabolism			
BM080471	0.00016	1.32	argininosuccinate synthase
BM078436	0.00064	1.24	Putative pyruvate kinase, EC 2.7.1.40
DN212830	0.00066	0.86	Lecithin:cholesterol acyltransferase-like, EC 2.3.1.43
DN206428	0.00024	0.77	Putative phospholipase D protein
CD527719	0.00009	0.72	O-methyltransferase, family 2, EC 2.1.1.-
CB604839	0.00046	0.63	Maize fructokinase 1, EC 2.7.1.4
CD670197	0.00071	1.20	Clavaminate synthase-like, EC 1.14.11.21
CD484712	0.00049	1.27	Phosphoenolpyruvate carboxylase, EC 4.1.1.31
CB381580	0.00053	1.29	Isocitrate dehydrogenase NADP-dependent, eukaryotic, EC 1.1.1.42
CB833458	0.00068	1.28	Putative NADH-ubiquinone oxidoreductase
CB885881	0.00035	1.30	Glyceraldehyde-3-phosphate dehydrogenase, cytosolic, EC 1.2.1.12
BM074122	0.00063	1.33	Cytoplasmic malate dehydrogenase
DV942641	0.00044	0.76	Putative oxysterol binding protein
DN213207	0.00064	0.50	Glycogenin glucosyl transferase-like
DN221082	0.00085	5.12	Phenylalanine ammonia-lyase; EC 4.3.1.5
DN204225	0.00045	1.44	Fructosamine kinase
DN207238	0.00050	1.49	LPD1 (lipoamide dehydrogenase 1), EC 1.8.1.4
DV550953	0.00059	0.69	D-glycerate 3-kinase, EC 2.7.1.31
DN215756	0.00082	1.51	Methionine synthase, vitamin-B12 independent
CD484410	0.00012	0.82	Superoxide dismutase [Cu-Zn] (MAIZE)
DV549937	0.00089	1.29	Putative multicopper oxidase, pollen-specific protein Bp10-like
CB380882	0.00086	0.77	Putative phosphomevalonate kinase, EC 2.7.1.36
CB885470	0.00052	0.78	Cysteine synthase
CB605278	0.00051	1.35	Putative NADH-dehydrogenase 39kDa subunit EC 1.6.5.3
DN227764	0.00009	0.69	Nucleoside-diphosphate kinase, EC 2.7.4.6
DN223790	0.00018	0.82	Trehalose-6-phosphate synthase
CD527174	0.00059	1.36	Cleft Lip and Palate Associated Transmembrane Protein-Related
Other			
CB381574	0.00001	0.62	Cyclin IaZm-like
CB886407	0.00080	1.34	Floral organ regulator 1-like
BM080403	0.00086	1.36	Frigida-like protein

Table 4.1 (continued): Genes differentially-expressed in the rgd2-R mutant SAM

Accession #	p value	Fold change	Putative Gene Identification
CB605145	0.00011	0.66	Plant lipid transfer protein/seed storage/trypsin-alpha amylase inhibitor
DN204081	0.00099	1.22	Statistically defined repeat DNA
BM332245	0.00068	1.24	Rho GDP-dissociation inhibitor
RNA binding or processing			
CA829318	0.00060	1.39	Hyaluronic Acid-Binding Protein 4, Nuclear RNA Binding Protein A-Like Protein
CB331714	0.00049	1.32	Putative Glycine-Rich RNA-Binding Protein
CB250115	0.00050	0.77	Putative THO Complex Subunit 3 WD-40 Repeat containing
CB380524	0.00096	0.71	Putative RNA Binding Protein RZ-1
CD527281	0.00060	0.82	putative snRNA Sm-like protein/ Putative SAD1 (Supersensitive to ABA and Drought 1)
CD568706	0.00060	0.76	Nucleolysin TIA-1-like
DN215403	0.00012	1.10	Potassium channel regulatory factor/Prp18 domain containing
Stress-related			
DN205512	0.00074	0.81	Jasmonate-induced protein-like, leaf thionin-like
DN226593	0.00006	0.73	Coronatine insensitive 1-like
DV490246	0.00044	0.79	Catalase isozyme 3, EC 1.11.1.6
DN210036	0.00074	0.13	Putative glutathione peroxidase, EC 1.11.1.9
Translation			
DN220078	0.00070	0.18	Ribosomal protein S11
CB833828	0.00005	1.19	Putative ribosomal protein L7AE
CB885416	0.00033	1.23	Maize 60S ribosomal protein L39
CB329860	0.00005	1.71	60S Ribosomal Protein L18a
CB815895	0.00021	1.28	Putative 60S ribosomal protein L18e
CB885847	0.00009	0.85	Putative Ribosomal Protein L3p
CB604439	0.00013	0.82	Putative 60S ribosomal protein L27e
CD568560	0.00010	1.13	Putative elongation factor-1 gamma
CB381712	0.00077	1.33	Putative Eukaryotic Translation Initiation Factor 3-related
CD573263	0.00028	1.23	Putative 60S Ribosomal Protein L6
CB604957	0.00048	1.48	40S ribosomal S4 protein
CB250114	0.00087	0.48	Ribosomal protein S12/S23
CB381080	0.00032	1.15	Putative ribosomal protein L13
CB381409	0.00071	0.83	Putative 60S ribosomal protein L27
CD001130	0.00052	0.75	Putative 40S ribosomal subunit S9
CB816014	0.00034	0.81	Zea mays translational initiation factor eIF-4A (tif-4A3)
DV621311	0.00096	1.35	Putative 50S Ribosomal Protein L4
DN209313	0.00013	1.32	Ribosomal protein S4
DN217693	0.00007	1.18	Putative translation initiation factor eIF-1A
DN211570	0.00046	0.71	30S Ribosomal Protein S16
DN213621	0.00092	1.19	Zea mays ribosomal protein L30 (rpl30)
DN206858	0.00021	1.54	Putative 40S ribosomal protein S10
DN211469	0.00073	1.42	Ribosomal L22e protein
DN232564	0.00038	1.12	Putative 60S Ribosomal Protein L14
DN220333	0.00035	1.31	Putative 40S ribosomal protein S12E
DN220643	0.00034	1.20	Putative 40S ribosomal protein S12E
DN231324	0.00010	1.27	Putative Eukaryotic Release Factor 1
DN211015	0.00068	0.78	Protein translation factor SUI1 homolog (Protein GOS2)
DN225978	0.00076	1.18	Putative Ribosomal protein L31e/ small nuclear ribonucleoprotein
CD651548	0.00029	0.79	Putative Ribosomal protein L11/ L5

Table 4.1 (continued): Genes differentially-expressed in the rgd2-R mutant SAM			
Accession #	**p value**	**Fold change**	**Putative Gene Identification**
DV494543	0.00021	1.22	Putative 60S Ribosomal Protein L1/L4
DV495826	0.00016	0.78	Putative 25S rRNA
CD651265	0.00018	0.73	Ribosomal Protein L1
DN213848	0.00083	0.82	Ribosomal protein S6-like
Transport			
CB604948	0.00099	1.19	Putative Nuclear transport factor 2
DV490645	0.00050	1.17	Putative Nucleotide-sugar transporter, Golgi
DN219736	0.00045	1.35	Putative importin beta-3
DN207153	0.00074	0.59	H+ plasma membrane transporting ATPase-like
DN208288	0.00089	0.79	Phosphatidylcholine transfer protein
Unknown			
DV491400	0.00068	1.48	Unknown
AA418251	0.00065	1.15	Unknown
BQ539499	0.00006	6.25	Unknown
BM338067	0.00080	1.11	Unknown
CD001382	0.00058	0.90	Unknown
DN227936	0.00066	1.13	Unknown
AW355896	0.00033	1.40	Unknown
DN214841	0.00051	1.42	Unknown
BM332481	0.00080	1.26	Unknown
DN230665	0.00051	0.76	Unknown
BM073021	0.00091	1.72	Unknown
BG874170	0.00071	0.16	Unknown
DN206792	0.00024	0.65	Unknown
BM382333	0.00794	0.45	Unknown
DN213263	0.00077	0.62	Unknown (contains cinful LTR sequence)
BM073135	0.00001	1.21	Unknown protein
CB833890	0.00004	1.29	Unknown protein
CB281935	0.00018	0.71	Translationally controlled tumor protein
DV621973	0.00062	0.74	Unknown protein
CD484827	0.00039	1.16	Protein of unknown function DUF1084
DV622068	0.00016	1.47	SH3 Domain containing protein
CD484854	0.00017	1.56	Unknown WD40 repeat domain containing
CD651226	0.00059	0.86	Unknown (RING finger domain containing)
DV490767	0.00039	0.76	Reticulon family protien
CB351408	0.00020	0.68	Unknown
DN210576	0.00008	0.74	Armadillo domain containing protein
BM334513	0.00062	0.41	Protein of unknown function DUF887, TLC-like
CB329358	0.00040	0.47	SAP domain containing protein-like
DV622445	0.00044	0.82	D111/G-patch domain containing protein
AW067277	0.00066	1.32	Unknown
CA829834	0.00038	0.83	Unknown protein
CD573387	0.00081	0.69	Unknown protein
CB815685	0.00039	0.71	Unknown protein
CD572904	0.00085	1.16	Protein of unknown function DUF791
DV493956	0.00097	0.79	Unkown
DN204133	0.00018	0.73	Unknown WD repeat containing protein
DN208195	0.00093	0.88	Unknown protein

Table 4.1 (continued): Genes differentially-expressed in the rgd2-R mutant SAM			
Accession #	**p value**	**Fold change**	**Putative Gene Identification**
AW066680	0.00091	0.82	Protein of unknown function DUF266
DN222728	0.00074	1.19	Unknown protein
DN221288	0.00094	0.86	Unknown protein
DN213503	0.00003	1.14	Unknown protein
DN207488	0.00067	0.76	Unnamed protein
DN217861	0.00088	0.54	Unknown protein
DN226040	0.00032	0.77	Unknown protein
DN207424	0.00091	0.72	Unknown protein
DV621240	0.00067	4.63	Unknown protein
DN227265	0.00082	4.50	Unknown protein
DN209651	0.00090	0.69	Kelch-related protein
DN203830	0.00052	0.87	Unknown protein
DN229135	0.00060	0.84	XYPPX repeat containing protein
DN212681	0.00789	0.11	Unknown protein
DV489660	0.00454	2.25	Unknown, DUF248 containing
DN223697	0.00564	0.18	Unknown protein
CD484665	0.00981	0.44	Spiral1-like
CD059054	0.00058	1.13	Putative Acyl-CoA-binding protein
DV621899	0.00060	1.21	Unknown protein
CB885420	0.00078	1.43	Unknown protein
Vessicle Trafficking			
CB334277	0.00060	0.82	Synaptobrevin-like
CD058733	0.00034	1.25	Putative Rab7 small GTPase
DN209289	0.00052	0.71	Arf GTPase activating protein, Glo3-like
BM079296	0.00095	1.61	Vesicle transport V-SNARE protein VTI1-related
BM078226	0.00047	1.16	Putative ADP Ribosylation Factor (Arf)

qRT-PCR and *in situ* Hybridizations: Corroborating the Differential Expression of Genes Identified by Microarray Data

Quantitative RT-PCR (qRT-PCR) was used to measure the relative transcript accumulation of 30 differentially-expressed microarray genes whose fold-change was > 2. Out of 30 genes tested, 21 showed compatible fold changes in rgd2-R versus non-mutant SAMs as predicted from microarray data (Pearson correlation coefficient was 0.6) (Table 4.2). Nine genes that were originally detected via microarray as differentially expressed in the rgd2-R mutant SAMs could not be verified by qRT-PCR and were excluded from further consideration. These false-positive data may be an artifact generated by cross-hybridization between related gene family members , which is an intrinsic drawback to the use of long cDNA arrays (Draghici et al., 2006).

In situ hybridization was used to further characterize the tissue-specific expression patterns of ten differentially expressed genes identified in our dataset. Two such genes displayed very weak or undetectable signal and could not be interpreted. Eight genes exhibited interesting mRNA accumulation patterns within the maize shoot apex and are good candidates for subsequent genetic analysis to test whether they may function during the RGD2-mediated patterning of maize shoot development (Table 4.3, Figures 4.3-4.7).

Table 4.2 qRT-PCR corroboration of rgd2-R differentially expressed genes

Accession #	p-value	Putative Gene Identification	microarray fold change	qRT-PCR fold-change	std of Δct in qRT-PCR
DN222016	0.00424	Putative DP transcription factor	0.42	0.47	0.59
DY397856	0.00125	Maize MADS box transcription factor	3.37	1.98	0.65
DN222770	0.00311	Transcription factor BTF3-like	0.42	0.42	0.03
DN224320	0.00001	Maize DNA-binding WRKY	0.28	0.29	1.14
DN225508	0.00031	Serine-Threonine Protein Kinase, Plant-Type	3.56	3.63	0.51
BM079608	0.00539	Putative p21-rho-binding domain containing	9.39	3.66	1.41
DN234378	0.00525	Leucine-rich repeat-containing protein	3.57	5.94	0.28
DV621240	0.00067	Ubiquitin protein ligase	4.63	3.66	0.64
DN232995	0.00556	Ubiquitin-specific protease-like	3.51	2.00	0.36
BG840965	0.00158	Putative ubiquitin ligase	0.10	0.13	0.74
BG841726	0.00448	Putative HSP70, ARM repeat containing	7.74	4.17	0.03
BM347967	0.00378	Putative ARP2/3 complex 20 kDa subunit	2.13	2.46	1.53
DN227265	0.00082	Unknown	4.50	2.69	0.49
DN212681	0.00789	Unknown	0.11	0.22	0.10
BM382333	0.00794	Unknown	0.45	0.17	0.11
DV489660	0.00454	Unknown, DUF248 containing	2.25	9.30	0.50
BM334513	0.00062	Protein of unknown function DUF887, TLC-like	0.41	0.10	1.46
CD484665	0.00981	Spiral1-like	0.44	0.35	0.39
DN223697	0.00564	Unknown protein	0.18	0.01	0.27
BQ539499	0.00006	Unknown	6.25	4.63	0.65
BG874170	0.00071	Unknown	0.16	0.04	1.58

Table 4.3 Genes chosen for *in situ* hybridization

Accession #	p-value	Fold change	Putative Gene Identification
DN224320	5.6E-06	0.28	Maize DNA-binding WRKY
DV621143	0.01077	0.45	Member of the HIR1 family of WD-repeat proteins
CD058851	0.00051	0.75	Putative zinc finger homeodomain protein
BM340951	0.00061	0.69	Serine-Threonine Protein Kinase, Plant-Type
CB331199	0.00027	1.53	Putative ring-box protein
BM073135	7.7E-06	1.21	Unknown protein
DN223697	0.00564	0.18	Unknown protein
DN212681	0.00789	0.11	Protein of unknown function

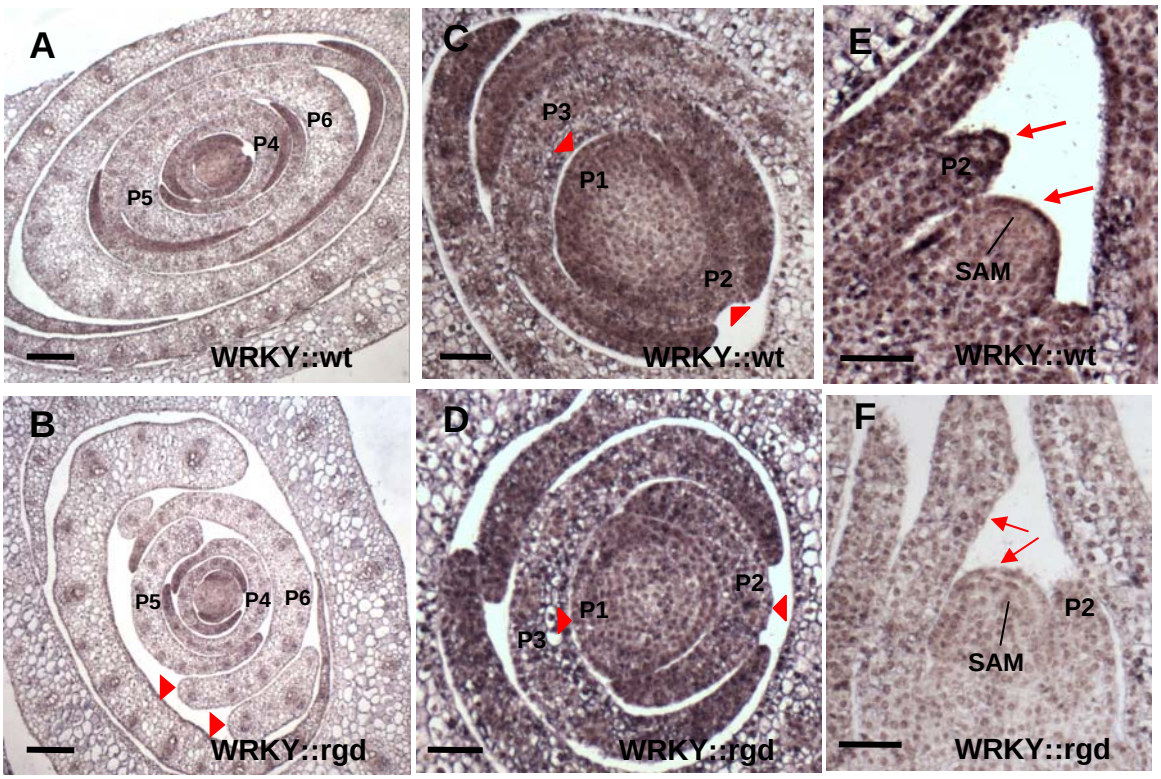

Figure 4.3 *In situ* hybridization analyses of the predicted WRKY transcription factor (DN224320). (A, C, E) Expression of DN224320 is shown in transverse (A, C) and longitudinal (E) sections of non-mutant shoot apics. Transcripts of DN224320 accumulated weakly in the SAM, strongly throughout the P1 and P2 leaf primordia, but was gradually restricted to the vascular bundles and leaf margins from P3 through P5 (A, C). Expression of DN224320 was also greatly enriched in the superficial cell layer (L1) of the SAM and in the L1-derived epidermis of leaf primordia (arrows in E). (B, D, F) Expression of DN224320 was shown in transverse (B, D) and longitudinal (F) sections of rgd2-R mutant. Expression of DN224320 is reduced in the margin area of older leaf primordia (P3-P5, arrow heads), the midrib regions of P1and P2 (arrow heads), and L1 or L1-derived tissue (arrow). Numbers denote leaf primordia. Scale bars = 200μm in A and B, scale bars = 50μm in C, D, E, F.

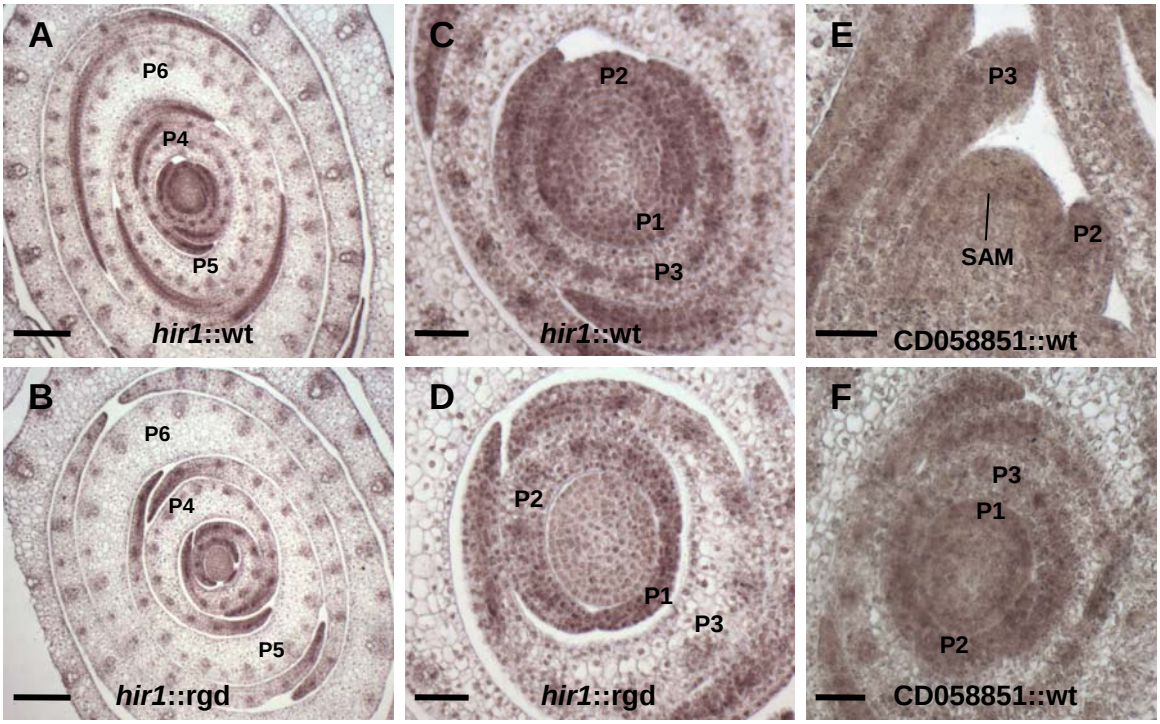

Figure 4.4 *In situ* hybridization analyses of two putative transcription factors *hir1* (DV621143) and CD058851. (A, C) Expression of the putative hir1 is localized to the peripheral region of the SAM, vascular bundles and leaf margins in the non-mutant. (B, D) Transcripts of the putative hir1 are greatly reduced in the peripheral regions of the SAM in the rgd2-R mutant apex. (E, F) Longitudinal (E) and transverse sections (F) showed that CD058851 is expressed in the SAM, especially in the crown, in the non-mutant maize shoot apex. Numbers denote leaf primordia. Scale bars = 200μm in A and B, scale bars = 50μm in C, D, E, F.

Transcription Factors and Chromatin Remodeling Genes are Differentially Expressed in the rgd2-R Mutant SAM

Our microarray data identified twelve differentially expressed genes that are predicted to encode transcription factors (Table 4.1), four of which were verified as misexpressed in the rgd2-R mutant SAM via qRT-PCR (Table 4.2). *In situ* hybridization was used to further characterize the transcript accumulation of three additional transcription factors, including a putative WRKY encoding gene (DN224320), a putative histone regulatory (HIR1) encoding gene (DV621143) and a putative zinc finger homeodomain encoding gene (CD058851) (Figure 4.3, 4.4). The putative WRKY (DN224320) gene is most similar to WRKY1 (98% identity, 687/700, 8 gaps), which encodes a maize protein that interacts with RS2 (Phelps-Durr et al., 2005). In the non-mutant SAM, transcripts of this WRKY (DN224320) accumulated weakly in the SAM, strongly throughout the P1 and P2 leaf primordia, but was gradually restricted to the vascular bundles and leaf margins from P3 through P5 (Figure 4.3, A, C). Expression of DN224320 was also greatly enriched in the tunica layer (L1) of the SAM and in the L1-derived epidermis of leaf primordia (arrows in the Figure 4.3 E). In the rgd2-R mutant SAM, however, transcripts of DN224320 in the midrib regions of the P1 and P2 were greatly reduced (Figure 4.3 D, arrow heads). In older leaf primordia (P3 –P5) one or both of the marginal accumulations were absent or diminished, in accord with the rgd2 mutant defect in mediolateral development (Figure 4.3 B, arrow heads). Moreover, DN224320 transcript accumulations in the L1 layer of the rgd2-R mutant SAM is reduced or patchy; a similar accumulation pattern is observed in the leaf primordial epidermis (Figure 4.3 F, arrows). These *in situ* data correlate with the downregulation of DN224320 observed in our microarray and qRT-PCR analyses (0.28 and 0.29 fold, respectively. The expression of a putative zinc finger homeodomain encoding gene (CD058851) was enriched in

the crown of the SAM, the vascular tissue, and the leaf margins in both non-mutant and rgd2-R mutant apex (Figure 4.4 E, F).

In addition, *in situ* hybridization was used to characterize the expression pattern of a predicted HIR1 (DV621143) encoding gene in the maize shoot apex. DV621143 is paralogous to the maize HIRA orthologue that has been identified to interact with RS2 in maize and with AS1 in *Arabidopsis* (Phelps-Durr et al., 2005). In the non-mutant, transcripts of the putative HIR1 (DV621143) accumulate low in the central zone (CZ), but high in the peripheral zone (PZ) of the SAM. In the leaf primordia DV621143 is abundant and throughout the P1, and becomes more limited to the vascular tissue and the leaf margins from P2 through P5 (Figure 4.4 A, C). In the rgd2-R mutant apex the expression of DV621143 in the leaf primordia was comparable to that of the non-mutant, but the transcript accumulation in the PZ of the SAM was remarkably reduced (Figure 4.4 B, D). These data are well-correlated with the mutant downregulation observed in our microaray data (0.45 fold), and may suggest that RGD2 functions as a positive regulator of this HIR1-encoding gene during early stage of leaf development.

In addition to its predicted function as a transcription factor, HIRA (the paralogue of DV621143) functions as a chromatin remodeling factor that mediates nucleosome assembly and chromatin structure (Spector et al., 1997; Magnaghi et al., 1998; Ray-Gallet et al., 2002). Eleven additional putative chromatin-related genes are differentially expressed in the rgd2-R mutant SAMs (Table 4.1), including three putative high mobility group proteins that are essential for chromatin dynamics during regulation of gene expression and cell differentiation, and eight putative histone proteins that provide the building blocks for nucleosome assembly and transcription regulation (Stein et al., 1992; Reichheld et al., 1998; Bianchi and Agresti, 2005; Hock et al., 2007).

Multiple Signal Transduction Genes are Differentially Expressed in the rgd2-R Mutant SAM

Signal transduction genes are implicated in numerous developmental-related processes, such as stem cell maintenance in the SAM, cell polarity, cell differentiation, leaf polarity and hormone response (Osada et al., 1997; Shiu and Bleecker, 2001; Becraft, 2002; Tichtinsky et al., 2003; Xu et al., 2003; Guyon et al., 2004; Qi et al., 2004). Ten genes predicted to be involved in signal transduction are significantly mis-expressed in the rgd2-R mutant SAMs (Table 4.1), including four putative Serine-Threonine protein kinases, three predicted receptor protein kinases and three putative signaling genes that mediate protein-protein or protein-RNA interaction. qRT-PCR corroborated the differential expression of three putative signaling genes (Table 4.2), and *in situ* hybridization of a putative plant type Serine-Threonine protein kinase encoding gene (BM340951) revealed its non-mutant expression is localized in the SAM proper, vascular bundles, leaf margins, and one or two cell layers on the abaxial side of older leaf primordia (P4-P6) (Figure 4.5 A, B, D, F). In the rgd2-R mutants, the tissue and domain-specific expression patterns of BM340951 are unaffected, but the signal is much weaker (Figure 4.5 D, E, G). These *in situ* expression data correlated with our microarray results, wherein BM340951 was downregulated 0.69 fold in the rgd2-R mutant SAM.

In addition, the putative maize ERECTA orthologue (DV491381), a protein kinase homologous to an *Arabidopsis* gene that functions redundantly with AS1 and AS2 to promote adaxial leaf identity (Xu et al., 2003; Qi et al., 2004; Li et al., 2005), was also upregulated in the rgd2-R mutant SAMs, suggesting that RGD2 may function to repress the expression of a maize ERECTA-like gene (DV491381).

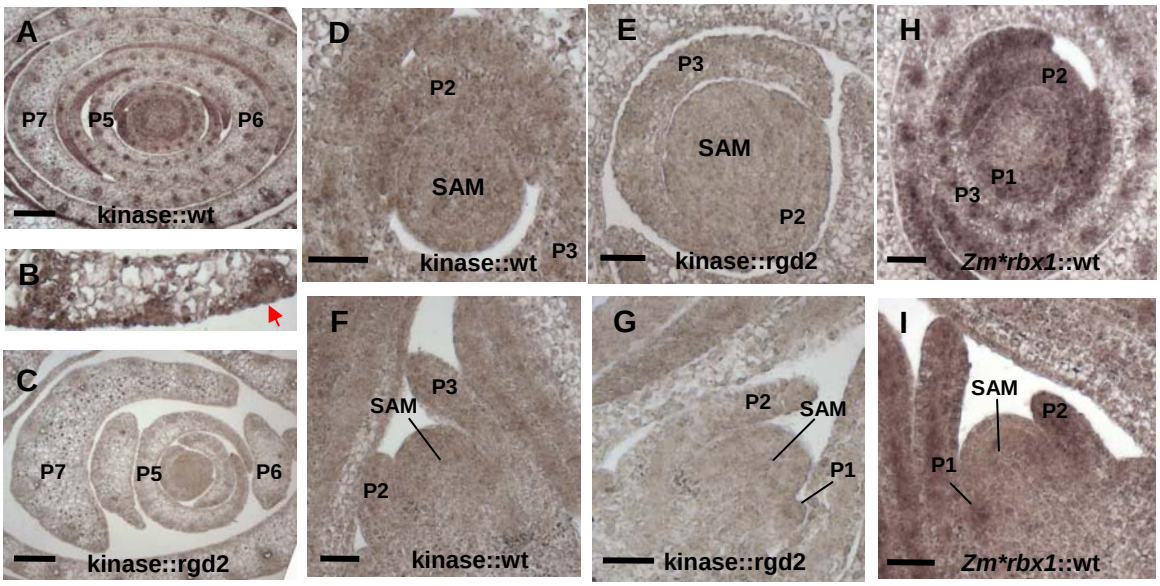

Figure 4.5 *In situ* hybridization analyses of a putative Serine-Threonine protein kinase (BM340951) and a putative ring box gene (*Zm*rbx*, CB331199). Transverse (A-E) and longitudinal (F-G) sections showed that BM340951 is expressed in the crown of meristem, vasculature, leaf margins and one-two cell layers in the abaxial sides of older leaf primordia (arrow) in non-mutant shoot apices (A, B, D, F). Expression of BM340951 is decreased in the rgd2-R mutant apex (C, E, G). (H-I) transverse (H) and longitudinal sections (I) showed that CB331199 is expressed in the founder cell ring and the newly initiating leaf primordia. Later, expression is predominant in the vasculature. Numbers denote leaf primordia. Scale bars = 200μm in A and C, scale bars = 50μm in B, D, E, F, G, H, I.

Genes Involved in Proteolysis/Protein Fate are Differentially Expressed in the rgd2-R Mutant SAM

Transcriptome analyses of rgd2-R mutant SAMs reveals that fourteen genes predicted to function during proteolysis and protein fate are significantly mis-expressed; these include nine genes involved in protein degradation and five genes involved in protein folding, assembly or processing (Table 4.1). qRT-PCR correlated the differential expression of three putative proteolysis genes implicated to function in the ubiquitin-20S proteasome pathway, as well as a heat shock protein (HSP70) putatively involved in protein metabolism and stress response (Gaitanaris et al., 1990; Sung et al., 2001) (Table 4.2). *In situ* hybridizations were performed for a predicted maize orthologue of the *rbx1* gene (*Zm*rbx1*) (CB331199), whose *Arabidopsis* homolog specifies targeted proteins for degradation in the ubiquitin-proteasome pathway (Hellmann and Estelle, 2002). Transcripts of *Zm*rbx1* are detected in newly initiating leaf primordia, including the P0; *Zm*rbx1* mRNA accumulation colocalizes with the leaf founder cell ring in transverse sections of the non-mutant SAM (Figure 4.5 H, I). No changes in expression pattern of *Zm*rbx1* are identified in rgd2-R mutant apices, suggesting that the 1.53 fold increase in transcript abundance detected in our microarray experiments is not easily differentiated via *in situ* hybridization protocols (Table 4.1).

Genes of Unknown Functions are Significantly Mis-expressed in the rgd2-R Mutant SAM

Out of the 202 maize genes that are identified as differentially expressed in the rgd2-R mutant SAM, 57 genes encode unknown predicted functions (Table 4.1). qRT-PCR corroborated the differential expression of nine unknown-encoding genes (Table 4.2), and *in situ*

hybridizations further characterized the expression patterns of three putative unknown genes (Figure 4.6).

In the non-mutant apex unknown DN212681 is enriched in the SAM (Figure 4.6 A), whereas unknown DN223697 is expressed in leaf vasculature and in the un-vascularized P1 primordium in a pattern that appears to precede and predict vein development (Figure 4.6 B). In the rgd2-R mutants, which are defective in lateral development, the expression domain of DN223697 is much reduced and sporadic (Figure 4.6 C). These data are consistent with the pronounced downregulation of DN223697 transcript accumulation in the rgd2-R SAM as measured in our microarray and qRT-PCR analyses (0.18 fold and 0.06 fold, respectively). Transcripts of yet another unknown maize gene (BM073135) are localized to the new and incipient leaf primordia in the non-mutant apex, whereas the expression of BM073135 is throughout the SAM in rgd2-R mutants (Figure 4.6 D, F). These data correlate with the observed upregulation of BM073135 in the microarray data (1.21 fold) (Table 4.1), indicating that RGD2 may negatively regulate BM073135 in the indeterminate meristematic cells.

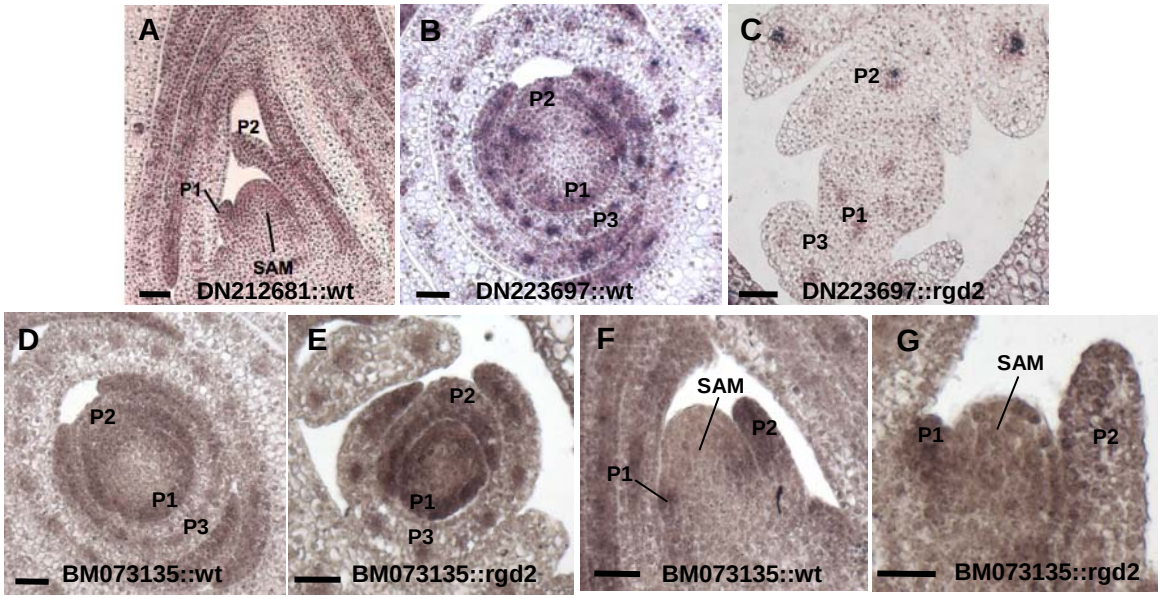

Figure 4.6 *In situ* hybridization analyses of three genes of unknown predicted function. (A) Unknown DN212681 is expressed in the crown of the SAM in the non-mutant longitudinal section. (B) Unknown DN223697 is expressed in leaf vasculature and in the un-vascularized P1 primordium in a pattern that appears to precede and predict vein development. (C) Expression of DN223697 is much reduced and sporadic in the rgd2-R mutant. (D-G) Transverse (D, E) and longitudinal (F, G) sections showed the expression of unknown BM073135 is localized in the new and incipient leaf primordia in the non-mutant apex (D, F), whereas the expression is throughout the SAM in the rgd2-R mutants (E, G). Numbers denote leaf primordia. Scale bars = 50μm.

Reverse Genetic analyses of Four Differentially Expressed Genes: a progress report

In order to characterize the biological functions of genes that are differentially expressed in the rgd2-R mutant apex, ten genes were selected and targeted for reverse mutagenesis using transposon *Mutator* (*Mu*) screening (Table 4.4). In this assay, DNA extracted from F2 individuals obtained via self-pollination of ~ 3,000 F1 plants harboring *Mu* transposon activity were screened using gene-specific primers paired with a *Mu*-specific primer (see Material and Methods). Four out of the ten selected genes were found to have putative *Mu* insertions, including the putative WRKY encoding gene (DN224320; ten putative independent insertions), the predicted HIR1 (DV621143; four putative independent insertions), the putative unknown (DN223697; eleven putative independent insertions) and a predicted protein kinase (DN225508; six putative independent insertions) (Table 4.4). Of these combined 31 putative gene-specific *Mu* insertion alleles identified in gel assays of PCR products (see Materials and Methods), 22 were verified by sequence analyses to indeed contain *Mu* transposon insertions in the targeted genes (Table 4.4). Siblings of the F2 plants that were PCR-screened were planted in the summer nursery in Aurora, NY, and will be analyzed for co-segregation of gene-specific *Mu* insertions and leaf developmental phenotypes. Phenotypic *Mu* insertion alleles will represent novel maize mutations. Subsequent morphological, genetic, and molecular analyses of gene expression performed on these new maize mutants will be used to ascertain the function of the corresponding gene products during maize leaf development.

Table 4.4 Genes chosen for reverse genetics in maize

Accession #	p-value	Fold change	Putative Gene Identification	Function	*Mu* hits*
DN225508	0.00031	3.56	Serine-Threonine Protein Kinase, Plant-Type	Signal transduction	6 (2)
DN224320	0.00001	0.28	Maize DNA-binding WRKY	Transcription	10 (7)
DV621143	0.01077	0.45	Member of the HIR1 family of WD-repeat proteins	Transcription/ chromatin	4 (3)
DN223697	0.00564	0.18	Unknown	Unknown	11 (10)
CD661819	0.01713	0.46	putative 26S proteasome subunit RPN9	Protein fate/proteolysis	0 (0)
BG840965	0.00158	0.10	ankyrin repeat-containing protein, putative ubiquitin ligase	Protein fate/proteolysis	0 (0)
DN219767	0.00594	0.11	protein binding / ubiquitin-protein ligase and putative RING zinc finger protein	Protein fate/proteolysis	0 (0)
DN223776	0.00107	0.06	Serine/threonine protein phosphatase PP2A-4 catalytic subunit	Signal Transduction	0 (0)
CB381167	0.00002	1.44	possible transcription factor	Transcription	0 (0)
DN222770	0.00311	0.42	Transcription factor BTF3-like	Transcription	0 (0)

***:** First number designates putative *Mu* insertions detected by agarose gel electrophoresis of PCR fragments; the number in parentheses represents *Mu* insertions verified by sequencing of PCR fragments (see Materials and Methods).

DISCUSSION

Unlike all other radial-leaf mutants described in the literature, maize rgd2-R mutants display no reduction of adaxial or abaxial identity (Henderson et al., 2005; Henderson et al., 2006). Transcripts of multiple leaf patterning genes such as NS1, YABBY14, Zm*KAN2 and RLD1 are greatly reduced in the rgd2-R mutant apex, although the expression patterns and domain-specificities of these transcripts are unaffected. These previous analyses suggest that RGD2 is required to coordinate dorsiventral and mediolateral patterning during maize leaf development, although the molecular mechanisms of RGD2 function are completely unknown. Here we utilized a genomic approach to identify genes and genetic pathways that function downstream of RGD2, and to provide novel insight into the molecular mechanisms of leaf patterning and lateral expansion.

Laser Microdissection is Effective to Restrict Microarray Analyses to the SAM

rgd2-R mutant plants display narrow to filamentous leave with defective founder cell recruitment, minimal lateral expansion and odd adaxial/abaxial pattering (Henderson et al., 2005; Henderson et al., 2006). Molecular expression analyses revealed that multiple developmental marker genes are aberrantly expressed in the rgd2-R mutant SAM, suggesting that RGD2 functions quite early during shoot development, prior to the formation of leaf primordia. Micoarray comparisons of non-mutant and rgd2-R mutant seedlings are likely to give rise to a skewed dataset that is biased toward post-primordial differences in gene expression, owing to the enormous differences in leaf expansion and patterning observed in mutant and non-mutant seedlings. Therefore, laser microdissection was used to limit our transcriptome analyses to

genes expressed in the shoot apex (i.e. SAM and P1), in an attempt to identify the earliest events downstream of RGD2 function. Among the genes represented in our SAM microarray dataset, genes predicted to be involved in transcription regulation, chromatin remodeling, signal transduction, proteolysis/protein fate control, and unknown function are especially misexpressed in the rgd2-R mutant SAMs (discussed below). Eight genes selected from the above categories were characterized by *in situ* hybridization; all eight genes were expressed in the SAM, corroborating the effectiveness of laser microdissection to restrict microarray comparisons to specific developmental field.

RGD2 and LBL1 Function in Separate Pathways to Coordinate Leaf Patterning

Mutations in RGD2 and LBL1 display similar anatomy and morphology, although lbl1 mutant leaves are described as abaxialized whereas rgd2 mutant leaves exhibit no reduction in adaxial or abaxial identity. LBL1 encodes a maize SGS3 orthologue that functions via the ta-siRNA pathway to promote adaxial cell fate (Nogueira et al., 2007); as yet the RGD2 gene product is unknown. Double mutants of rgd2 lbl1 are shootless and embryo lethal, suggesting that RGD2 functions redundantly with LBL1 but in a different genetic pathway to mediate leaf patterning (Henderson et al., 2005; Henderson et al., 2006). Laser microdissection microarray analyses of LBL1 function identified only two maize genes that are differentially expressed in both RGD2 and LBL1, including a predicated ribosomal protein (DN213621) and a predicted unknown protein DN212681 (A Sarkar and M Timmermans, personal communication of unpublished data). This low level of shared differential gene expression identified in our microarray analyses is consistent with previous genetic analyses, which predicted that that RGD2 and LBL function in separate genetic pathways to affect similar developmental traits.

RGD2 may function through ARP pathway to regulate leaf development?

ARP genes encode MYB domain proteins that are required to maintain *knox* gene expression in the "off" state within leaf primordia (Kidner and Martienssen, 2004; Chitwood et al., 2007). Loss of RS2 function in maize results in ectopic but variegated *knox* accumulation in the leaf tissue. Therefore, RS2 has been proposed to repress knox expression through an epigenetic mechanism (Timmermans et al., 1999; Tsiantis et al., 1999). Several protein partners have been shown to interact with RS2, including a putative transcription factor (WRKY1) and a predicted chromatin remodeling factor (HIRA) (Phelps-Durr et al., 2005). Notably, twelve putative transcription factors and eleven predicted chromatin remodeling genes are differentially expressed in the rgd2-R mutant SAM, including a putative paralogue of WRKY1(DN224320) and a predicted paralogue of HIRA (DV621143) (Table 4.1, Figure 4.3, 4.4). In particular, gene DN224320 is very similar to WRKY1 at the nucleotide sequence level (98% identity, 687/700, 8 gaps). In the non-mutant shoot apex, expression of DN24320 was observed throughout the P1 and P2 leaf primordia, but was gradually localized to the vascular bundles and leaf margins from P3 through P5 (Figure 4.3, A, C). This expression pattern is very similar to that of observed for RS2 (Timmermans et al., 1999; Tsiantis et al., 1999). Although DN24320 and RS2 are co-expression in maize leaf primordia, in the absence of genetics or biochemical data it is not possible to predict any shared function for these two gene products. Intriguingly, DN224320 is also expressed in the SAM and accumulates in the L1 layer (Figure 4.3). Laser ablation experiments and analyses of LBL1 function have revealed that the L1 layer of the SAM is a required source of developmental signals controlling adaxial/abaxial leaf patterning (Reinhardt et al., 2003a; Reinhardt et al., 2003b; Reinhardt et al., 2005; Nogueira et al., 2007). In the rgd2-R mutant apex, transcripts of DN224320 are reduced in the midrib regions of young leaf primordia,

marginal regions of old leaf primordia, and in the L1 layer in the SAM (Figure 4.3), suggesting that RGD2 has a positive effect on DN224320 expression during maize leaf development. Genetic analyses may reveal if the predicted WRKY (DN224320) contributes to dorsiventral patterning functions of the L1 layer.

A putative *hir1* gene (DV621143) is also significantly downregulated in the rgd2-R mutant SAMs. DV621143 is paralogous to the maize RS2-interacting gene HIRA. In yeast and animals, HIRA is known to modulate heterochromatic gene silencing and euchromatic gene expression via chromatin remodeling (Spector et al., 1997; Magnaghi et al., 1998). In *Arabidopsis* HIRA has been shown to interact with AS1 and functions to maintain leaf determinacy and *knox* gene silencing (Phelps-Durr et al., 2005). Transcripts of DV621143 accumulate in the maize meristem and in developing leaf primordia; this expression pattern closely resembles that of HIRA in *Arabidopsis* (Figure 4.4) (Phelps-Durr et al., 2005). In the rgd2-R mutant apex, expression of DV621143 was remarkably reduced in the PZ of the SAM (Figure 4.4), indicating that RGD2 is required to maintain expression of DV621143 in the maize meristem.

HIRA also has been shown to interact with a HISTONE DEACETYLASE (HDAC) and CHROMATIN ASSEMBLY FACTOR-1 (Ahmad et al., 2003, 2004). In *Arabidopsis*, HDACs function independently and convergently with AS1/ AS2 to regulate leaf dorsiventrality. Blocking HDACs activity in an *as1* or *as2* mutant background leads to abaxialized radial leaves and ectopic accumulation of miR165/166 (Ueno et al., 2007), although solo *as1* or *as2* mutants result in no dorsiventral patterning defects (Byrne et al., 2000; Iwakawa et al., 2002). Whether maize HIRA and its putative paralogue *hir1* (DV621143) have similar functions is not clear; Further genetic analyses are required to give a more definitive answer.

ERECTA (ER), a receptor-like protein kinase, acts redundantly with the ARP gene and the LATERAL ORGAN BOUNDARY (LOB) gene AS2 to promote adaxial fate in *Arabidopsis* (Xu et al., 2003; Qi et al., 2004; Li et al., 2005). Although solo mutants in *as1* or *as2* display no dorsiventral defects, mutations in either *as1* or *as2* in an *er* mutant background leads to increased accumulation of miR166/5 and partial loss of adaxial identity (Xu et al., 2003; Qi et al., 2004; Li et al., 2005). Our microrray identified ten predicted signaling genes that are significantly mis-expressed in the rgd2-R mutant SAM (Table 4.1), including a putative ERECTA protein kinase encoding gene (DV491381). DV491381 is orthologous to the *er* gene in *Arabidopsis* and may play a similar role in maize leaf patterning. Taken together, RGD2 may function through modulating multiple genes that are paralogous to ARP interactors or cooperators to coordinate leaf lateral expansion and dorsiventral patterning. The misregulation of KNOX accumulation in rgd2-R mutants is consistent with the hypothesis that RGD2 functions in an ARP related pathway, as are genetic analyses that RGD2 and LBL function in separate pathways (Henderson et al., 2005; Henderson et al., 2006). Cloning of the rgd2 gene will enable tests of this now speculative model.

RGD2 may regulate leaf dorsiventrality via novel proteolytic pathway?

Genes involving in proteolysis/protein fate may regulate biological function at the post-translational level, including degradation, folding, assembly and processing of cellular proteins. Our microarray data identified fourteen such genes that are differentially expressed in the rgd2-R mutant SAM, including five genes predicted to be involved in the Skp1-Cul1-F-box-protein (SCF) proteolytic pathway (Table 4.1). The SCF complex is a multi-subunit ubiquitin protein ligase (E3) that is comprised of S-phase kinase associated protein1 (Skp1), Cullin1 (Cul1), an F-

box protein and a ring box protein (RBX). E3 mediates the transfer of activated UBIQUITIN to a targeted protein substrate, which is then recognized and degraded by the 26S proteasome (Hellmann and Estelle, 2002; Cardozo and Pagano, 2004). The UBIQUITIN-SCF-proteasome pathway is involved in multiple cellular and developmental processes such as auxin response and light signaling (Callis and Vierstra, 2000; Hellmann and Estelle, 2002; Dharmasiri and Estelle, 2004). Degradation of AUX/IAA by the SCF^{TIR1}-proteasome leads to the activation of AUXIN RESPONSE FACTORS (ARFs), transcription factors regulating auxin-induced signaling (Hellmann and Estelle, 2002; Dharmasiri and Estelle, 2004).

Recently, AUXIN RESPONSE FACTOR 3 (ARF3) and ARF4 have been shown to promote abaxial identity in *Arabidopsis* (Fahlgren et al., 2006). ARF3 is expressed throughout the meristem and leaf primordia, and ARF4 is expressed in the abaxial side of leaf primordia (Pekker et al., 2005). Double mutants in *arf3 arf4* display narrow and abaxialized leave (Pekker et al., 2005). In addition, the ta-siRNA pathway mediates leaf patterning by targeting the transcripts of ARF3 and ARF4 for destruction in *Arabidopsis* (Fahlgren et al., 2006; Hunter et al., 2006). Leaves of lbl1 null mutants, which harbor mutations in the ta-siRNA biosynthetic gene SGS3, are thread-like and abaxialized. The lbl1 mutant phenotype is accompanied by upregulation of miR166 and downregulation of the HD-ZIPIII genes ROLLED1 and ROLLED2, which correlates with the over-accumulation of maize ARF3 and ARF4 transcripts (Juarez et al., 2004; Nogueira et al., 2007). In keeping with the similar phenotypes of rgd2 and lbl1 mutants, perhaps RGD2 may function to coordinate dorsiventral and mediolateral patterning by regulating the proteolysis of ARF4 via the UBIQUITIN-SCF-proteasome pathway. RLD1 transcript accumulation is reduced in the rgd2-R mutant, and the newly identified co-expression of putative proteolysis gene *Zm*rbx1* (Figure 4.5 H, I) and ARF3/ARF4 (Noguiera etal.,2007) in the newly

initiating leaf primordia and P0, support the above hypothesis (Henderson et al., 2006). Alternatively, RGD2 might function via the proteolysis of genes upstream of the ARP pathway to coordinate leaf lateral growth and dorsiventral patterning. Cloning of RGD2, biochemical analysis of ARF3/ARF4 in rgd2 mutant plants, and reverse mutagenesis of the implicated genes will help test the efficacy of these hypothesized RGD2 functions.

Transcripts in unvascularized tissue, what for?

Notably, three differentially expressed genes, the putative *Zm*rbx1 gene* (CB331199) and two predicted unknown genes (DN223697 and BM073135), are expressed in leaf vasculature as well as in unvascularized tissues such as the P1 and the founder cells within the SAM. Expression of these three genes within the P1 and SAM appears to precede and predict the eventual location of developing vasculature (Figure 4.5 H, I, Figure 4.6 B-G). Given that lateral leaf development is disrupted in the rgd2-R mutant and that vasculature is required for lateral expansion, it is not surprising to identify vasculature genes that are differentially expressed in rgd2-R mutant leaves (Henderson et al., 2005; Cnops et al., 2006; Henderson et al., 2006). However, the microarray data used to detect these genes was generated from laser microdissected SAM and P1, tissues devoid of vasculature. These findings suggest perhaps *Zm*rbx1,* DN223697 and BM073135 perform different functions in the vascularized primordia and in the unvascularized SAM/P1? More intriguingly, these data may comprise the first evidence that vascular patterning actually begins at the founder cell stage, well before the appearance of provascular tissues. Genetic analyses and identification of these gene functions may determine which of these hypotheses is more likely.

MATERIALS AND METHODS

Plant materials

The *rgd2*-R was introgressed into Mo17 for 5 generations. Non-mutant and rgd2-R mutant maize siblings were grown in controlled conditions with 15 hours light with intensity 220-250 $\mu ES^{-1}M^{-2}$ at 25°C; and 9 hours dark at 20°C. Humidity was set at 50%. Siblings were harvested for laser microdissection at 14 days after germination.

Isolation of maize SAM RNAs

Siblings were fixed with acetone and embedded in paraffin as described (Emrich et al., 2007). The P.A.L.M. Laser Microbeam (Bernried, Germany) was used to collect SAM cells from 10 µm sections. Each SAM typically comprised 10-12 longitudinal sections for laser microdissection. Six biological replicates were captured independently. Each replicate consisted of 3-5 whole non-mutant or rgd2-R SAMs with harvested areas varying from 0.57 mm^2 to 0.95 mm^2 (Supplementary Table 4.1). RNA from the captured SAMs was extracted using the PicoPure™ RNA extraction kit (Arcturus Molecular Devices, Sunnyvale, CA) and amplified twice (RiboAmp™ HS RNA amplification kit; Arcturus Molecular Devices, Sunnyvale, CA) to yield 28 µg to 74 µg antisense RNA (Supplementary Table 4.1).

First strand cDNA was synthesized from the amplified SAM RNA using Superscript II (Invitrogen, Carlsbad, CA) and purified with QIAquick PCR purification kit (QIAGEN, Valencia, CA). Purified cDNA (2.5 ug) was indirectly labeled with Cy dye as described (Nakazono et al., 2003). Dye swapping was performed between biological replicates to minimize dye bias. Microarrays were hybridized according to Nakazono et al (2003).

Maize chips

Maize SAM 1.1 (GPL3333) and SAM 3.0 (GPL3538) gene chips containing a combined total of 28,671 cDNAs were used in this experiment (Emrich et al., 2007; Zhang et al., 2007). Detailed information about these chips is available at http://www.plantgenomics.iastate.edu/maizechip/ or MADI (MicroArray Data Interface http://schnablelab.plantgenomics.iastate.edu:8080/madi/ , and in Zhang et al., 2007).

Microarray data analyses and annotation

Each hybridized microarray gene chip was scanned with ScanArray Lite (Packard Bioscience, Meriden, CT) at 10μm resolution. Image quantification was performed with ScanArray Express (PerkinElmer, Waltham, MA). Raw signals were first corrected by background intensity within each slide, followed by LOWESS normalization to remove intensity-dependent dye bias (Dudoit et al., 2002). Median centering was used to normalize data across slides from each channel (Yang et al., 2002). A mixed linear model was applied to the normalized data to identify the differentially expressed genes among rgd2-R mutant and non-mutant samples as described (Dudoit et al., 2002; Zhang et al., 2007). The identified differentially expressed genes were functionally annotated as described in Buckner et al., 2007.

Quantitative RT-PCR and *in situ* hybridization

SYBR green-based real time RT-PCR arrays were performed on cDNA templates reverse transcribed from the same amplified RNA sources used in the microarray analyses (Gomes-Ruiz et al., 2006). Two biological replicates from each genotype (rgd2-R mutant and non-mutant) were analyzed in triplicate for each target gene. Transcript accumulations were normalized to

control *ubiquitin* expression, and the relative expression ratios were calculated as described (Livak and Schmittgen, 2001). Target gene specific primers are listed in the Supplemental Table 4.2.

Maize two-week-old seedlings were fixed in FAA and processed for *in situ* hybridization as described (Juarez et al., 2004; Buckner et al., 2007; Zhang et al., 2007). At least six plants from each genotype (rgd2-R mutant and non-mutant sibling) were compared for each gene-specific probe presented in the text.

Reverse genetic analyses

For each target gene, 3,456 DNA samples prepared from F2 progeny obtained by self-pollination of active *Mutator* transposon stocks were subjected to PCR-based screens using gene-specific primers and a *Mu* specific primer (*Mu*). Three primers were designed for each target gene (Supplementary table 4.3). The gene specific forward primer T1 was used to optimize PCR amplification conditions for two gene specific reverse primers M1 and M2 (M2 is upstream of M1). The first round of PCR analysis (pooled PCR) was performed with the *Mu* and M1 primers, on 96-well PCR plates with pooled four DNA samples in each well. PCR reactions were screened for specific fragments using 1% agarose gels. The corresponding DNA samples in the selected DNA sample pools were rearrayed for a second round of PCR analysis using the same primer set (*Mu* and M1) (deconvolution PCR). PCR reactions were then analyzed by agarose gel electrophoresis to identify individual DNA samples with specific fragments. The identified DNA samples were used for the third round of PCR amplification with the *Mu* and M2 primers (nested PCR). Meanwhile, to rule out the false-positive results derived from multiple *Mu* insertions, control reactions were performed with the *Mu* primer only. PCR reactions with

specific products only from the nested PCR amplifications were sequenced to verify the *Mutator* transposon insertion.

Supplementary Table 4.1 Laser Microdissection Microarray samples used in this study

Sample Information	rgd1	wt1	rgd2	wt2	rgd3	wt3	rgd4	wt4	rgd5	wt5	rgd6	wt6
mm^2 captured[i]	0.60	0.75	0.72	0.95	0.60	0.78	0.72	0.75	0.58	0.62	0.59	0.57
aRNA yield (µg)	38	74	46	72	63	43	50	43	43	40	28	54
Labeling for SAM1	Cy3	Cy5	Cy5	Cy3	Cy5	Cy3	Cy3	Cy5	Cy3	Cy5	Cy5	Cy3
Labeling for SAM3	Cy5	Cy3	Cy5	Cy3	Cy3	Cy5	Cy3	Cy5	Cy3	Cy5	Cy5	Cy3

[i] square surface area of SAM tissue isolated by laser microdissection

Supplemental table 4.2 Primers used for quantitative real time RT-PCR

Accession #	Forward primer 5'-3'	Reverse primer 5'-3'
DV621240	GCGGTCAGGCAGTAAAAGAG	GTGACATCTGACTGCCAGGA
DN232995	GCAGGGGCCATCATACTAGA	GCCTGTGCTGAGGCCTATAC
BG840965	CCATCACGAGCACTTTCTGA	AGGGTCTTTCGAGGCAGACT
DN222016	TGCACCAGCTGCATATCTTC	GAGCTTGTGGGACTGAAAGG
DY397856	AATCCATTGCCAACATGTGA	TCTTCAGAGGAGGGAGCAAA
DN222770	TTAAACCGACGACCCTTCAC	AAGCTGGCTGAGATTTTCCA
DN224320	GAGCATGGAAGGGAGTCTTG	GGGATGTCTGCAACCTTGTT
DN225508	GTCTGCGACCTCCTTCTGAG	ACAAACAACGTCATGCTGGA
BM079608	TGTCGTCTCATGCTCTACGC	CCATTTGATTGCTTCACACG
DN234378	CGAATGCACATTAGGCAAAA	AGACCCCAGAAATGTCATCG
BM347967	CTTCAGCTCGCTGATCTCCT	TCCCCTCTTATCTTGCCGTA
BG841726	TGCATCATCAGCTTTGGAAG	CGTCATAACCAGCCTGGAGT
DN227265	AAGTCCTTCTTCCGTCAGCA	GGTGACGAGAGACGAATCAA
DN212681	GAGAAAAGCGATCTGCAAGG	AAGTGGTGGTGGCAAATAGC
BM382333	CGCCATTAAAAGTCGCTGAT	AGGTGACCTGCCATTACAGC
DV489660	CAAAATTAAGGGAGCGCAAG	GCCAGACGTAGTAGCCAAGG
BM334513	CAGCCATCGAACAGCTCATA	ACACCTTGAGGGATCGTTTG
CD484665	GGAAGTTTCCGGTGTTCTGA	CACCAGCTGTAAGTGCTCCA
DN223697	CTTGCCATGGATGAATGATG	CCGAGTTTCAGCCTTTTCAG
BQ539499	ATGGGTTGTTCCCCCTTATC	GCCACAACATGCAGTCAAGA
BG874170	GCCTGATGCGTAGTGTGAGA	CACCAGCAACCAATGTTGTC

Supplemental table 4.3 Primers used for reverse genetic screening of *Mutator* stocks

Accession #	Primer name	Sequence (5' to 3')	Length (bp)	Tm*	Amplicon / tester (bp)
CD661819	X1-M1	CCACAGTTGTGTAGGCCAGAT	21	61	327
	X1-M2	CATGAACTGTGGGATCGACAT	21	60	228
	X1-T1	CTTCTCGCCAGTACCCTGATAA	22	62	
BG840965	X2-M1	CTTGGACACCTTGAATCGAAAC	22	60	132
	X2-M2	CGAAACAGATAACCACCATCG	21	60	116
	X2-T1	GTTCAGACGCTGCTGCTGTT	20	60	
DN219767	X3-M1	CTGTGCTCCATTTGTCAGGAG	21	61	728
	X3-M2	ATGGTCCAGTTCCGTCTTGAT	21	60	667
	X3-T1	AGAGGAACATCCGAGCTAATCC	22	62	
DN223776	X4-M1	GCGAGAGCTGTAACAAATGGA	21	60	~900
	X4-M2	CTGGGAATTGGTAACACCACA	21	60	~700
	X4-T1	CACGTGGTGCTGGCTACACT	20	63	
DN225508	X5-M1	GGTAGAGCCCGAAGTCTGAGAT	22	64	158
	X5-M2	GTCCAGCATGACGTTGTTTGT	21	60	118
	X5-T1	GTGGGAGATAATCTGCAAGCTG	22	62	
CB381167	X6-M1	CTGCAGTTTGAGGGCTTCAG	20	60	525
	X6-M2	CACCCAAAATGGCTCATAAGG	21	60	143
	X6-T1	ACCGATAACAAAGACCCAGGA	21	60	
DV621143	X7-M1	GATTAGTTTGGCGCGGATTT	20	56	121
	X7-M2	TGAGTGTCCAATCTGAGAGGTG	22	62	101
	X7-T1	CCTTTCCTTTCCCTTTTTGC	20	56	
DN222770	X8-M1	TTCTCATCCTGCTCCAGTTGA	21	60	954
	X8-M2	CTGGAAAATCTCAGCCAGCTT	21	60	835
	X8-T1	AGAGCACCTTGAAAAGGATCG	21	60	
DN224320	X9-M1	CAAACTCGCAAGACTCCCTTC	21	61	549
	X9-M2	TCTTCATCATCTCGCTCTGGA	21	60	394
	X9-T1	CTGCACATCTTCGACAGCAAC	21	61	
DN223697	X11-M1	GAGTCCGCAATCTCCATCAAC	21	61	257
	X11-M2	CCTGCAACTGAATCTGTCCAA	21	60	116
	X11-T1	AGGGATTCATGCTACCCAGAG	21	61	

*Tm calculator**:** http://www.basic.northwestern.edu/biotools/oligocalc.html (salt adjusted)

REFERENCE

Adenot, X., Elmayan, T., Lauressergues, D., Boutet, S., Bouche, N., Gasciolli, V., and Vaucheret, H. (2006). DRB4-dependent TAS3 trans-acting siRNAs control leaf morphology through AGO7. Curr Biol **16,** 927-932.

Ahmad, A., Takami, Y., and Nakayama, T. (2003). WD dipeptide motifs and LXXLL motif of chicken HIRA are necessary for transcription repression and the latter motif is essential for interaction with histone deacetylase-2 in vivo. Biochem Biophys Res Commun **312,** 1266-1272.

Ahmad, A., Takami, Y., and Nakayama, T. (2004). WD dipeptide motifs and LXXLL motif of chicken HIRA are essential for interactions with the p48 subunit of chromatin assembly factor-1 and histone deacetylase-2 in vitro and in vivo. Gene **342,** 125-136.

Allen, E., Xie, Z., Gustafson, A.M., and Carrington, J.C. (2005). microRNA-directed phasing during trans-acting siRNA biogenesis in plants. Cell **121,** 207-221.

Baumberger, N., and Baulcombe, D.C. (2005). *Arabidopsis* ARGONAUTE1 is an RNA Slicer that selectively recruits microRNAs and short interfering RNAs. Proc Natl Acad Sci U S A **102,** 11928-11933.

Becraft, P.W. (2002). Receptor kinase signaling in plant development. Annu Rev Cell Dev Biol **18,** 163-192.

Bianchi, M.E., and Agresti, A. (2005). HMG proteins: dynamic players in gene regulation and differentiation. Curr Opin Genet Dev **15,** 496-506.

Bowman, J.L., Eshed, Y., and Baum, S.F. (2002). Establishment of polarity in angiosperm lateral organs. Trends Genet **18,** 134-141.

Buckner, B., Beck, J., Browning, K.F., Fritz, A.E., Hoxha, E., Grantham, L.D., Kamvar, Z.N., Lough, A.N., Nikolova, O., Schnable, P.S., Scanlon, M.J., and Janick-Buckner, D. (2007). Involving Undergraduates in the Annotation and Analysis of Global Gene Expression Studies: Creation of a Maize Shoot Apical Meristem Expression Database. Genetics.

Byrne, M.E., Barley, R., Curtis, M., Arroyo, J.M., Dunham, M., Hudson, A., and Martienssen, R.A. (2000). Asymmetric leaves1 mediates leaf patterning and stem cell function in *Arabidopsis*. Nature **408,** 967-971.

Callis, J., and Vierstra, R.D. (2000). Protein degradation in signaling. Curr Opin Plant Biol **3,** 381-386.

Cardozo, T., and Pagano, M. (2004). The SCF ubiquitin ligase: insights into a molecular machine. Nat Rev Mol Cell Biol **5,** 739-751.

Chitwood, D.H., Guo, M., Nogueira, F.T., and Timmermans, M.C. (2007). Establishing leaf polarity: the role of small RNAs and positional signals in the shoot apex. Development **134,** 813-823.

Cnops, G., Neyt, P., Raes, J., Petrarulo, M., Nelissen, H., Malenica, N., Luschnig, C., Tietz, O., Ditengou, F., Palme, K., Azmi, A., Prinsen, E., and Van Lijsebettens, M. (2006). The TORNADO1 and TORNADO2 genes function in several patterning processes during early leaf development in *Arabidopsis thaliana*. Plant Cell **18,** 852-866.

Dharmasiri, N., and Estelle, M. (2004). Auxin signaling and regulated protein degradation. Trends Plant Sci **9,** 302-308.

Draghici, S., Khatri, P., Eklund, A.C., and Szallasi, Z. (2006). Reliability and reproducibility issues in DNA microarray measurements. Trends Genet **22,** 101-109.

Dudoit, S., Yang, Y.H., Callow, M.J., and Speed, T.P. (2002). Statistical methods for identifying genes with differential expression in replicated cDNA microarray experiments. Statistical Sinica**,** 111-139.

Emery, J.F., Floyd, S.K., Alvarez, J., Eshed, Y., Hawker, N.P., Izhaki, A., Baum, S.F., and Bowman, J.L. (2003). Radial patterning of *Arabidopsis* shoots by class III HD-ZIP and KANADI genes. Curr Biol **13,** 1768-1774.

Emrich, S.J., Barbazuk, W.B., Li, L., and Schnable, P.S. (2007). Gene discovery and annotation using LCM-454 transcriptome sequencing. Genome Res **17,** 69-73.

Eshed, Y., Baum, S.F., Perea, J.V., and Bowman, J.L. (2001). Establishment of polarity in lateral organs of plants. Curr Biol **11,** 1251-1260.

Eshed, Y., Izhaki, A., Baum, S.F., Floyd, S.K., and Bowman, J.L. (2004). Asymmetric leaf development and blade expansion in *Arabidopsis* are mediated by KANADI and YABBY activities. Development **131,** 2997-3006.

Fahlgren, N., Montgomery, T.A., Howell, M.D., Allen, E., Dvorak, S.K., Alexander, A.L., and Carrington, J.C. (2006). Regulation of AUXIN RESPONSE FACTOR3 by TAS3 ta-siRNA affects developmental timing and patterning in *Arabidopsis*. Curr Biol **16,** 939-944.

Gaitanaris, G.A., Papavassiliou, A.G., Rubock, P., Silverstein, S.J., and Gottesman, M.E. (1990). Renaturation of denatured lambda repressor requires heat shock proteins. Cell **61,** 1013-1020.

Gasciolli, V., Mallory, A.C., Bartel, D.P., and Vaucheret, H. (2005). Partially redundant functions of *Arabidopsis* DICER-like enzymes and a role for DCL4 in producing trans-acting siRNAs. Curr Biol **15,** 1494-1500.

Gomes-Ruiz, A.C., Nascimento, R.T., de Paula, S.O., and da Fonseca, B.A. (2006). SYBR green and TaqMan real-time PCR assays are equivalent for the diagnosis of dengue virus type 3 infections. J Med Virol **78,** 760-763.

Grigg, S.P., Canales, C., Hay, A., and Tsiantis, M. (2005). SERRATE coordinates shoot meristem function and leaf axial patterning in *Arabidopsis*. Nature **437,** 1022-1026.

Guyon, V., Tang, W.H., Monti, M.M., Raiola, A., Lorenzo, G.D., McCormick, S., and Taylor, L.P. (2004). Antisense phenotypes reveal a role for SHY, a pollen-specific leucine-rich repeat protein, in pollen tube growth. Plant J **39,** 643-654.

Hellmann, H., and Estelle, M. (2002). Plant development: regulation by protein degradation. Science **297,** 793-797.

Henderson, D.C., Muehlbauer, G.J., and Scanlon, M.J. (2005). Radial leaves of the maize mutant ragged seedling2 retain dorsiventral anatomy. Dev Biol **282,** 455-466.

Henderson, D.C., Zhang, X., Brooks, L., 3rd, and Scanlon, M.J. (2006). RAGGED SEEDLING2 is required for expression of KANADI2 and REVOLUTA homologues in the maize shoot apex. Genesis **44,** 372-382.

Hock, R., Furusawa, T., Ueda, T., and Bustin, M. (2007). HMG chromosomal proteins in development and disease. Trends Cell Biol **17,** 72-79.

Hudson, A. (2001). Plant development: Two sides to organ asymmetry. Curr Biol **11,** R756-758.

Hunter, C., Willmann, M.R., Wu, G., Yoshikawa, M., de la Luz Gutierrez-Nava, M., and Poethig, S.R. (2006). Trans-acting siRNA-mediated repression of ETTIN and ARF4 regulates heteroblasty in *Arabidopsis*. Development **133,** 2973-2981.

Iwakawa, H., Ueno, Y., Semiarti, E., Onouchi, H., Kojima, S., Tsukaya, H., Hasebe, M., Soma, T., Ikezaki, M., Machida, C., and Machida, Y. (2002). The ASYMMETRIC

LEAVES2 gene of *Arabidopsis thaliana*, required for formation of a symmetric flat leaf lamina, encodes a member of a novel family of proteins characterized by cysteine repeats and a leucine zipper. Plant Cell Physiol **43,** 467-478.

Jackson, D., Veit, B., and Hake, S. (1994). Expression of the maize KNOTTED-1 related homeobox genes in the shoot apical meristem predicts patterns of morphogenesis in the vegetative shoot. Development**,** 405-413.

Juarez, M.T., Kui, J.S., Thomas, J., Heller, B.A., and Timmermans, M.C. (2004). microRNA-mediated repression of rolled leaf1 specifies maize leaf polarity. Nature **428,** 84-88.

Kerstetter, R.A., Bollman, K., Taylor, R.A., Bomblies, K., and Poethig, R.S. (2001). KANADI regulates organ polarity in *Arabidopsis*. Nature **411,** 706-709.

Kidner, C.A., and Martienssen, R.A. (2004). Spatially restricted microRNA directs leaf polarity through ARGONAUTE1. Nature **428,** 81-84.

Kidner, C.A., and Timmermans, M.C. (2007). Mixing and matching pathways in leaf polarity. Curr Opin Plant Biol **10,** 13-20.

Kim, M., McCormick, S., Timmermans, M., and Sinha, N. (2003). The expression domain of PHANTASTICA determines leaflet placement in compound leaves. Nature **424,** 438-443.

Li, H., Xu, L., Wang, H., Yuan, Z., Cao, X., Yang, Z., Zhang, D., Xu, Y., and Huang, H. (2005). The Putative RNA-dependent RNA polymerase RDR6 acts synergistically with ASYMMETRIC LEAVES1 and 2 to repress BREVIPEDICELLUS and MicroRNA165/166 in *Arabidopsis* leaf development. Plant Cell **17,** 2157-2171.

Livak, K.J., and Schmittgen, T.D. (2001). Analysis of relative gene expression data using real-time quantitative PCR and the 2(-Delta Delta C(T)) Method. Methods **25,** 402-408.

Magnaghi, P., Roberts, C., Lorain, S., Lipinski, M., and Scambler, P.J. (1998). HIRA, a mammalian homologue of Saccharomyces cerevisiae transcriptional co-repressors, interacts with Pax3. Nat Genet **20,** 74-77.

McConnell, J.R., and Barton, M.K. (1998). Leaf polarity and meristem formation in *Arabidopsis*. Development **125,** 2935-2942.

McConnell, J.R., Emery, J., Eshed, Y., Bao, N., Bowman, J., and Barton, M.K. (2001). Role of PHABULOSA and PHAVOLUTA in determining radial patterning in shoots. Nature **411,** 709-713.

Nakazawa, Y., Hiraguri, A., Moriyama, H., and Fukuhara, T. (2007). The dsRNA-binding protein DRB4 interacts with the Dicer-like protein DCL4 in vivo and functions in the trans-acting siRNA pathway. Plant Mol Biol **63,** 777-785.

Nakazono, M., Qiu, F., Borsuk, L.A., and Schnable, P.S. (2003). Laser-capture microdissection, a tool for the global analysis of gene expression in specific plant cell types: identification of genes expressed differentially in epidermal cells or vascular tissues of maize. Plant Cell **15,** 583-596.

Nogueira, F.T., Madi, S., Chitwood, D.H., Juarez, M.T., and Timmermans, M.C. (2007). Two small regulatory RNAs establish opposing fates of a developmental axis. Genes Dev **21,** 750-755.

Osada, S., Izawa, M., Koyama, T., Hirai, S., and Ohno, S. (1997). A domain containing the Cdc42/Rac interactive binding (CRIB) region of p65PAK inhibits transcriptional activation and cell transformation mediated by the Ras-Rac pathway. FEBS Lett **404,** 227-233.

Otsuga, D., DeGuzman, B., Prigge, M.J., Drews, G.N., and Clark, S.E. (2001). REVOLUTA regulates meristem initiation at lateral positions. Plant J **25,** 223-236.

Pekker, I., Alvarez, J.P., and Eshed, Y. (2005). Auxin response factors mediate *Arabidopsis* organ asymmetry via modulation of KANADI activity. Plant Cell **17,** 2899-2910.

Peragine, A., Yoshikawa, M., Wu, G., Albrecht, H.L., and Poethig, R.S. (2004). SGS3 and SGS2/SDE1/RDR6 are required for juvenile development and the production of trans-acting siRNAs in *Arabidopsis*. Genes Dev **18,** 2368-2379.

Phelps-Durr, T.L., Thomas, J., Vahab, P., and Timmermans, M.C. (2005). Maize rough sheath2 and its *Arabidopsis* orthologue ASYMMETRIC LEAVES1 interact with HIRA, a predicted histone chaperone, to maintain knox gene silencing and determinacy during organogenesis. Plant Cell **17,** 2886-2898.

Poethig, R.S. (1984). Cellular parameters of leaf morphogenesis in maize and tobacco. Contemporary Problems of Plant Anatomy (eds. R. A. White and W. C. Dickinson)**,** 235-238.

Poethig, R.S., and Szymkowiak, E.J. (1995). Clonal analysis of leaf development in maize. Maydica**,** 67-76.

Prigge, M.J., Otsuga, D., Alonso, J.M., Ecker, J.R., Drews, G.N., and Clark, S.E. (2005). Class III homeodomain-leucine zipper gene family members have overlapping, antagonistic, and distinct roles in *Arabidopsis* development. Plant Cell **17,** 61-76.

Qi, Y., Sun, Y., Xu, L., Xu, Y., and Huang, H. (2004). ERECTA is required for protection against heat-stress in the AS1/ AS2 pathway to regulate adaxial-abaxial leaf polarity in *Arabidopsis*. Planta **219,** 270-276.

Ray-Gallet, D., Quivy, J.P., Scamps, C., Martini, E.M., Lipinski, M., and Almouzni, G. (2002). HIRA is critical for a nucleosome assembly pathway independent of DNA synthesis. Mol Cell **9,** 1091-1100.

Reichheld, J.P., Gigot, C., and Chaubet-Gigot, N. (1998). Multilevel regulation of histone gene expression during the cell cycle in tobacco cells. Nucleic Acids Res **26,** 3255-3262.

Reinhardt, D., Frenz, M., Mandel, T., and Kuhlemeier, C. (2003a). Microsurgical and laser ablation analysis of interactions between the zones and layers of the tomato shoot apical meristem. Development **130,** 4073-4083.

Reinhardt, D., Frenz, M., Mandel, T., and Kuhlemeier, C. (2005). Microsurgical and laser ablation analysis of leaf positioning and dorsoventral patterning in tomato. Development **132,** 15-26.

Reinhardt, D., Pesce, E.R., Stieger, P., Mandel, T., Baltensperger, K., Bennett, M., Traas, J., Friml, J., and Kuhlemeier, C. (2003b). Regulation of phyllotaxis by polar auxin transport. Nature **426,** 255-260.

Schneeberger, R., Tsiantis, M., Freeling, M., and Langdale, J.A. (1998). The rough sheath2 gene negatively regulates homeobox gene expression during maize leaf development. Development **125,** 2857-2865.

Shiu, S.H., and Bleecker, A.B. (2001). Plant receptor-like kinase gene family: diversity, function, and signaling. Sci STKE **2001,** RE22.

Siegfried, K.R., Eshed, Y., Baum, S.F., Otsuga, D., Drews, G.N., and Bowman, J.L. (1999). Members of the YABBY gene family specify abaxial cell fate in *Arabidopsis*. Development **126,** 4117-4128.

Smith, L.G., Greene, B., Veit, B., and Hake, S. (1992). A dominant mutation in the maize homeobox gene, Knotted-1, causes its ectopic expression in leaf cells with altered fates. Development **116,** 21-30.

Spector, M.S., Raff, A., DeSilva, H., Lee, K., and Osley, M.A. (1997). Hir1p and Hir2p function as transcriptional corepressors to regulate histone gene transcription in the Saccharomyces cerevisiae cell cycle. Mol Cell Biol **17,** 545-552.

Stein, G.S., Stein, J.L., van Wijnen, A.J., and Lian, J.B. (1992). Regulation of histone gene expression. Curr Opin Cell Biol **4,** 166-173.

Sung, D.Y., Vierling, E., and Guy, C.L. (2001). Comprehensive expression profile analysis of the *Arabidopsis* Hsp70 gene family. Plant Physiol **126,** 789-800.

Theodoris, G., Inada, N., and Freeling, M. (2003). Conservation and molecular dissection of ROUGH SHEATH2 and ASYMMETRIC LEAVES1 function in leaf development. Proc Natl Acad Sci U S A **100,** 6837-6842.

Tichtinsky, G., Vanoosthuyse, V., Cock, J.M., and Gaude, T. (2003). Making inroads into plant receptor kinase signalling pathways. Trends Plant Sci **8,** 231-237.

Timmermans, M.C., Hudson, A., Becraft, P.W., and Nelson, T. (1999). ROUGH SHEATH2: a Myb protein that represses knox homeobox genes in maize lateral organ primordia. Science **284,** 151-153.

Tsiantis, M., Schneeberger, R., Golz, J.F., Freeling, M., and Langdale, J.A. (1999). The maize rough sheath2 gene and leaf development programs in monocot and dicot plants. Science **284,** 154-156.

Ueno, Y., Ishikawa, T., Watanabe, K., Terakura, S., Iwakawa, H., Okada, K., Machida, C., and Machida, Y. (2007). Histone deacetylases and ASYMMETRIC LEAVES2 are involved in the establishment of polarity in leaves of *Arabidopsis*. Plant Cell **19,** 445-457.

Vaucheret, H. (2005). MicroRNA-dependent trans-acting siRNA production. Sci STKE **2005,** pe43.

Waites, R., and Hudson, A. (1995). *phantastica*: a gene required for dorsoventrality of leaves in *Antirrhinum-majus*. Development **121,** 2143-2154.

Waites, R., Selvadurai, H.R., Oliver, I.R., and Hudson, A. (1998). The PHANTASTICA gene encodes a MYB transcription factor involved in growth and dorsoventrality of lateral organs in Antirrhinum. Cell **93,** 779-789.

Williams, L., Grigg, S.P., Xie, M., Christensen, S., and Fletcher, J.C. (2005). Regulation of *Arabidopsis* shoot apical meristem and lateral organ formation by microRNA miR166g and its AtHD-ZIP target genes. Development **132,** 3657-3668.

Xu, L., Xu, Y., Dong, A., Sun, Y., Pi, L., Xu, Y., and Huang, H. (2003). Novel as1 and as2 defects in leaf adaxial-abaxial polarity reveal the requirement for ASYMMETRIC LEAVES1 and 2 and ERECTA functions in specifying leaf adaxial identity. Development **130,** 4097-4107.

Yang, Y.H., Dudoit, S., Luu, P., Lin, D.M., Peng, V., Ngai, J., and Speed, T.P. (2002). Normalization for cDNA microarray data: a robust composite method addressing single and multiple slide systematic variation. Nucleic Acids Res **30,** e15.

Yoshikawa, M., Peragine, A., Park, M.Y., and Poethig, R.S. (2005). A pathway for the biogenesis of trans-acting siRNAs in *Arabidopsis*. Genes Dev **19,** 2164-2175.

Zhang, X., Madi, S., Borsuk, L., Nettleton, D., Elshire, R.J., Buckner, B., Janick-Buckner, D., Beck, J., Timmermans, M., Schnable, P.S., and Scanlon, M.J. (2007). Laser microdissection of narrow sheath mutant maize uncovers novel gene expression in the shoot apical meristem PLoS Genet **3(6),** e101.

CHAPTER 5

CONCLUSIONS AND PERSPECTIVES

CENH3 phosphorylation extends "histone code" to centromeres

All eukaryotic genetic information is wrapped around octamers comprised of four core histones, H3, H4, H2A, and H2B. The globular domains of these core histones are involved in protein-protein interactions, while the amino termini are exposed outside of the nucleosomes and subjected to a diverse array of posttranslational modifications such as methylation, acetylation, phosphorylation, and ubiquitylation. Distinct histone amino-terminal modifications can potentially act synergistically or antagonistically to modulate gene expression (Daujat et al., 2002; Noma and Grewal, 2002; Hirota et al., 2005). The combinatorial histone modifications were envisioned as a "histone code" that provides coding information other than the genetic code conferred by DNA sequence (Strahl and Allis, 2000). Recently, abundant evidence has accumulated in support of the "histone code" model (Barski et al., 2007; Kouzarides, 2007).

As a well-characterized reversible histone modification, phosphorylation occurs on four distinct residues on histone H3 (Ser10/28 and thr3/11) and has been implicated in diverse biological processes (Hendzel et al., 1997; Zeitlin et al., 2001b; Zeitlin et al., 2001a; Gernand et al., 2003; Preuss et al., 2003; Polioudaki et al., 2004). However, these conserved histone H3 phosphorylation events are restricted to certain chromosomal domains such as chromosome arms and pericentromeres. The centromere is a unique chromosomal domain that interacts with the kinetochore and coordinates microtubule attachment during cell division (Dawe and Henikoff, 2006). At centromeres, histone H3-containing subdomains are interspersed with domains containing a centromeric histone H3 variant (CENH3) (Blower et al., 2002; Chueh et al., 2005). Our data show that maize CENH3 is phosphorylated at Ser50 in a cell-cycle dependent manner similar to known H3 phosphorylation events (Figure 2.5). Thus CENH3 phosphorylation extends the "histone code" to centromeres. We further propose that the primary role of histone H3

phosphorylation is to demarcate distinct chromosomal domains (i.e. centromere, pericentromere, chromosome arm) so that chromosomes can align and segregate properly.

Maize CENH3 phosphorylation may participate in other cellular processes beyond a biological marker for active centromeres. One possibility is that CENH3 phosphorylation functions as a component of the spindle checkpoint via an as-yet-unknown mechanism. CENH3 phosphorylation is undetectable until prophase, reaches and maintains its maximum until metaphase-anaphase transition, and drops sharply upon anaphase initiation (Figure 2.6). The second possibility is that CENH3 is phosphorylated by an unspecified aurora kinase, and mediates kinetochore assembly and function through the recruitment of other kinetochore proteins. A good candidate kinase is aurora kinase 3, a conserved plant serine/threonine kinase that localizes at centromeres in prophase and move to cell plate in anaphase in *Arabidopsis*, and is capable of phosphorylating histone H3 Ser10/28 in vitro (Demidov et al., 2005; Kawabe et al., 2005; Kurihara et al., 2006). However, two questions remain to be addressed. One is whether a maize aurora 3 is able to phosphorylate H3 Ser10/28 and CENH3 Ser50 in vivo. Aurora kinase specific inhibitors such as Hesperadin or VX-680 may give a clue to this question (Hauf et al., 2003; Harrington et al., 2004; Kurihara et al., 2006). Knock-down of Aurora 3 via reverse genetics approaches are required to provide direct evidence. Another question is how aurora 3 recognizes two quite divergent proteins, if it phosphorylates both histone H3 and CENH3 indeed. Crystal structure analysis of the kinase and its substrate(s) may reveal the configurational information to tackle the question (Sessa et al., 2005).

To further unravel the biological functions of CENH3 phosphorylation, mutation of Ser50 to an unphosphorylatable amino acid (i.e., alanine) is a feasible, but time-consuming and expensive, strategy in maize. Given the interspecies-exchangeable nature of CENH3s (Wieland

et al., 2004), the availability of T-DNA insertion lines (Azpiroz-Leehan and Feldmann, 1997), and the convenience of genetic manipulation of *A. thaliana* (Clough and Bent, 1998; Zhang et al., 2006), it may be possible to use *Arabidopsis* to carry out this experiment. Wild-type and mutated (Ser50-to-Ala50) maize CENH3 could be transformed into *A. thaliana* in a HTR12 (the CENH3 homologue in *Arabidopsis*; Talbert et al., 2002) null background, phenotypic comparison between plants from these two transformation events can reveal the function of phosphorylation at Ser50. Additional genetic and biochemical (i.e. yeast two-hybrid) analysis will help answer whether phCENH3 interacts with other kinetochore proteins. Moreover, fluorescent fusion proteins in live cells can demonstrate accurate kinetics of each phosphorylation event, so that the phosphorylation order of CENH3-Ser50, H3-Ser28, H3-Ser10, H3-Thr3 and H3-Thr11 can be determined during cell division, which can help understand their functions (Reddy et al., 2004; Reddy et al., 2007). Finally, given the diverse modifications on histone H3, it is intriguing to test whether other covalent modifications (i.e., methylation and acetylation) apply to CENH3 as well. If yes, what is the function of each modification and how different modifications interact? Is there any difference from that on histone H3 with respect to the functions and interactions? These studies promise to better understand the conservation or diversity of the proposed "histone code".

Laser microdissection microarray: advantages and limitations

Most biological processes occur in heterogeneous tissues or organs comprised of distinct cell types with specialized morphology and function. Understanding the specific function of each cell type is of particular interest to cell and developmental biologists. Traditional methods, such as DNA or RNA *in situ* hybridization, immunolocalization and histochemical staining, have been

used to characterize the cellular distribution of individual transcripts, proteins and metabolites. However, these methods are greatly compromised by their low efficiency, in that just a single molecule per experiment is typically measured. Owing to their potential to measure biomolecules on a global scale, genomic- and proteomic technologies hold great promise toward understanding biological complexity.

Laser microdissection is a newly developed technology that enables the accurate and efficient isolation of selected cells based on histological appearance or biomolecular staining. Microarrays, on the other hand, are an effective high-throughput technology for analyses of molecular systems and networks (Schena et al., 1995; Templin et al., 2002; Abd El-Rehim et al., 2005; Bertone and Snyder, 2005; Mockler et al., 2005). The combined use of laser microdissection and microarrays enables cell- and tissue-specific analysis of DNA, RNA, protein or metabolite accumulation on a global scale (Scutt et al., 1997; Kerk et al., 2003; Schad et al., 2005b; Schad et al., 2005a; Nelson et al., 2006a).

However, the use of laser microdissection microarray analysis also has certain limitations. First, the process of tissue fixation, dehydration and embedding utilized in laser microdissectionis a trade-off between maintaining anatomical integrity and preservation of biomolecules in the target cells (Nelson et al., 2006b; Murray, 2007). Secondly, the ability to extract quantities of biomolecules from laser -captured cells is limited; subsequent sample amplifications is required to obtain sufficient quantities of biomolecules for use in microarrays (Nygaard and Hovig, 2006). Therefore, it is crucial that the amplification protocol utilized is linear and unbiased. Thirdly, similar to conventional microarray technology, laser microdissection microarray experiments are unable to detect RNAs expressed at low levels, and can only analyze biomolecules contained on the microarray platform (Schena et al., 1995;

Murray, 2007). Genome-wide analyses are not possible unless a completed genome sequence is available, and rare transcripts are undetectable. Lastly, the instrumentation currently employed in laser microdissection microarray analyses is costly (Nelson et al., 2006b).

New insights into the NS-mediated founder cell recruitment and mediolateral pattering

NS1 and NS2 encode paralogous WUSCHEL1-like homeobOX (WOX) transcription factors that are expressed at two lateral foci within the SAM (Nardmann et al., 2004). NS1 and NS2 function non-cell autonomously and redundantly to direct the recruitment of founder cells that give rise to a large lateral domain in mature maize leaves (Scanlon et al., 1996; Scanlon and Freeling, 1997; Scanlon, 2000; Nardmann et al., 2004). Multiple genes involved in two-component signaling, auxin response, jasmonate-induced/sugar signaling pathways and GTP-binding proteins, have been implicated in NS-mediated founder cell recruitment and mediolateral patterning via laser microdissection microarray analyses of the ns mutant SAM (chapter 3). More importantly, six genes identified in our LMM analyses are shown to be transcribed in a distinct founder cell domain that mirrors or overlaps the NS-expression foci within the SAM (Figure 3.5, Figure 3.6). Therefore, these genes are excellent candidates for subsequent reverse genetic and molecular/biochemical analyses, and may shed more light on mechanisms of early events in maize leaf development. In addition, our analyses reveal that repression of specific, two-component signaling pathways and activation of lectin gene expression are conserved functions for the WOX genes WUSCHEL and NARROW SHEATH1 (Leibfried et al., 2005) (chapter 3). Taken together with studies of developmental mutations in WOX9 (Wu et al., 2005), WOX5 (Gonzali et al., 2005), ATHB13 (Hanson et al., 2001), and RAMOSA3 (Satoh-Nagasawa et al.,

2006), our data reveal the importance of sugar-binding lectins and sugar transport during plant development, which may become an especially active research area in the near future.

RGD2 coordinates leaf patterning along the mediolateral and dorsiventral axes

Leaf patterning mutants, harboring mutations in class III *hd-zip* genes, *kan* genes, *phan*, *lbl1* and *arf3/ arf4* double mutants display narrow and radial leaf phenotypes, accompanied with a loss or reduction in adaxial or abaxial identity. These mutant phenotypes support a model wherein juxtaposition of adaxial and abaxial developmental fields generates a positional signal that is required for mediolateral expansion and proximodistal patterning (Waites and Hudson, 1995; Eshed et al., 2001; Hudson, 2001; Bowman et al., 2002). The maize mutant ragged seedling2-R (rgd2-R) also displays a narrow/filamentous leaf phenotype but no net loss of adaxial or abaxial identity, despite the fact that adaxial/abaxial tissues may be rotated or swapped (Henderson et al., 2005; Henderson et al., 2006). RGD2 is required for normal transcript accumulation of multiple leaf developmental genes, including NS1, YABBY14, Zm*KAN2 and RLD1, and may be required to coordinate dorsiventral and mediolateral patterning in maize leaves (Henderson et al., 2005; Henderson et al., 2006). These data suggest that juxtaposition of adaxial and abaxial identity is not sufficient to promote leaf lateral expansion, additional factors are required for competency to expand mediolaterally. The RGD2 gene product is unknown, although the mutant phenotype of rgd2-R is very similar to that of leafbladeless1 (lbl1) mutants (Henderson et al., 2006). LBL1 encodes an SGS3 orthologue required for tas3-siRNA biogenesis; loss of LBL1function leads to abaxialized leaves and over-accumulation of maize ARF3 and ARF4 transcripts (Nogueira et al., 2007). Double mutants in *rgd2/lbl1* are shootless

and embryo-lethal. This synergistic effect indicates that RGD2 functions redundantly with, but in a separate genetic pathway than, the ta3-siRNA regulator LBL1(Henderson et al., 2006).

We have characterized the genetic mechanisms downstream of RGD2 gene function using SAM-specific transcript profiling (Chapter 4). Genes predicted to be involved in transcriptional regulation, chromatin remodeling, signal transduction, and proteolysis/protein fate are especially misexpressed in the rgd2-R mutant apex. In consideration of the synergistic rgd2/lbl1 double mutant phenotypes and the role of LBL in ta-siRNA-mediated destruction of *arf3* and *arf4* transcripts, our LMM data may suggest that RGD2 functions in a novel proteolytic pathway targeting ARF4 proteins. Alternatively, three putative paralogues of RS2 interacting genes, including a WRKY-like gene (DN224320), a HIR1-like gene (DV621143) and the maize ERECTA-like gene (DV491381), are differentially expressed in specific domains of the rgd2-R mutant apex (Figure 4.3, Figure 4.4). These data suggest that RGD2 may function through the previously-described ARP pathway, to coordinate dorsiventral patterning and mediolateral growth during maize leaf development. Cloning RGD2, together with biochemical and reverse genetics analyses of genes identified as differentially-expressed in rgd2-R mutant apices will help to elucidate RGD2 function during maize leaf development.

Interestingly, all the differentially expressed genes characterized by *in situ* hybridization in chapter 4, and many published leaf dorsiventral patterning genes, are expressed in the vascular tissue in the leaf primordia (Figure 4.3-4.6) (Chitwood et al., 2007; Kidner and Timmermans, 2007). More intriguingly, the predicted unknown DN223697 is expressed in leaf vasculature and in the un-vascularized P1 primordium in a pattern that appears to precede and predict vein development (Figure 4.6 B, C). Genes specifically regulating xylem and phloem differentiation are useful molecular genetic tools to explore the correlation between vasculature specification

and leaf patterning along the mediolateral and dorsiventral axes. Currently, very few studies have been performed in maize vasculature tissue, probably due to difficulties in analyses of lethal genes. Application of new technologies, such as RNAi (Cigan et al., 2005; McGinnis et al., 2005), fluorescent protein tagging (Wymer et al., 2001) and live-cell imaging (Reddy et al., 2004; Reddy et al., 2007), will help to address these developmental questions in maize.

REFERENCE

Abd El-Rehim, D.M., Ball, G., Pinder, S.E., Rakha, E., Paish, C., Robertson, J.F., Macmillan, D., Blamey, R.W., and Ellis, I.O. (2005). High-throughput protein expression analysis using tissue microarray technology of a large well-characterised series identifies biologically distinct classes of breast cancer confirming recent cDNA expression analyses. Int J Cancer **116,** 340-350.

Azpiroz-Leehan, R., and Feldmann, K.A. (1997). T-DNA insertion mutagenesis in *Arabidopsis*: going back and forth. Trends Genet **13,** 152-156.

Barski, A., Cuddapah, S., Cui, K., Roh, T.Y., Schones, D.E., Wang, Z., Wei, G., Chepelev, I., and Zhao, K. (2007). High-resolution profiling of histone methylations in the human genome. Cell **129,** 823-837.

Bertone, P., and Snyder, M. (2005). Advances in functional protein microarray technology. Febs J **272,** 5400-5411.

Blower, M.D., Sullivan, B.A., and Karpen, G.H. (2002). Conserved organization of centromeric chromatin in flies and humans. Dev Cell **2,** 319-330.

Bowman, J.L., Eshed, Y., and Baum, S.F. (2002). Establishment of polarity in angiosperm lateral organs. Trends Genet **18,** 134-141.

Chitwood, D.H., Guo, M., Nogueira, F.T., and Timmermans, M.C. (2007). Establishing leaf polarity: the role of small RNAs and positional signals in the shoot apex. Development **134,** 813-823.

Chueh, A.C., Wong, L.H., Wong, N., and Choo, K.H. (2005). Variable and hierarchical size distribution of L1-retroelement-enriched CENP-A clusters within a functional human neocentromere. Hum Mol Genet **14,** 85-93.

Cigan, A.M., Unger-Wallace, E., and Haug-Collet, K. (2005). Transcriptional gene silencing as a tool for uncovering gene function in maize. Plant J **43,** 929-940.

Clough, S.J., and Bent, A.F. (1998). Floral dip: a simplified method for Agrobacterium-mediated transformation of *Arabidopsis thaliana*. Plant J **16,** 735-743.

Daujat, S., Bauer, U.M., Shah, V., Turner, B., Berger, S., and Kouzarides, T. (2002). Crosstalk between CARM1 methylation and CBP acetylation on histone H3. Curr Biol **12,** 2090-2097.

Dawe, R.K., and Henikoff, S. (2006). Centromeres put epigenetics in the driver's seat. Trends Biochem Sci **31,** 662-669.

Demidov, D., Van Damme, D., Geelen, D., Blattner, F.R., and Houben, A. (2005). Identification and dynamics of two classes of aurora-like kinases in *Arabidopsis* and other plants. Plant Cell **17,** 836-848.

Eshed, Y., Baum, S.F., Perea, J.V., and Bowman, J.L. (2001). Establishment of polarity in lateral organs of plants. Curr Biol **11,** 1251-1260.

Gernand, D., Demidov, D., and Houben, A. (2003). The temporal and spatial pattern of histone H3 phosphorylation at serine 28 and serine 10 is similar in plants but differs between mono- and polycentric chromosomes. Cytogenet. Genome Res. **101,** 172-176.

Gonzali, S., Novi, G., Loreti, E., Paolicchi, F., Poggi, A., Alpi, A., and Perata, P. (2005). A turanose-insensitive mutant suggests a role for WOX5 in auxin homeostasis in *Arabidopsis thaliana*. Plant J **44,** 633-645.

Hanson, J., Johannesson, H., and Engstrom, P. (2001). Sugar-dependent alterations in cotyledon and leaf development in transgenic plants expressing the HDZhdip gene ATHB13. Plant Mol Biol **45,** 247-262.

Harrington, E.A., Bebbington, D., Moore, J., Rasmussen, R.K., Ajose-Adeogun, A.O., Nakayama, T., Graham, J.A., Demur, C., Hercend, T., Diu-Hercend, A., Su, M., Golec, J.M., and Miller, K.M. (2004). VX-680, a potent and selective small-molecule inhibitor of the Aurora kinases, suppresses tumor growth in vivo. Nat Med **10,** 262-267.

Hauf, S., Cole, R.W., LaTerra, S., Zimmer, C., Schnapp, G., Walter, R., Heckel, A., van Meel, J., Rieder, C.L., and Peters, J.M. (2003). The small molecule Hesperadin reveals a role for Aurora B in correcting kinetochore-microtubule attachment and in maintaining the spindle assembly checkpoint. J Cell Biol **161,** 281-294.

Henderson, D.C., Muehlbauer, G.J., and Scanlon, M.J. (2005). Radial leaves of the maize mutant ragged seedling2 retain dorsiventral anatomy. Dev Biol **282,** 455-466.

Henderson, D.C., Zhang, X., Brooks, L., 3rd, and Scanlon, M.J. (2006). RAGGED SEEDLING2 is required for expression of KANADI2 and REVOLUTA homologues in the maize shoot apex. Genesis **44,** 372-382.

Hendzel, M.J., Wei, Y., Mancini, M.A., Van Hooser, A., Ranalli, T., Brinkley, B.R., Bazett-Jones, D.P., and Allis, C.D. (1997). Mitosis-specific phosphorylation of histone H3 initiates primarily within pericentromeric heterochromatin during G2 and spreads in an ordered fashion coincident with mitotic chromosome condensation. Chromosoma **106,** 348-360.

Hirota, T., Lipp, J.J., Toh, B.H., and Peters, J.M. (2005). Histone H3 serine 10 phosphorylation by Aurora B causes HP1 dissociation from heterochromatin. Nature **438,** 1176-1180.

Hudson, A. (2001). Plant development: Two sides to organ asymmetry. Curr Biol **11,** R756-758.

Kawabe, A., Matsunaga, S., Nakagawa, K., Kurihara, D., Yoneda, A., Hasezawa, S., Uchiyama, S., and Fukui, K. (2005). Characterization of plant Aurora kinases during mitosis. Plant Mol Biol **58,** 1-13.

Kerk, N.M., Ceserani, T., Tausta, S.L., Sussex, I.M., and Nelson, T.M. (2003). Laser capture microdissection of cells from plant tissues. Plant Physiol **132,** 27-35.

Kidner, C.A., and Timmermans, M.C. (2007). Mixing and matching pathways in leaf polarity. Curr Opin Plant Biol **10,** 13-20.

Kouzarides, T. (2007). Chromatin modifications and their function. Cell **128,** 693-705.

Kurihara, D., Matsunaga, S., Kawabe, A., Fujimoto, S., Noda, M., Uchiyama, S., and Fukui, K. (2006). Aurora kinase is required for chromosome segregation in tobacco BY-2 cells. Plant J **48,** 572-580.

Leibfried, A., To, J.P., Busch, W., Stehling, S., Kehle, A., Demar, M., Kieber, J.J., and Lohmann, J.U. (2005). WUSCHEL controls meristem function by direct regulation of cytokinin-inducible response regulators. Nature **438,** 1172-1175.

McGinnis, K., Chandler, V., Cone, K., Kaeppler, H., Kaeppler, S., Kerschen, A., Pikaard, C., Richards, E., Sidorenko, L., Smith, T., Springer, N., and Wulan, T. (2005). Transgene-induced RNA interference as a tool for plant functional genomics. Methods Enzymol **392,** 1-24.

Mockler, T.C., Chan, S., Sundaresan, A., Chen, H., Jacobsen, S.E., and Ecker, J.R. (2005). Applications of DNA tiling arrays for whole-genome analysis. Genomics **85,** 1-15.

Murray, G.I. (2007). An overview of laser microdissection technologies. Acta Histochem **109,** 171-176.

Nardmann, J., Ji, J., Werr, W., and Scanlon, M.J. (2004). The maize duplicate genes narrow sheath1 and narrow sheath2 encode a conserved homeobox gene function in a lateral domain of shoot apical meristems. Development **131,** 2827-2839.

Nelson, T., Tausta, S.L., Gandotra, N., and Liu, T. (2006a). Laser Microdissection of Plant Tissue: What You See Is What You Get. Annu Rev Plant Biol.

Nelson, T., Tausta, S.L., Gandotra, N., and Liu, T. (2006b). Laser microdissection of plant tissue: what you see is what you get. Annu Rev Plant Biol **57,** 181-201.

Noma, K., and Grewal, S.I. (2002). Histone H3 lysine 4 methylation is mediated by Set1 and promotes maintenance of active chromatin states in fission yeast. Proc Natl Acad Sci U S A **99 Suppl 4,** 16438-16445.

Nygaard, V., and Hovig, E. (2006). Options available for profiling small samples: a review of sample amplification technology when combined with microarray profiling. Nucleic Acids Res **34,** 996-1014.

Polioudaki, H., Markaki, Y., Kourmouli, N., Dialynas, G., Theodoropoulos, P.A., Singh, P.B., and Georgatos, S.D. (2004). Mitotic phosphorylation of histone H3 at threonine 3. FEBS Lett **560,** 39-44.

Preuss, U., Landsberg, G., and Scheidtmann, K.H. (2003). Novel mitosis-specific phosphorylation of histone H3 at Thr11 mediated by Dlk/ZIP kinase. Nucleic Acids Res **31,** 878-885.

Reddy, G.V., Gordon, S.P., and Meyerowitz, E.M. (2007). Unravelling developmental dynamics: transient intervention and live imaging in plants. Nat Rev Mol Cell Biol **8,** 491-501.

Reddy, G.V., Heisler, M.G., Ehrhardt, D.W., and Meyerowitz, E.M. (2004). Real-time lineage analysis reveals oriented cell divisions associated with morphogenesis at the shoot apex of *Arabidopsis thaliana*. Development **131,** 4225-4237.

Satoh-Nagasawa, N., Nagasawa, N., Malcomber, S., Sakai, H., and Jackson, D. (2006). A trehalose metabolic enzyme controls inflorescence architecture in maize. Nature **441,** 227-230.

Scanlon, M.J. (2000). NARROW SHEATH1 functions from two meristematic foci during founder-cell recruitment in maize leaf development. Development **127,** 4573-4585.

Scanlon, M.J., and Freeling, M. (1997). Clonal sectors reveal that a specific meristematic domain is not utilized in the maize mutant narrow sheath. Dev Biol **182,** 52-66.

Scanlon, M.J., Schneeberger, R.G., and Freeling, M. (1996). The maize mutant narrow sheath fails to establish leaf margin identity in a meristematic domain. Development **122,** 1683-1691.

Schad, M., Mungur, R., Fiehn, O., and Kehr, J. (2005a). Metabolic profiling of laser microdissected vascular bundles of *Arabidopsis thaliana*. Plant Methods **1,** 2.

Schad, M., Lipton, M.S., Giavalisco, P., Smith, R.D., and Kehr, J. (2005b). Evaluation of two-dimensional electrophoresis and liquid chromatography--tandem mass spectrometry for tissue-specific protein profiling of laser-microdissected plant samples. Electrophoresis **26,** 2729-2738.

Schena, M., Shalon, D., Davis, R.W., and Brown, P.O. (1995). Quantitative monitoring of gene expression patterns with a complementary DNA microarray. Science **270,** 467-470.

Scutt, C.P., Kamisugi, Y., Sakai, F., and Gilmartin, P.M. (1997). Laser isolation of plant sex chromosomes: studies on the DNA composition of the X and Y sex chromosomes of Silene latifolia. Genome **40,** 705-715.

Sessa, F., Mapelli, M., Ciferri, C., Tarricone, C., Areces, L.B., Schneider, T.R., Stukenberg, P.T., and Musacchio, A. (2005). Mechanism of Aurora B activation by INCENP and inhibition by hesperadin. Mol Cell **18,** 379-391.

Strahl, B.D., and Allis, C.D. (2000). The language of covalent histone modifications. Nature **403,** 41-45.

Talbert, P.B., Masuelli, R., Tyagi, A.P., Comai, L., and Henikoff, S. (2002). Centromeric localization and adaptive evolution of an *Arabidopsis* histone H3 variant. Plant Cell **14,** 1053-1066.

Templin, M.F., Stoll, D., Schrenk, M., Traub, P.C., Vohringer, C.F., and Joos, T.O. (2002). Protein microarray technology. Trends Biotechnol **20,** 160-166.

Waites, R., and Hudson, A. (1995). *phantastica*: a gene required for dorsoventrality of leaves in *Antirrhinum-majus*. Development **121,** 2143-2154.

Wieland, G., Orthaus, S., Ohndorf, S., Diekmann, S., and Hemmerich, P. (2004). Functional complementation of human centromere protein A (CENP-A) by Cse4p from Saccharomyces cerevisiae. Mol Cell Biol **24,** 6620-6630.

Wu, X., Dabi, T., and Weigel, D. (2005). Requirement of homeobox gene STIMPY/WOX9 for *Arabidopsis* meristem growth and maintenance. Curr Biol **15,** 436-440.

Wymer, C.L., Fernandez-Abalos, J.M., and Doonan, J.H. (2001). Microinjection reveals cell-to-cell movement of green fluorescent protein in cells of maize coleoptiles. Planta **212,** 692-695.

Zeitlin, S.G., Shelby, R.D., and Sullivan, K.F. (2001a). CENP-A is phosphorylated by Aurora B kinase and plays an unexpected role in completion of cytokinesis. J Cell Biol **155,** 1147-1157.

Zeitlin, S.G., Barber, C.M., Allis, C.D., and Sullivan, K.F. (2001b). Differential regulation of CENP-A and histone H3 phosphorylation in G2/M. J Cell Sci **114,** 653-661.

Zhang, X., Henriques, R., Lin, S.S., Niu, Q.W., and Chua, N.H. (2006). Agrobacterium-mediated transformation of *Arabidopsis thaliana* using the floral dip method. Nat Protoc **1,** 641-646.

APPENDICS

From: Diane McCauley <diane@aspb.org>

To: Xiaolan Zhang <xzhang@plantbio.uga.edu>

Date: 05/31/2007 10:17 AM

Subject: copyright permission for dissertation

Hello, Xiaolan

ASPB allows authors to reuse their material without written permission from the society. We just ask that you provide a bibliographic citation and acknowledge ASPB as copyright holder.

Regards,

Diane McCauley
Publications Assistant
American Society of Plant Biologists
15501 Monona Drive
Rockville, MD 20855
phone: 301-251-0560 ext. 133
fax: 301-279-2996
diane@aspb.org
http://www.aspb.org

From: PLoS Genetics <plosgenetics@plos.org>

To: Xiaolan Zhang <xzhang@plantbio.uga.edu> **Cc:** CJ Pub <cj_pub@plos.org>

Date: 05/29/2007 06:53 AM

Subject: RE: ask for copy right permission for dissertation

Dear Xiaolan,

Thanks for your message. Since the early online version is already in the public domain (http://genetics.plosjournals.org/perlserv/?request=get-document&doi=10.1371/journal.pgen.0030101.eor), you are free to download, use, distribute, and reproduce or use this in any way you wish (with attribution), including within your dissertation (but please be aware that there will be differences between the provisional version and the final published version). Further information is available at http://www.plos.org/oa/index.html and http://journals.plos.org/plosgenetics/license.php (as we apply the Creative Commons Attribution License to all works we publish, those accessing our content do not even need to request permission from us with respect to the use or reuse of it). The final version is currently scheduled for publication on June 15.

I hope this helps.

Best wishes,

Andy

Andy Collings
Publications Manager, *PLoS Genetics*
plosgenetics@plos.org / http://www.plosgenetics.org/
Email Alerts: http://register.plos.org/